ARES-3, the Ariel School

Google

Outils

https://

Ariel

On Sept

Ariel Sch

Backgrou

http://www.i

Index AR

ARES II: ARI

Beaulieu, Pier

https://www.bbc. Traduire cette page

The schoolkids who said they saw 'aliens'


LES AZALEES
1 à 2
DONT
MAKE YOUR
OWN
molly
KRACKEN

Jean-Philippe Beaulieu

With slides from Amélie Gressier, Alice Maurel, Emilie Panek, Pierre-Olivier Lagage

Exoplanet and JWST

Planet discovered by years

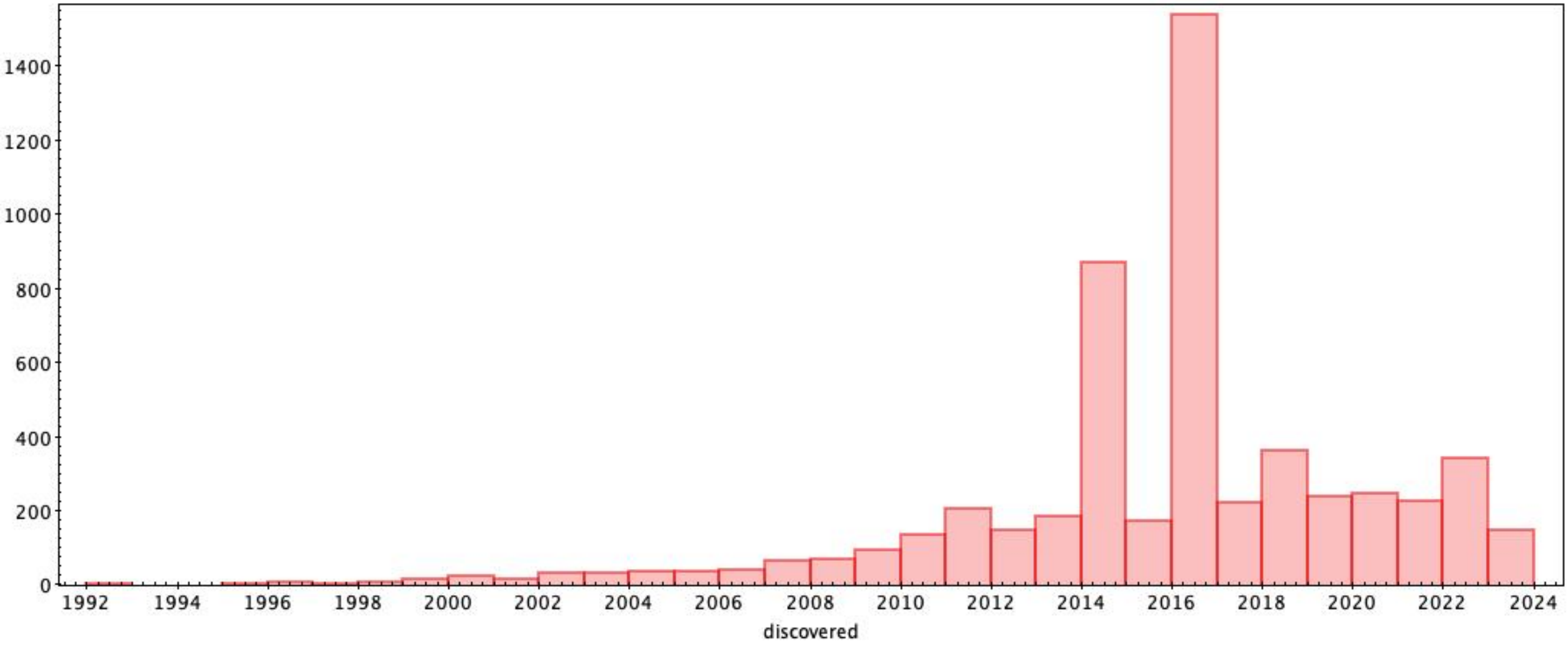

transit and eclipses

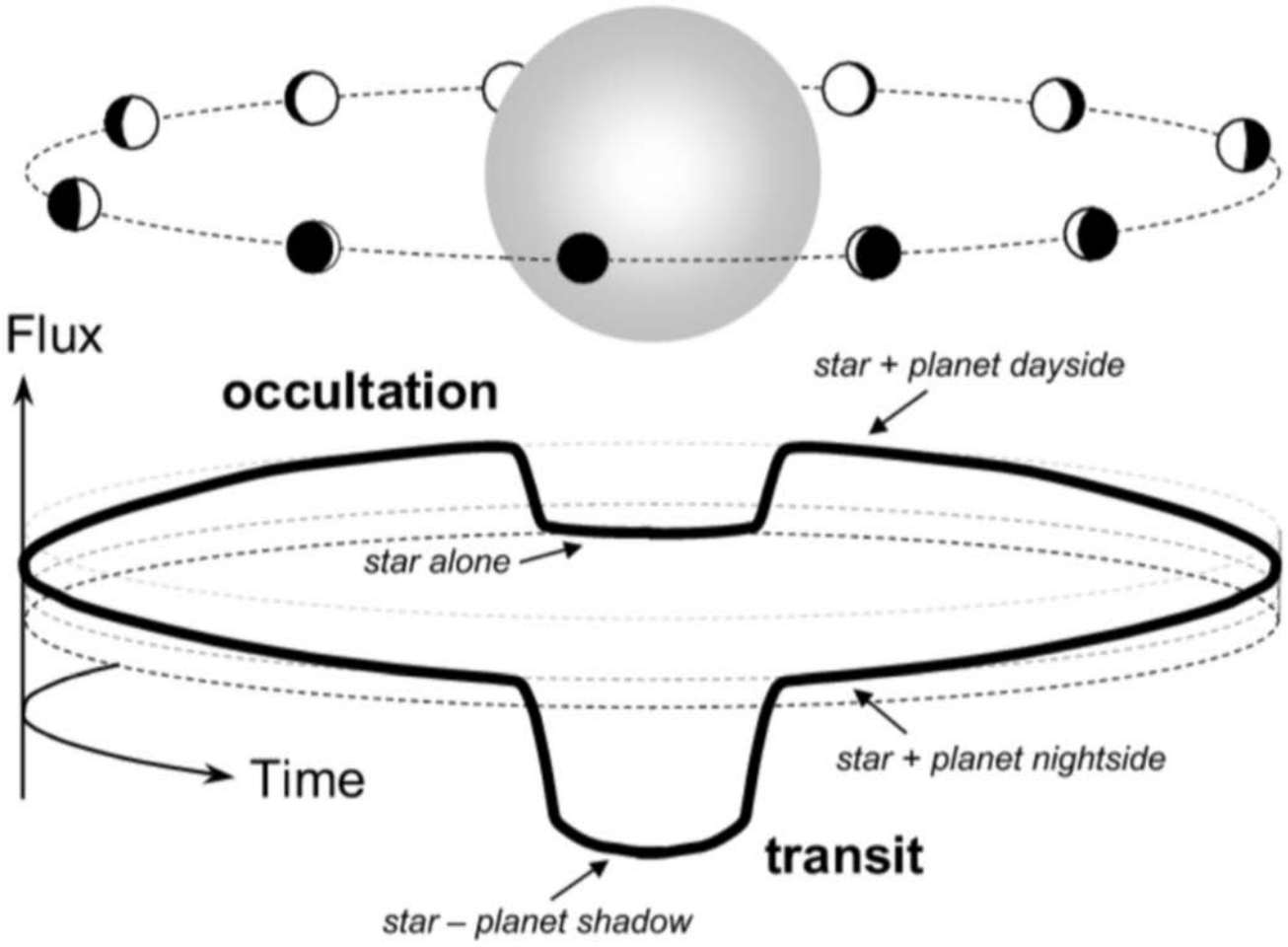

Transit depth:

$$\delta_{tra} = \left(\frac{R_p}{R_\star}\right)^2$$

Occultation depth:

$$\delta_{occ} = \frac{I_p}{I_\star}\left(\frac{R_p}{R_\star}\right)^2$$

Flux ratio day side of the planet / star

Kepler
BY THE NUMBERS

9.6 YEARS IN SPACE

530,506 STARS OBSERVED

2,662 PLANETS CONFIRMED

61 SUPERNOVAE DOCUMENTED
FROM EARLIEST STAGES OF EXPLOSION

2 MISSIONS COMPLETED

678 GB SCIENCE DATA COLLECTED

2,946 SCIENTIFIC PAPERS PUBLISHED

732,128 COMMANDS EXECUTED

94 MILLION MILES AWAY

3.12 GALLONS FUEL USED

www.nasa.gov/kepler

As of October 24, 2018

@NASAKepler

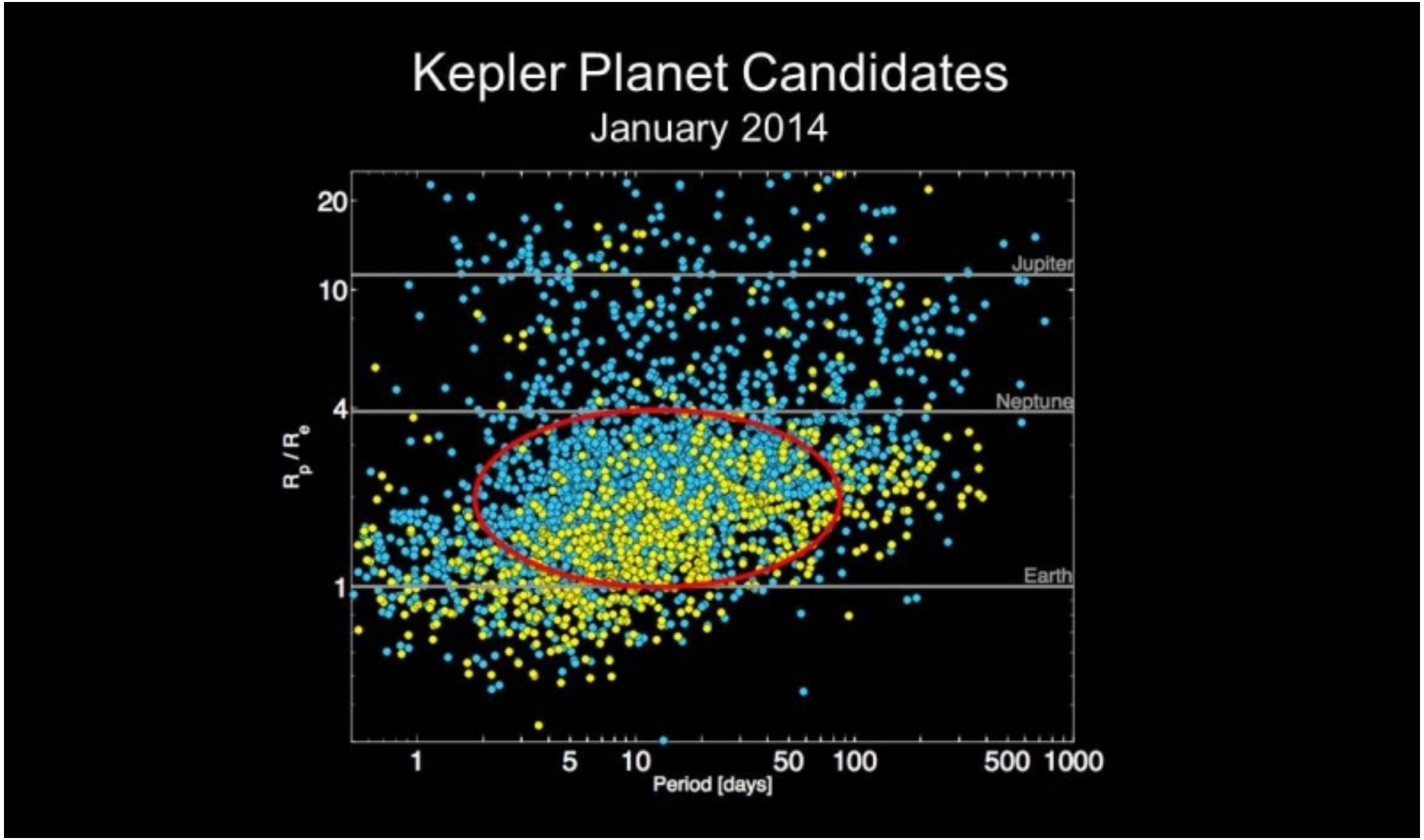
Kepler Planet Candidates
January 2014
20
10
4
1
Jupiter
Neptune
Earth
R_p / R_e
1
5
10
50
100
500
1000
Period [days]

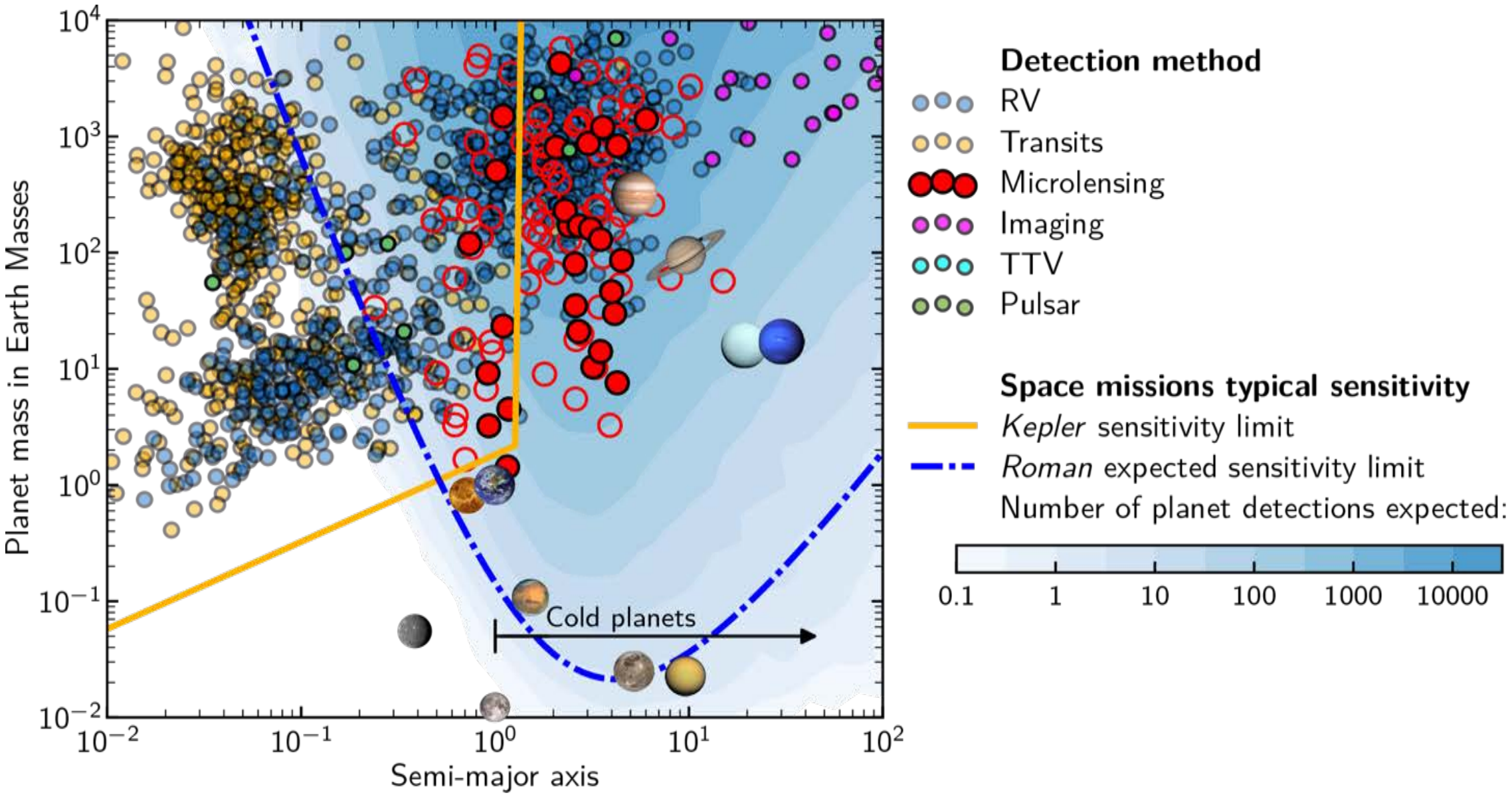
Planet mass in Earth Masses
10^4
10^3
10^2
10^1
10^0
10^{-1}
10^{-2}
10^{-2}
10^{-1}
10^0
10^1
10^2
Semi-major axis
Cold planets
Detection method
RV
Transits
Microlensing
Imaging
TTV
Pulsar
Space missions typical sensitivity
Kepler sensitivity limit
Roman expected sensitivity limit
Number of planet detections expected:
0.1
1
10
100
1000
10000

Mass radius relations and isodensity curves with first batch of small planets

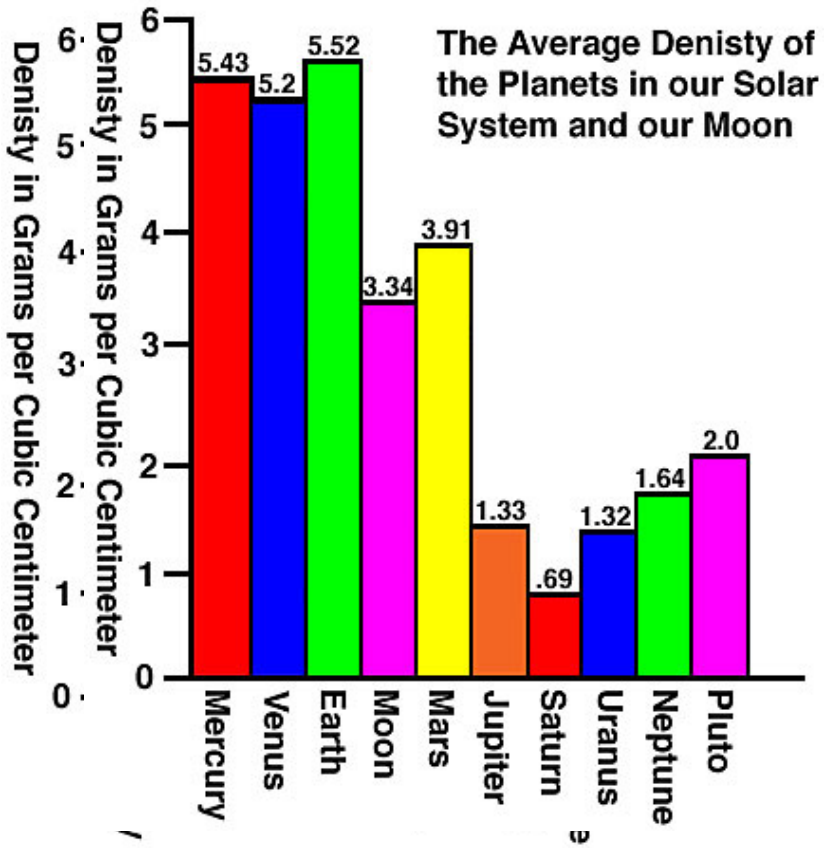

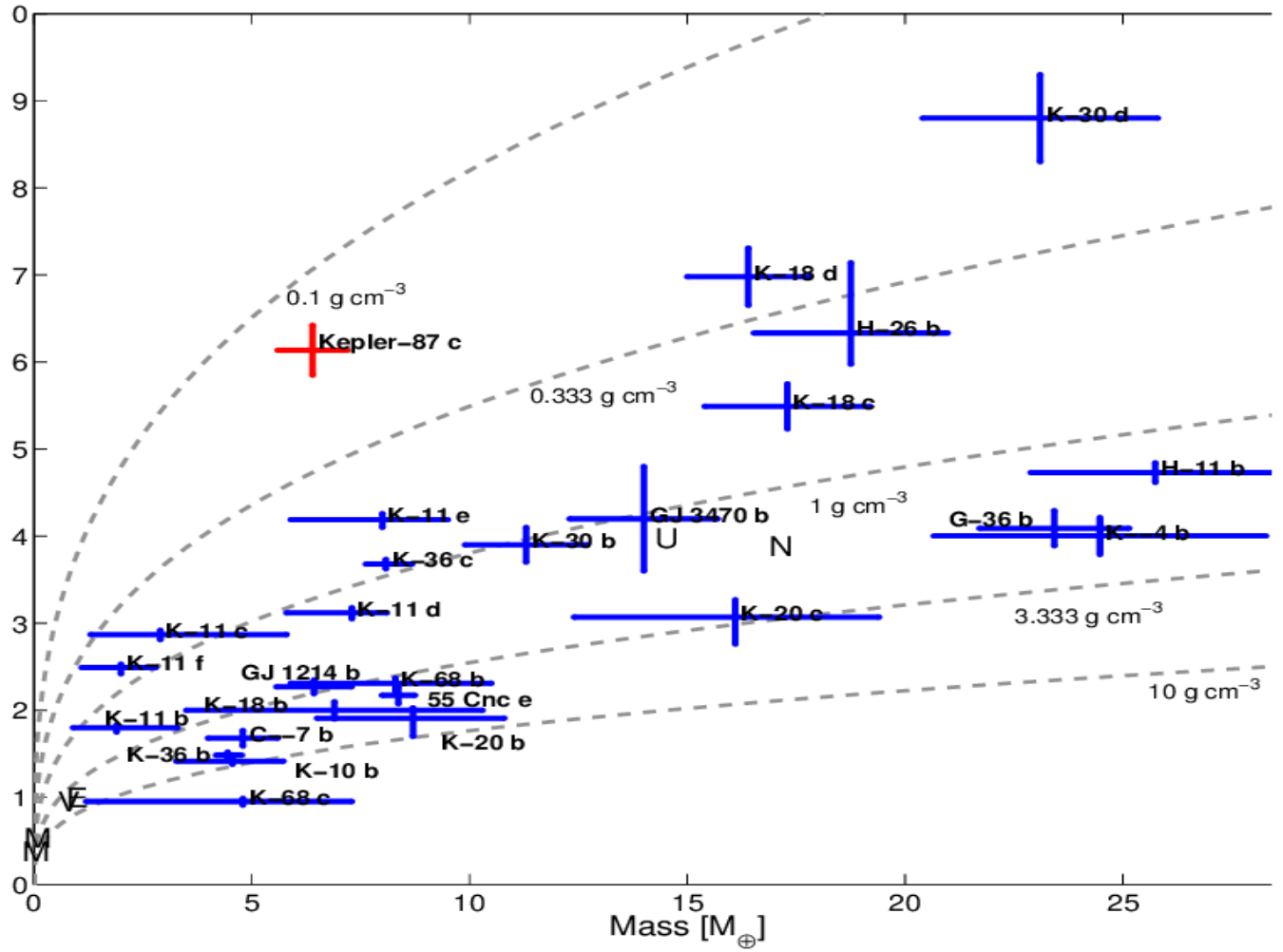

Histogram of planet radii, 2 peaks, super-Earth and Mini-Neptune

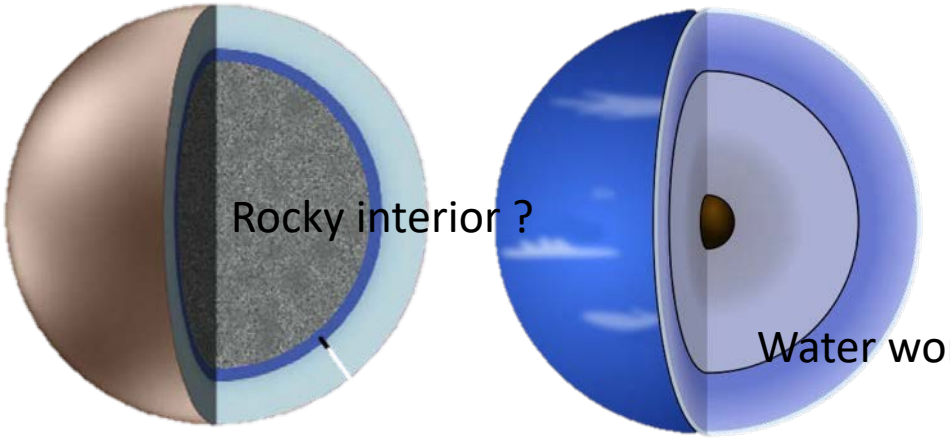

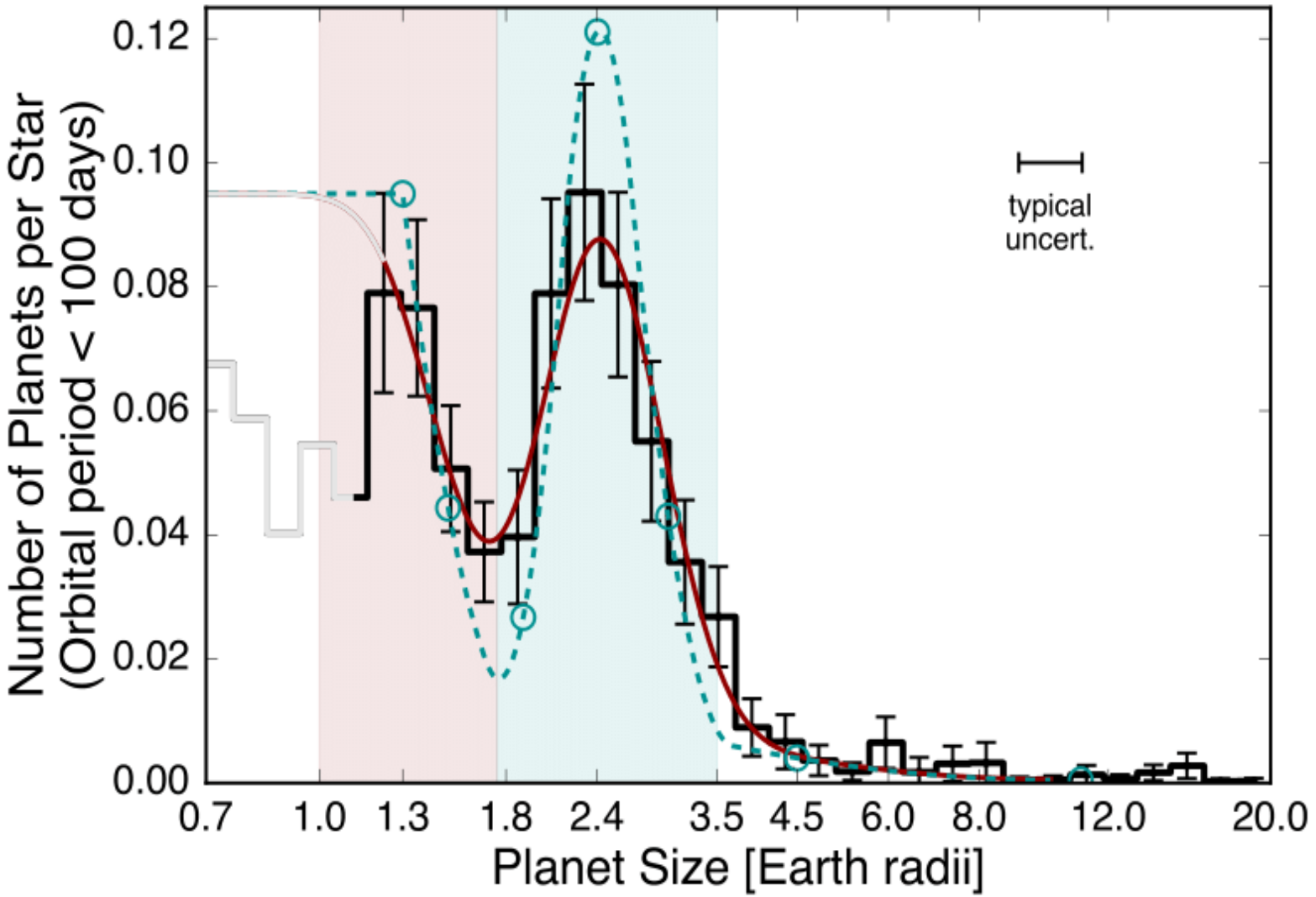

Completeness-corrected histogram of planet radii for planets with orbital periods shorter than 100 days.

Lightly shaded regions encompass our definitions of “super-Earths” (light red) and “sub-Neptunes” (light cyan). The dashed cyan line is a plausible model for the underlying occurrence distribution after removing the smearing caused by uncertainties on the planet radii measurements.

Classification according to density

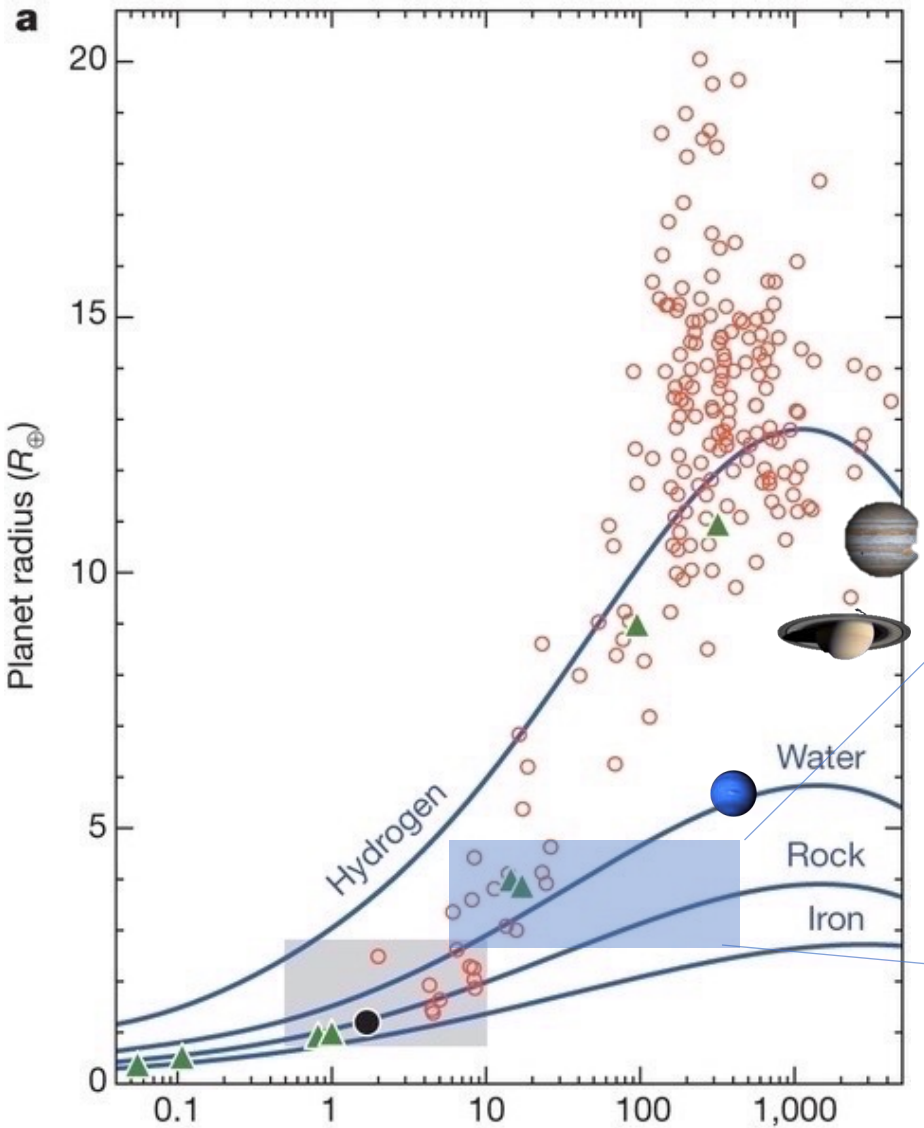

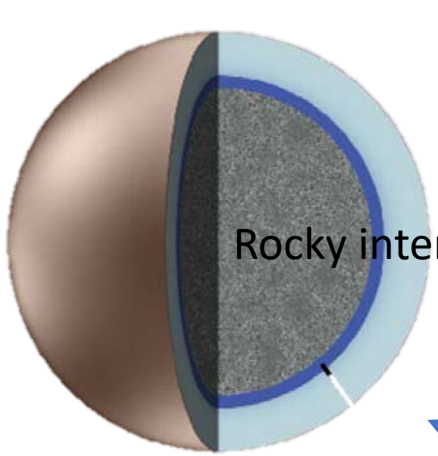

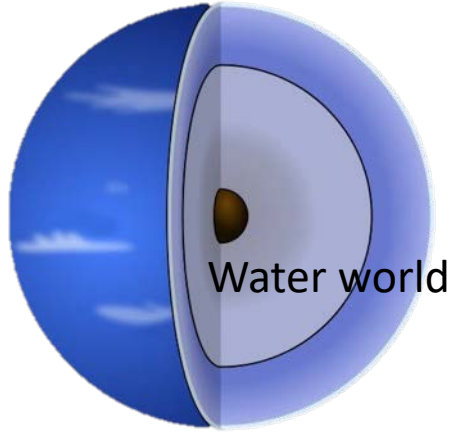

Or ?

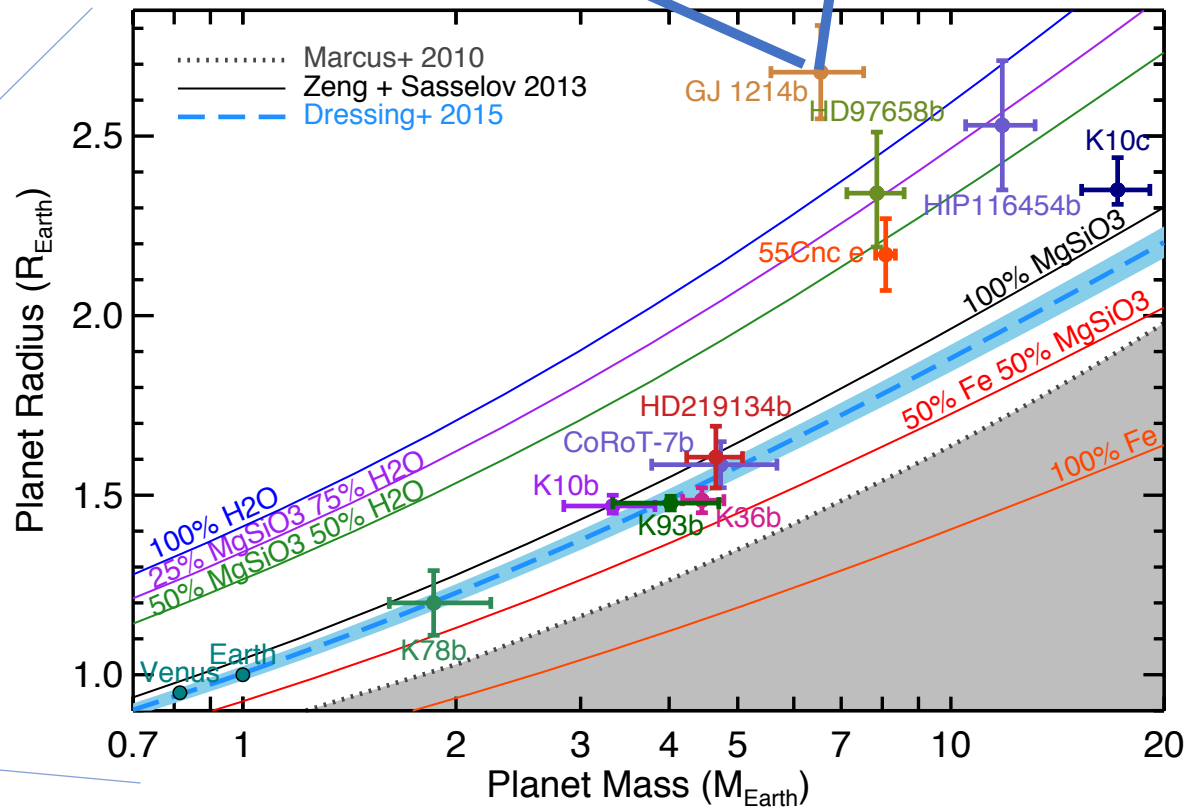

Howard et al., 2013; Motalebi et al., 2015

A fabulous diversity in the exoplanet zoo

Mass and Radius are not enough

5 Super Earth / Mini Neptunes in Kepler 11. Very different atmospheres !

(Lissauer et al. 2011, Valencia et al., 2013)

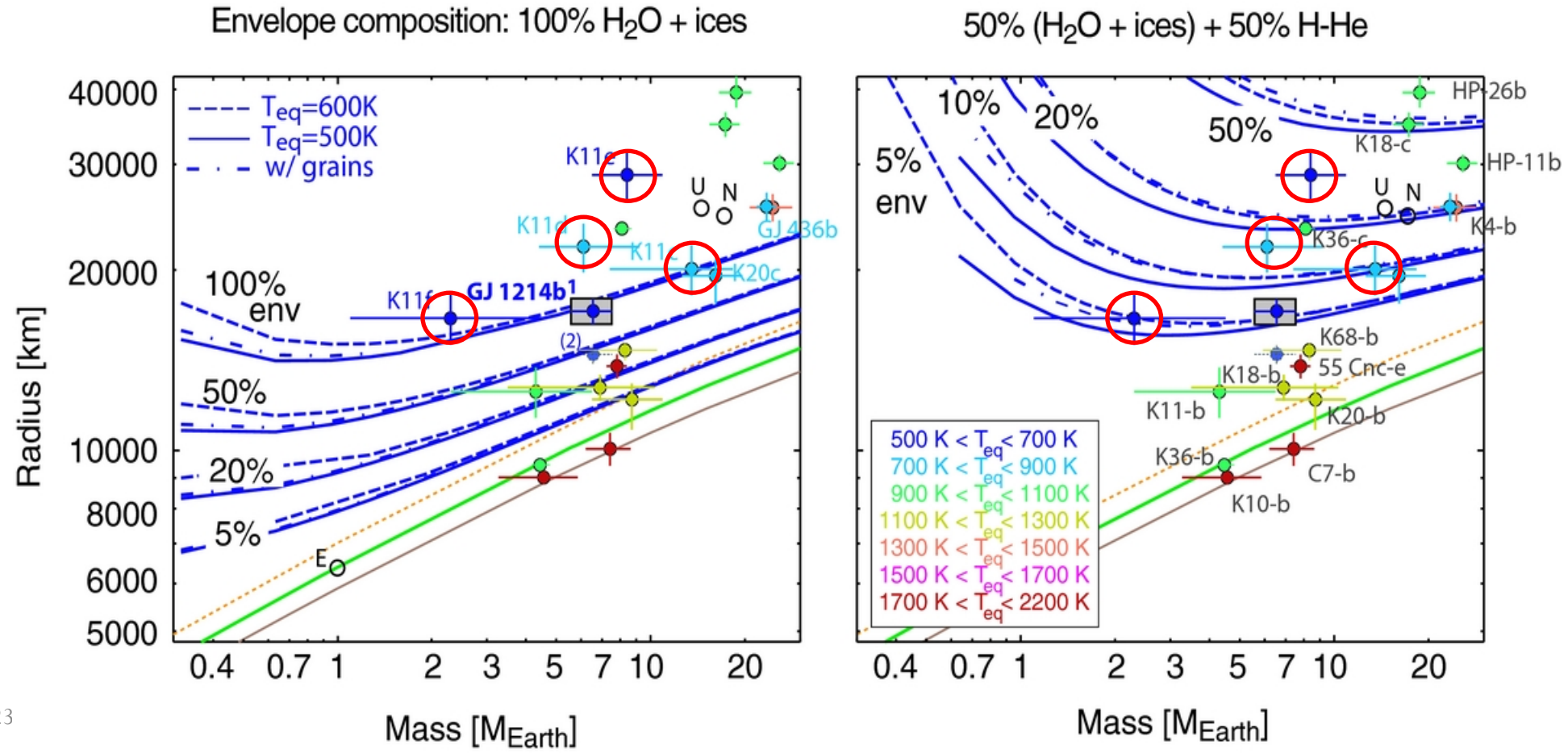

The Sun's planets are cold

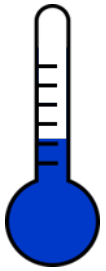

SOME KEY O, C, N, S MOLECULES ARE **NOT** IN GAS FORM

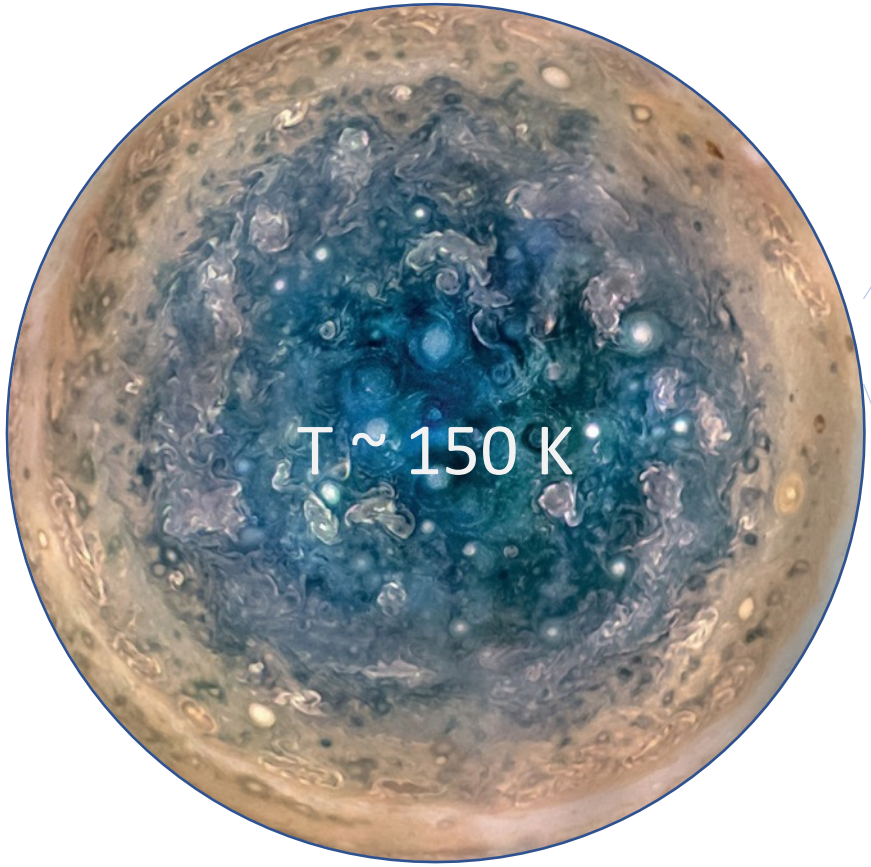

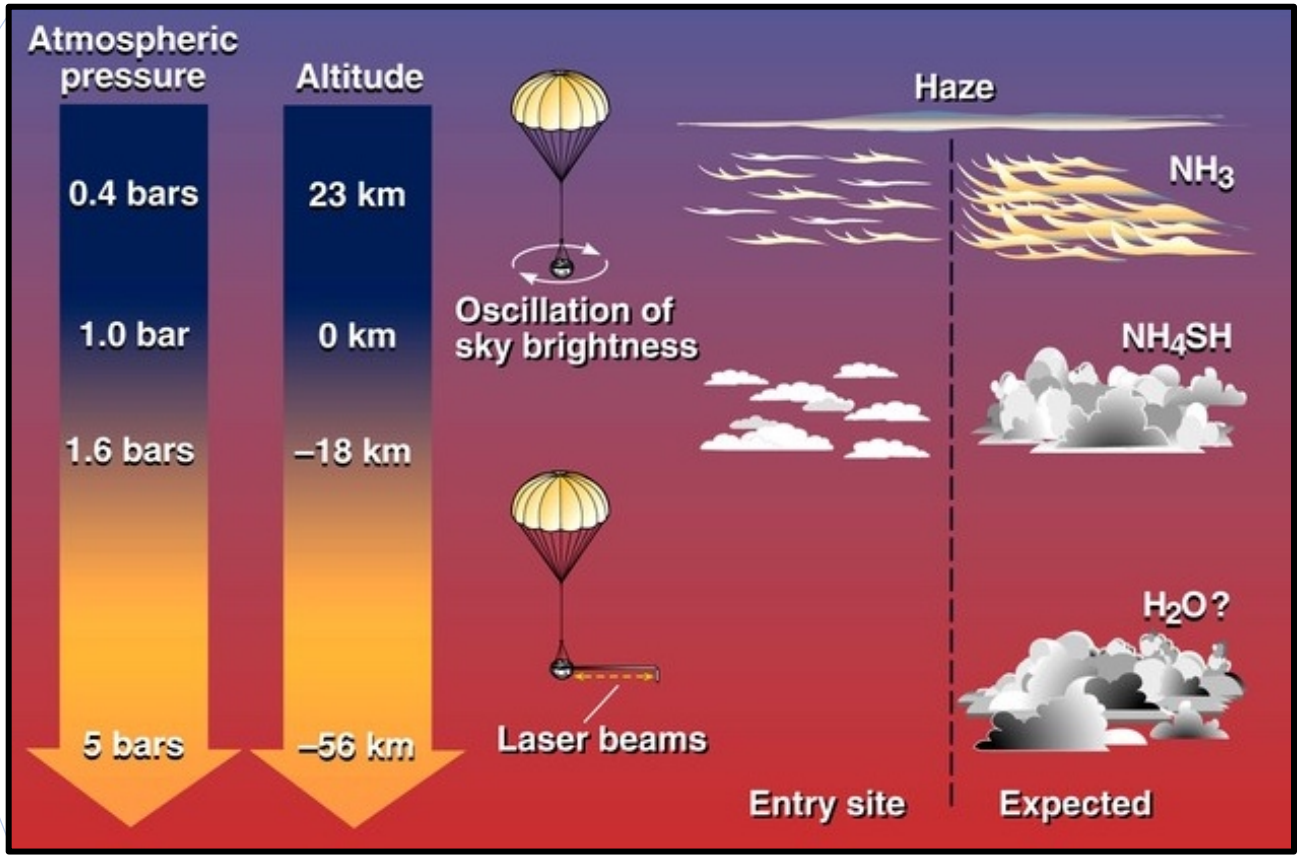

Warm/hot exoplanets

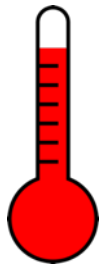

O, C, N, S (Ti, VO, Si) molecules are in gas form

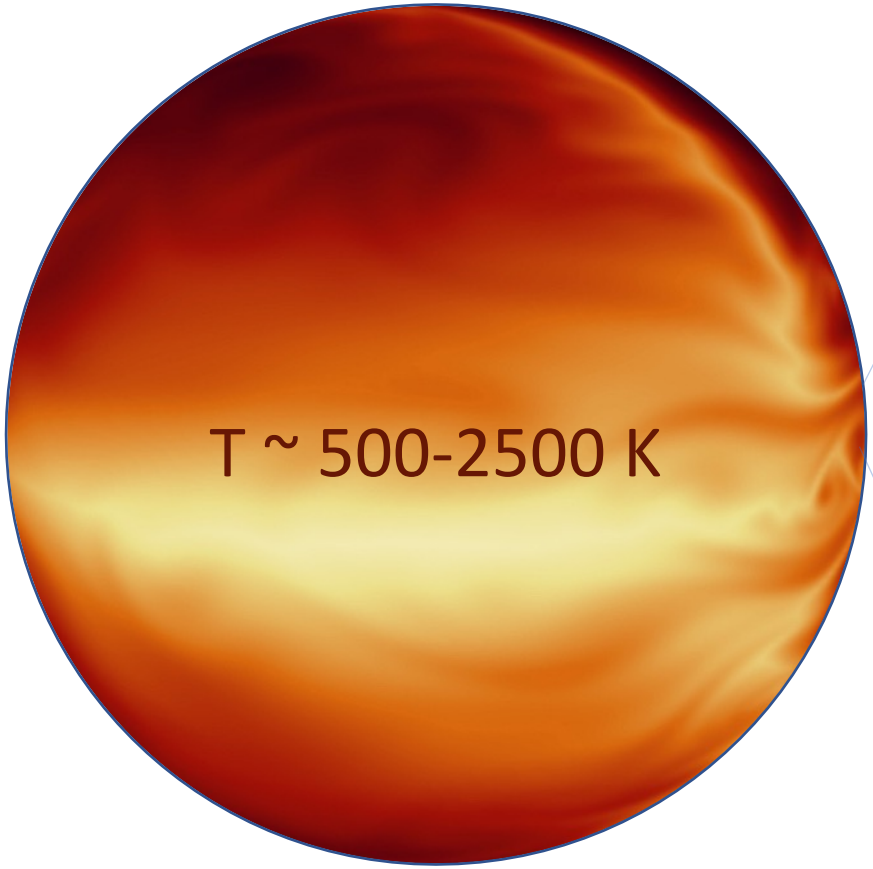

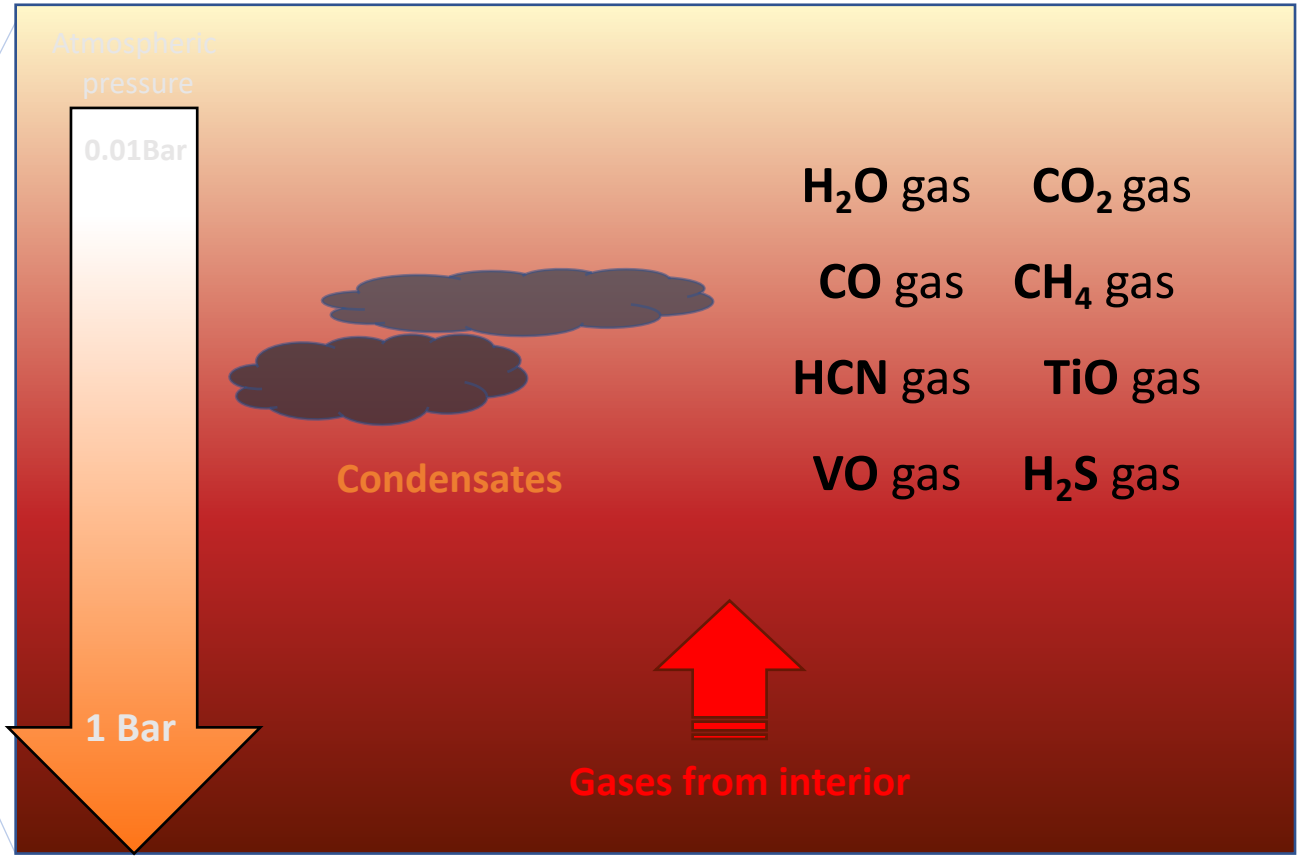

We need good line lists…
Exomol and other groups

Water vapour absorption as a function of temperature and wavelength

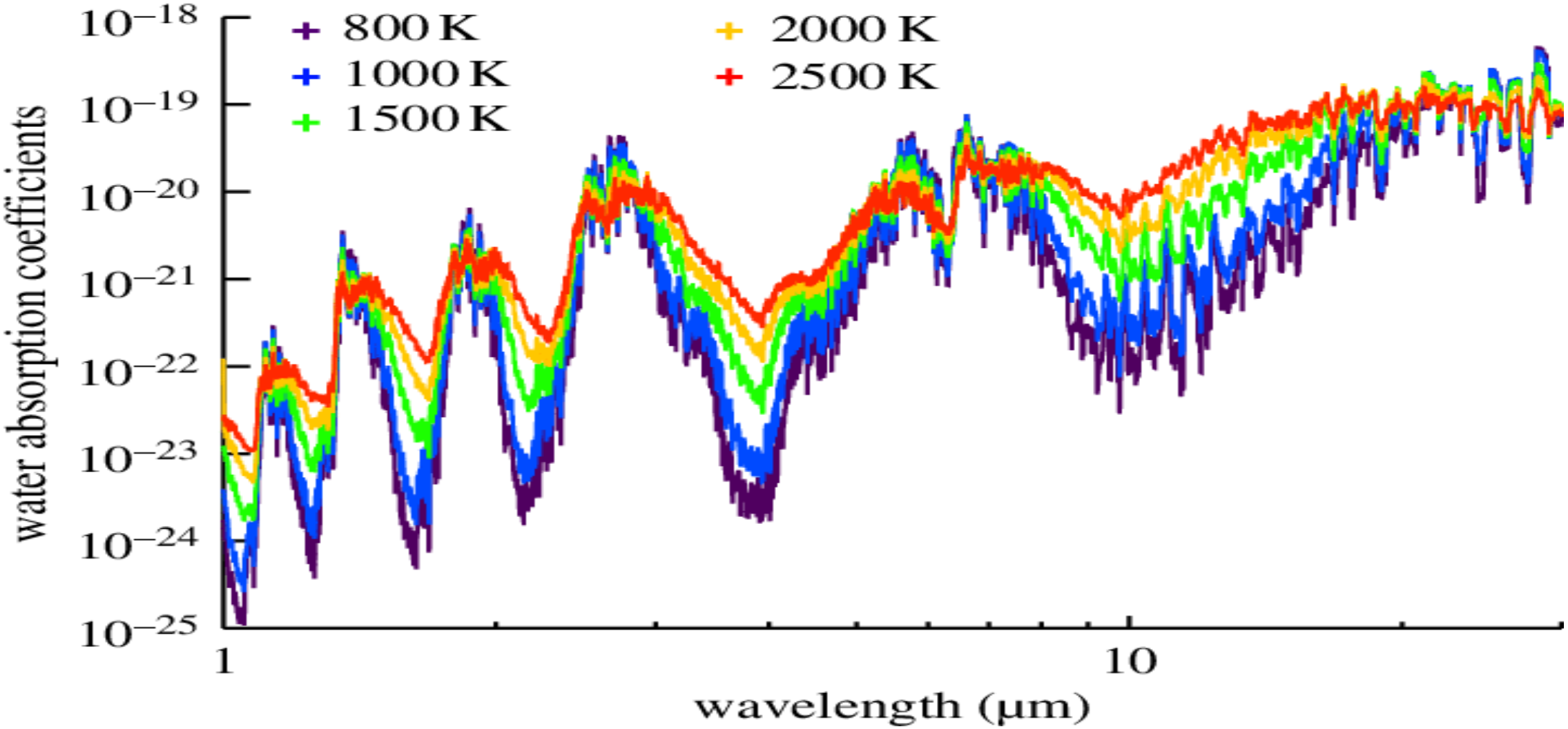

Key molecules absorbing in IR

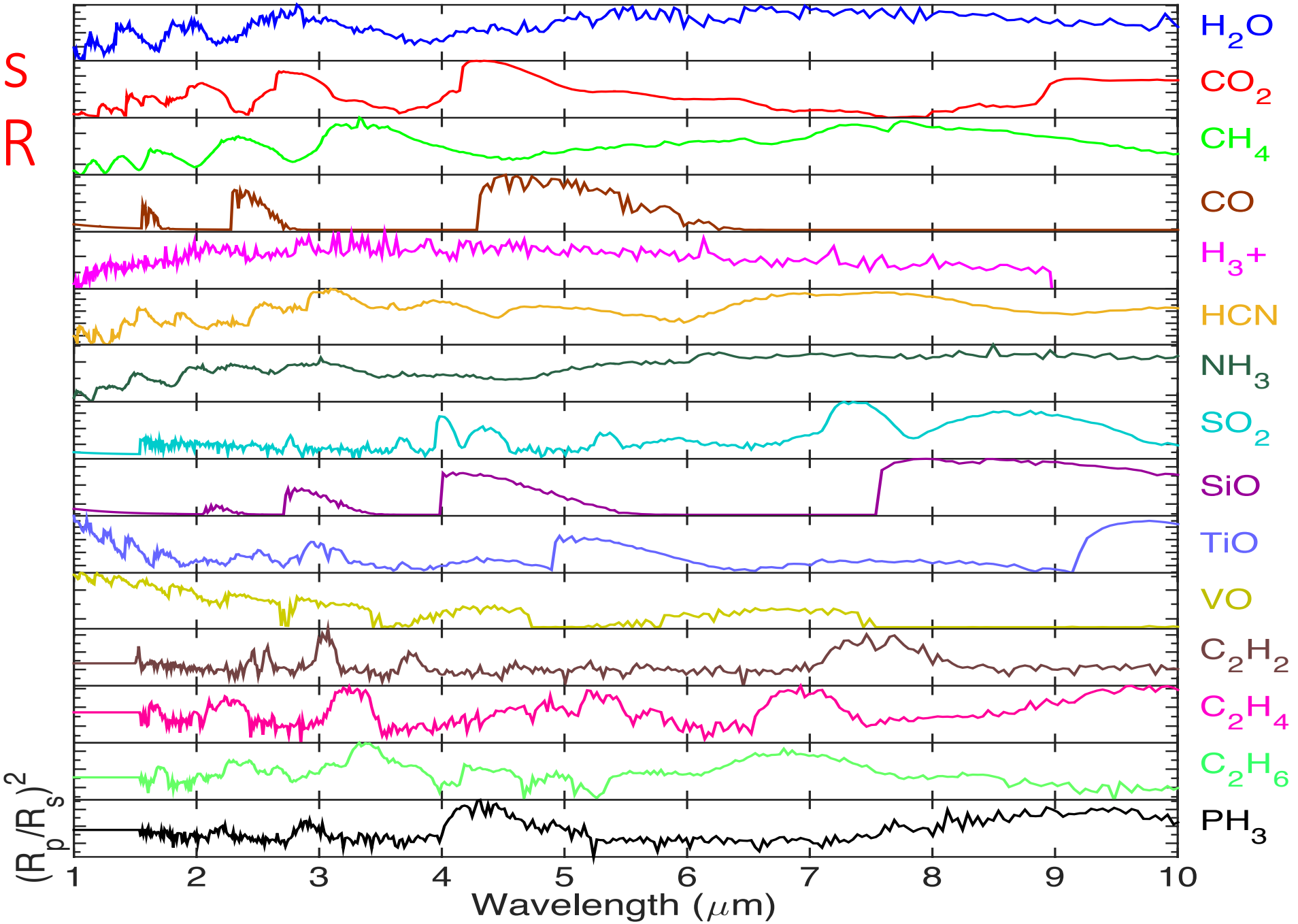

Temperature-Pressure profile in hot Jupiters

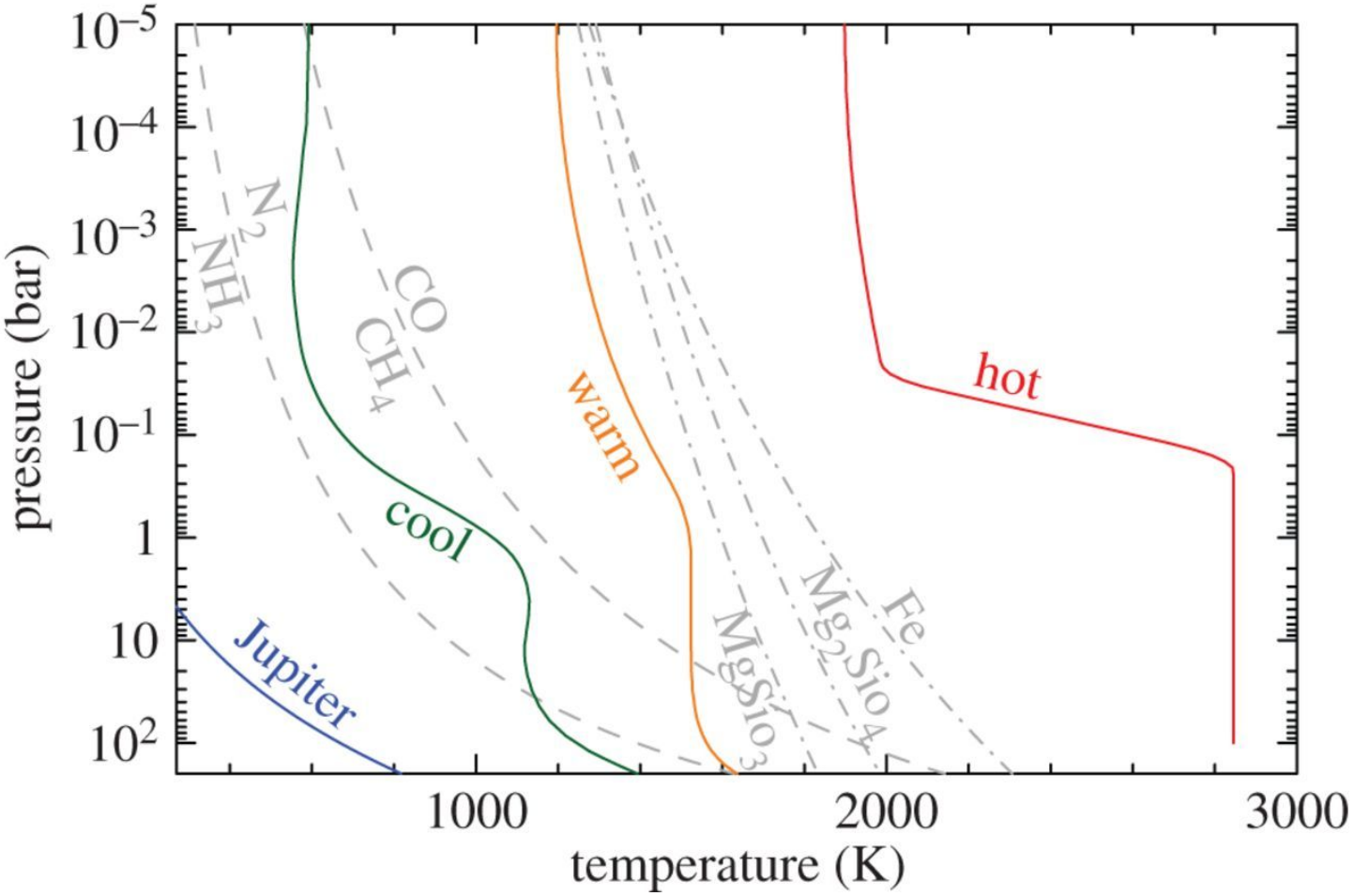

Thermal profiles for the hypothetical ‘hot’, ‘warm’ and ‘cool’ exoplanets (as labelled) used in the chemical models shown in figure. The grey dashed lines represent the equal-abundance curves for CH4–CO and NH3–N2. Profiles to the right of these curves are within the N2 and/or CO stability fields. The dot-dashed lines show the condensation curves for MgSiO3, Mg2SiO4 and Fe (solid, liquid). Moses 2014

Temperature matters !

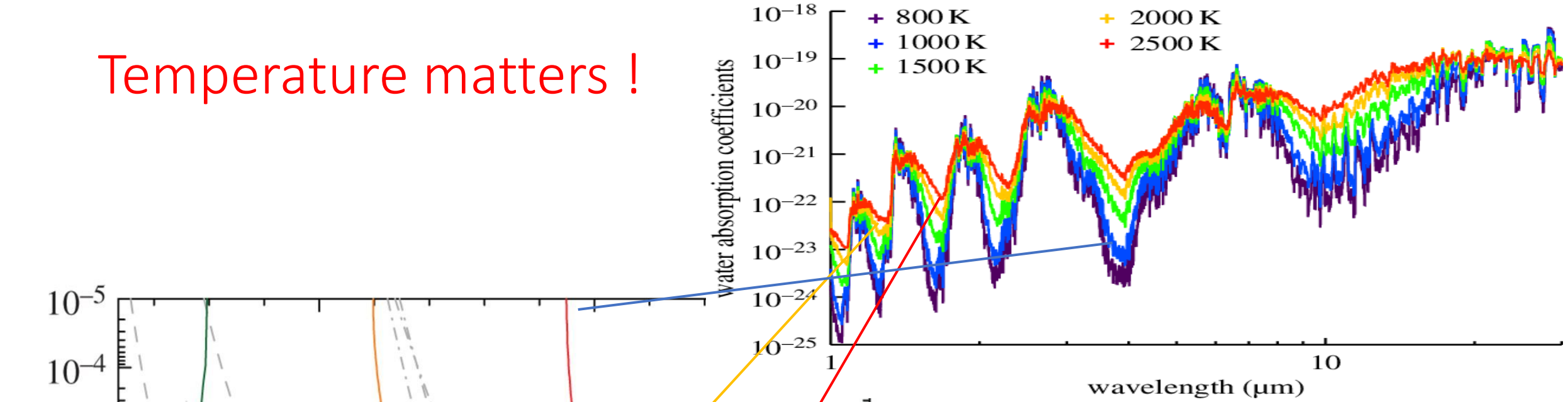

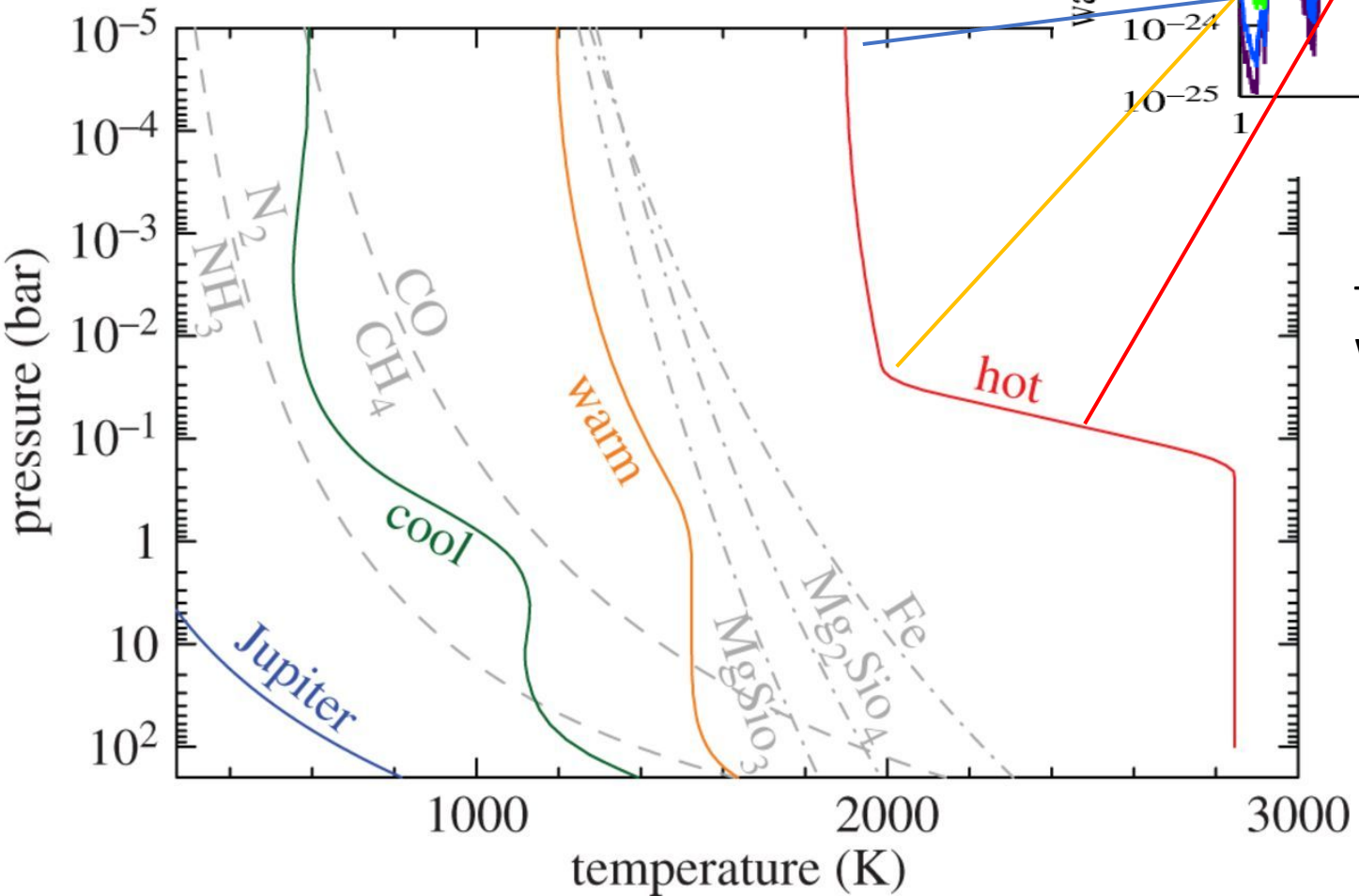

Temperature varies in the atmosphere
Water absorption depends on temperature too !

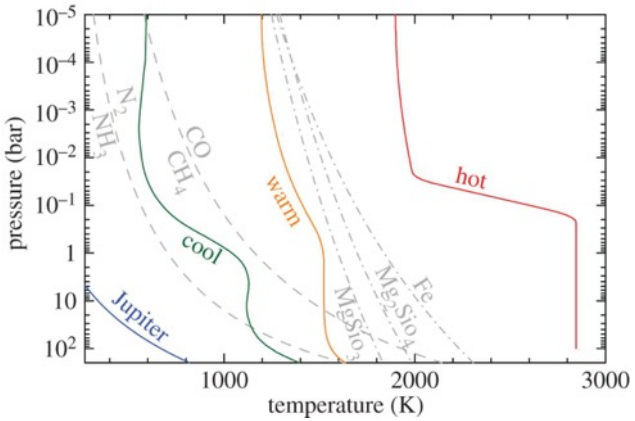

Temperature-pressure Profile

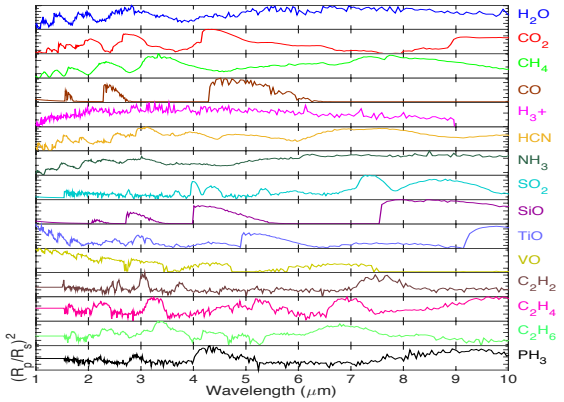

Molecules lines list

Chemistry in equilibrium

Which molecules are expected to be abundant ?

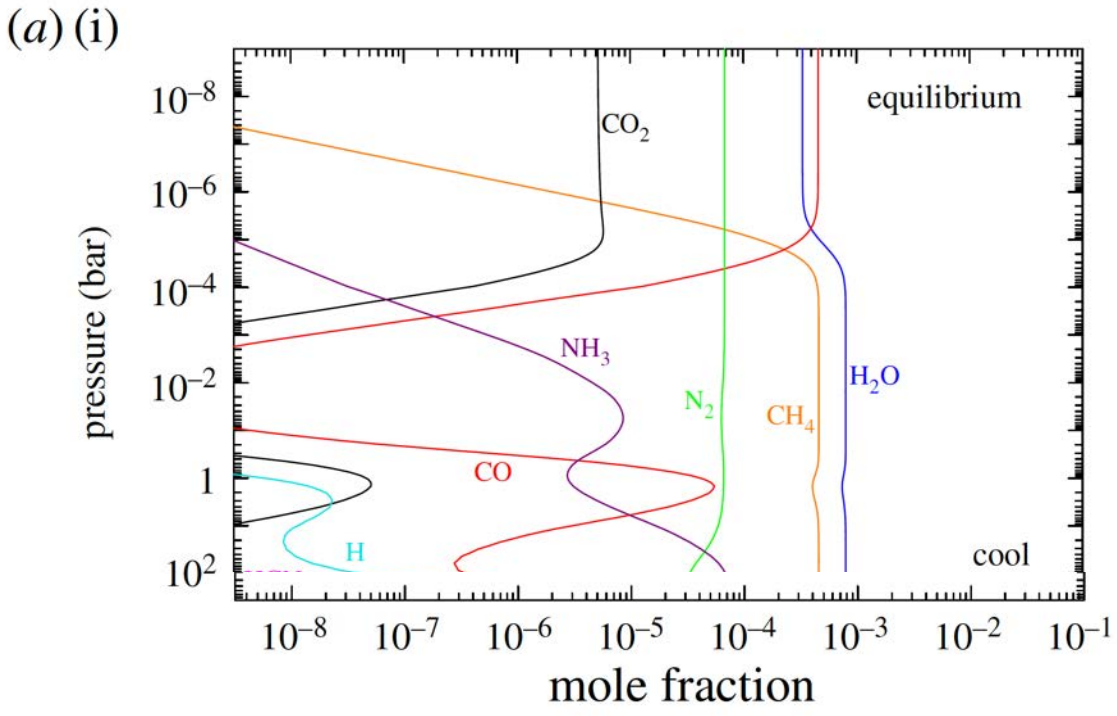

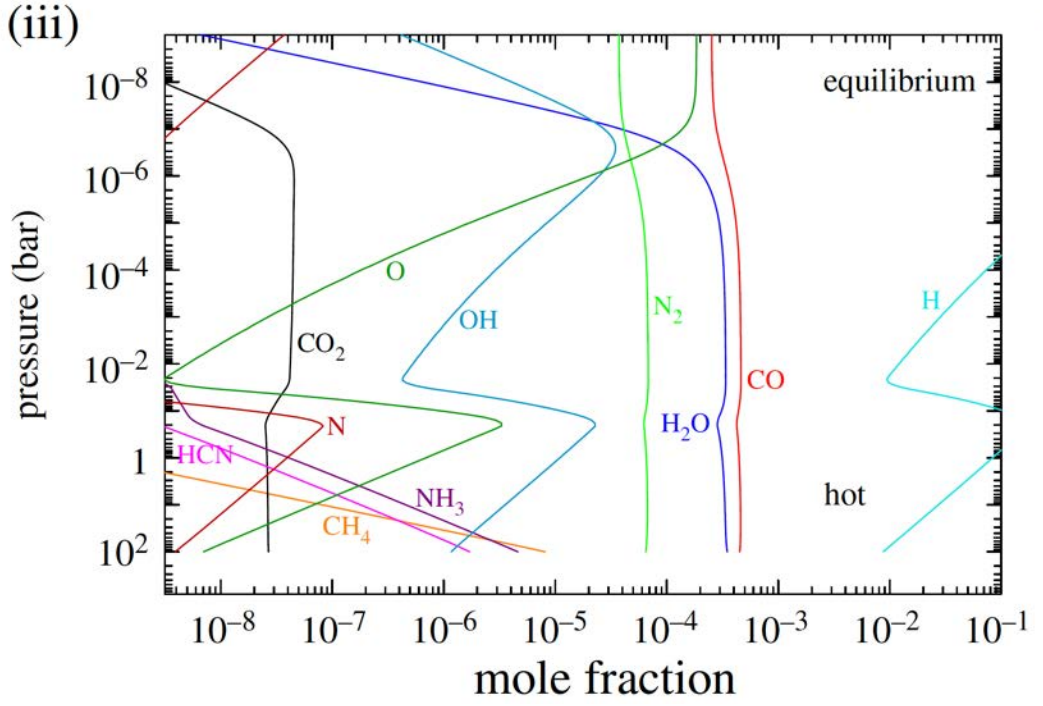

Spectral signature of a transiting planet

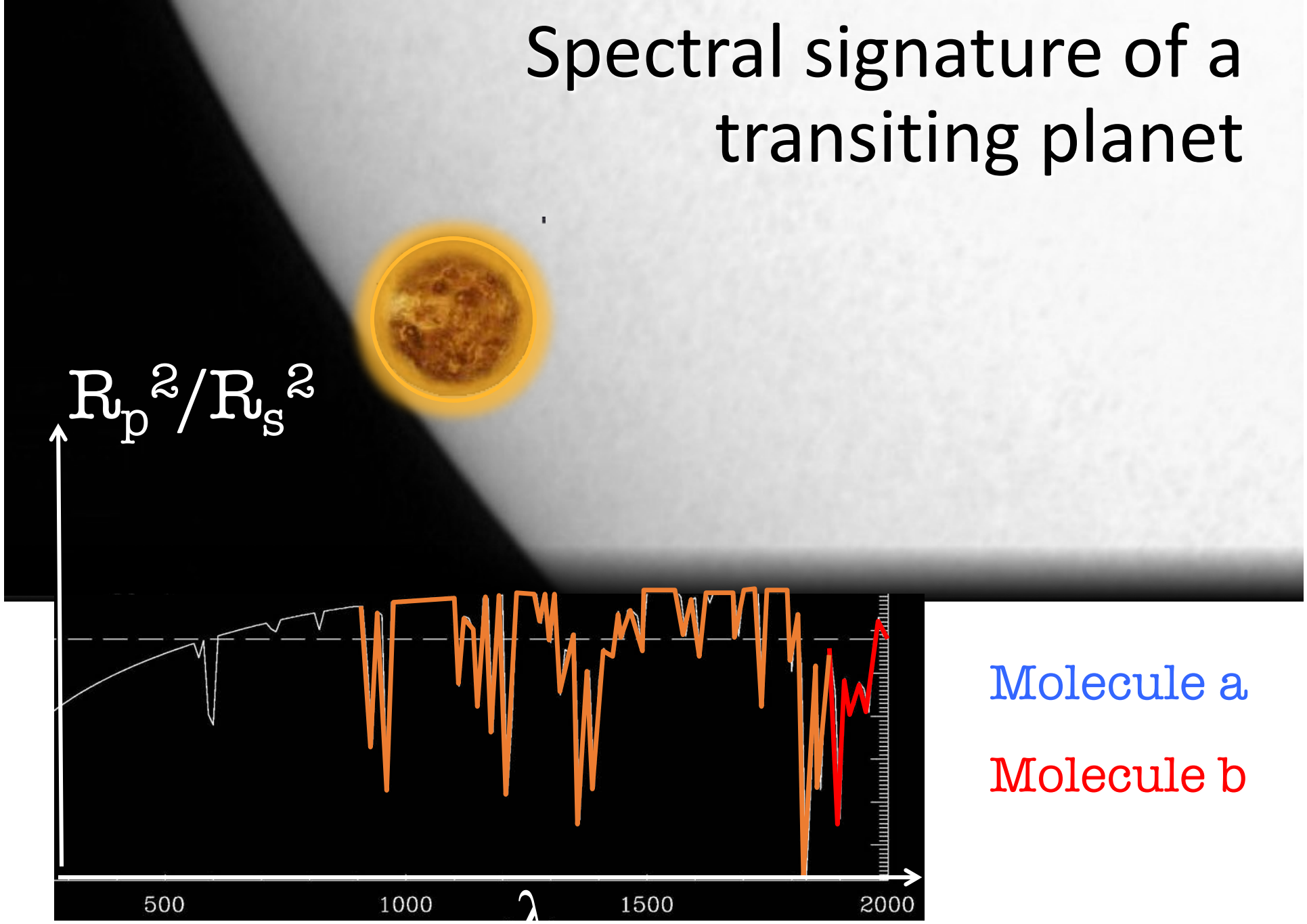

Phase curves
u Andromeda

Harrington et al. 2006

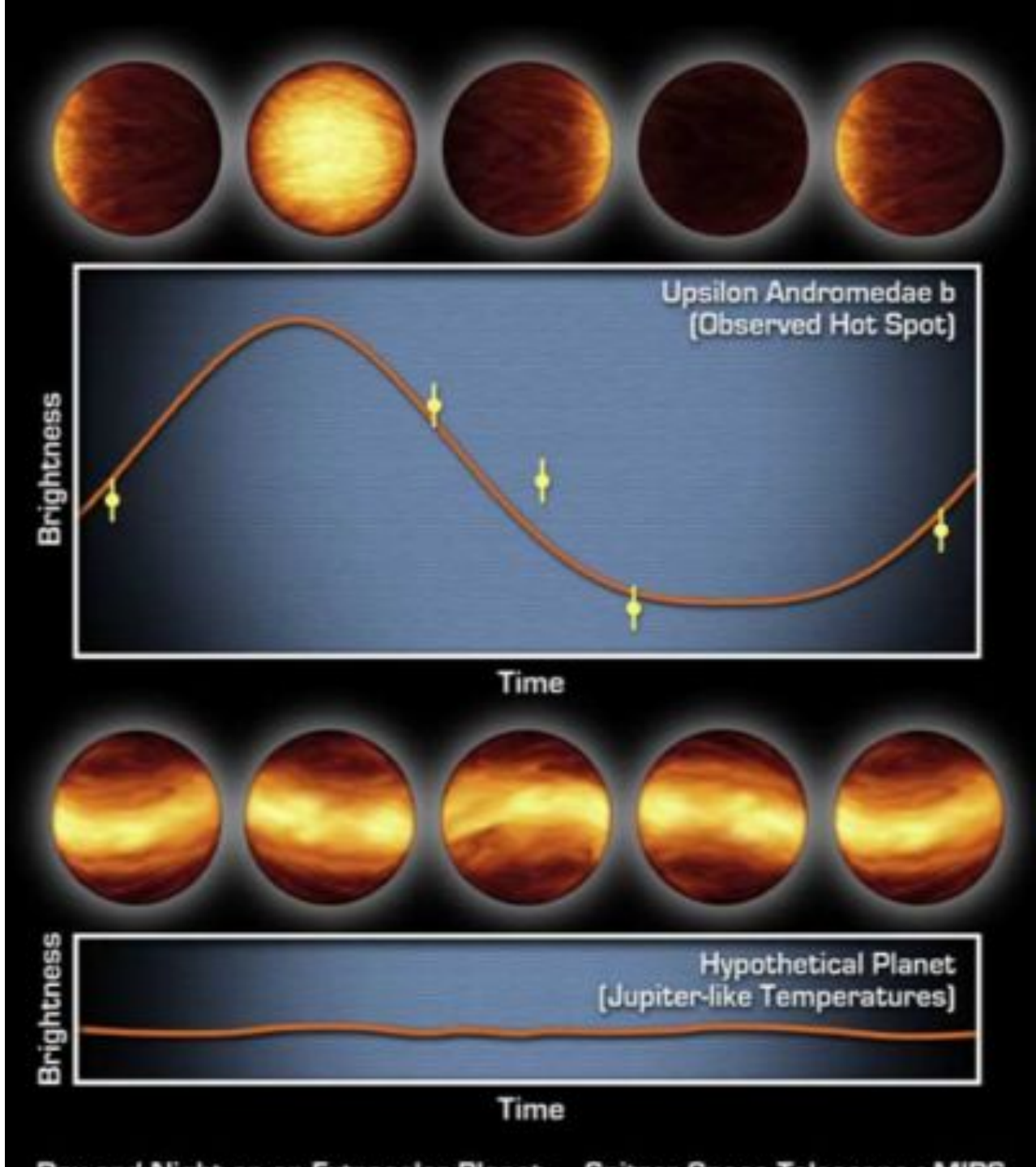

Day/Night phase curves, COROT-2b, HD190733b

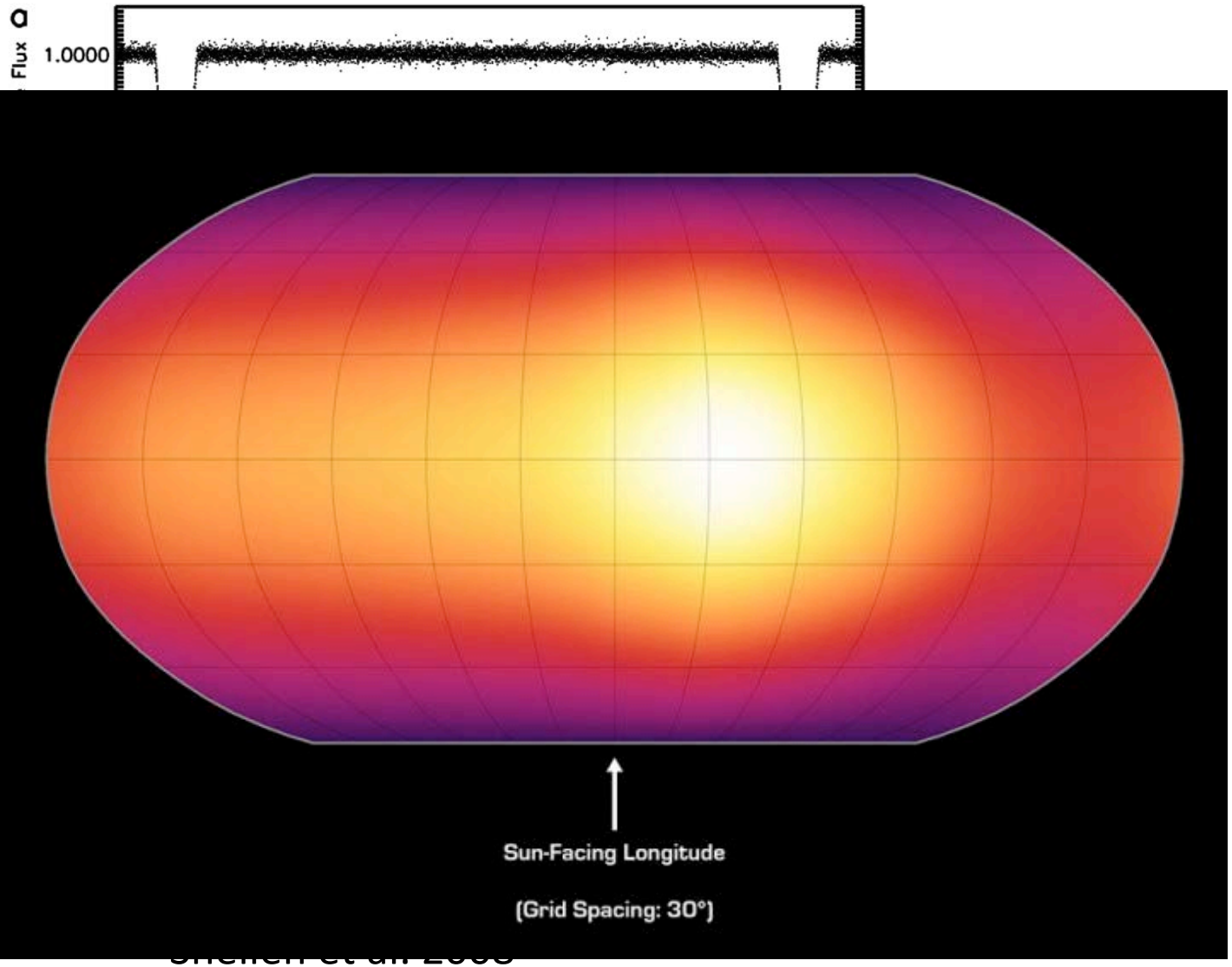

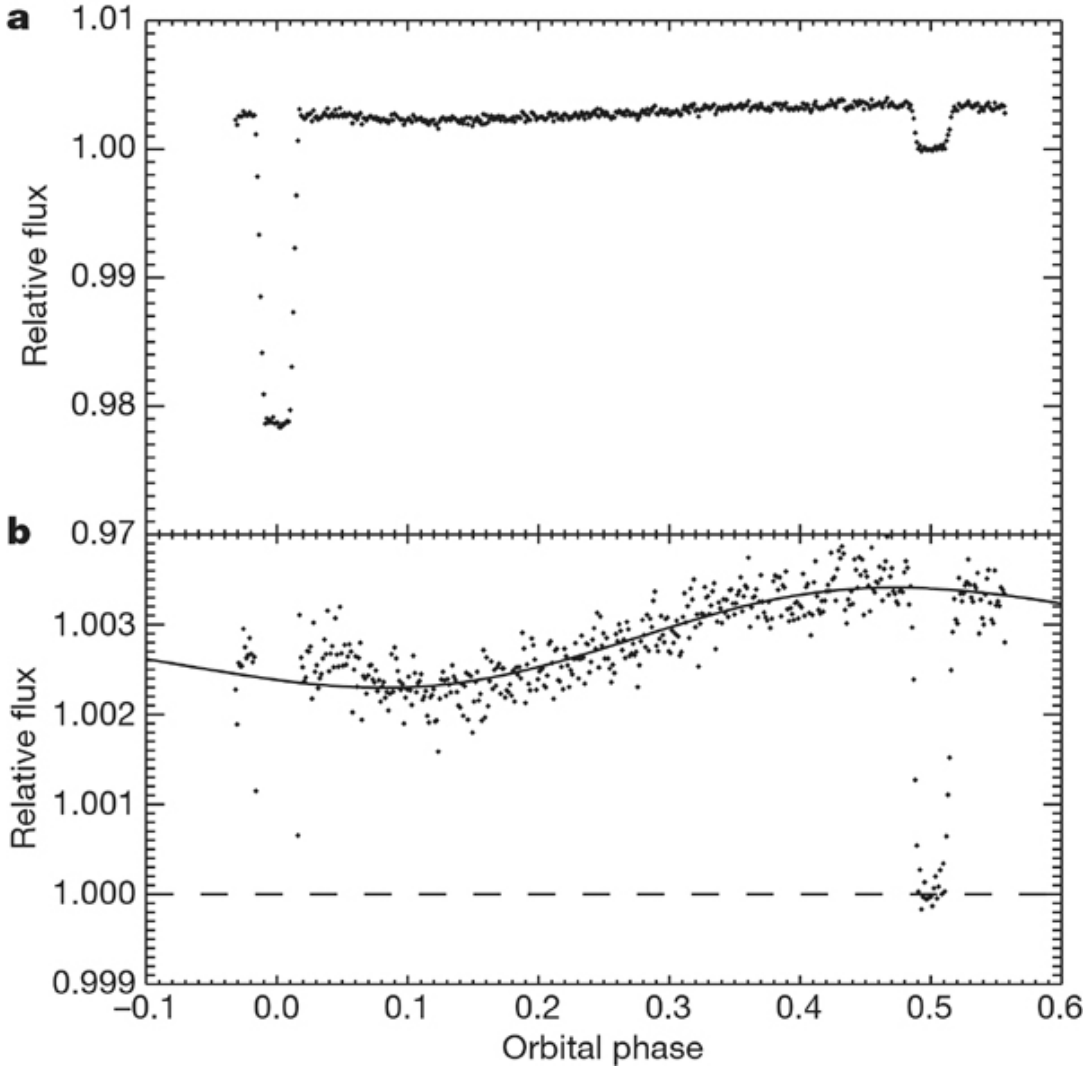

Knutson et al. 2007

Water vapor in the hot Jupiter HD189733b

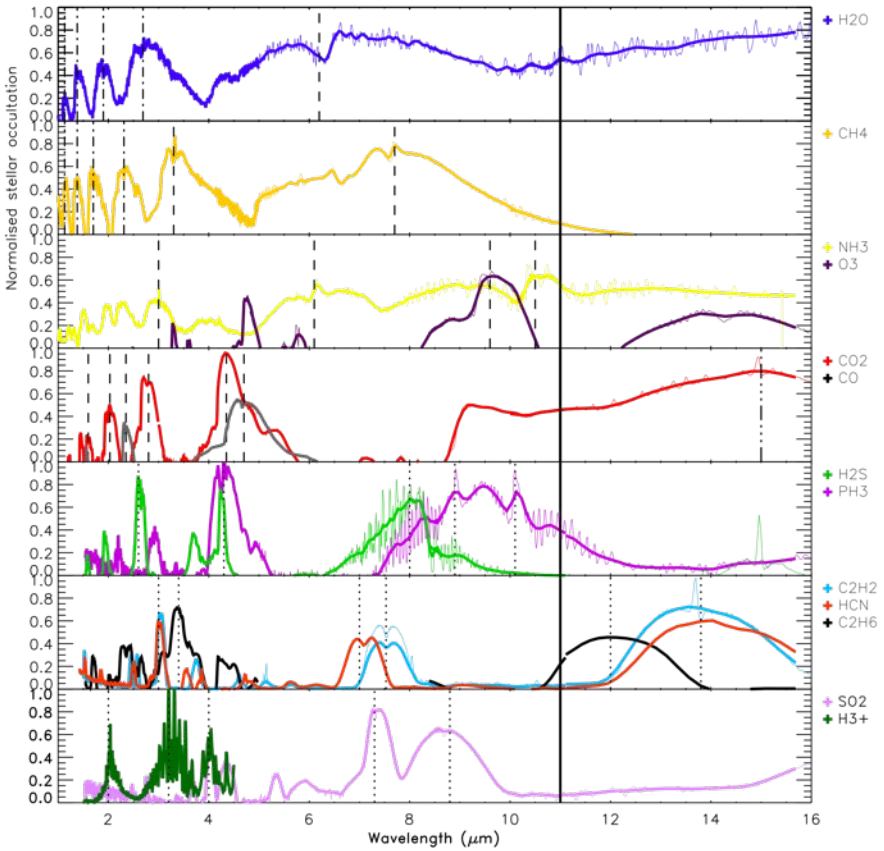

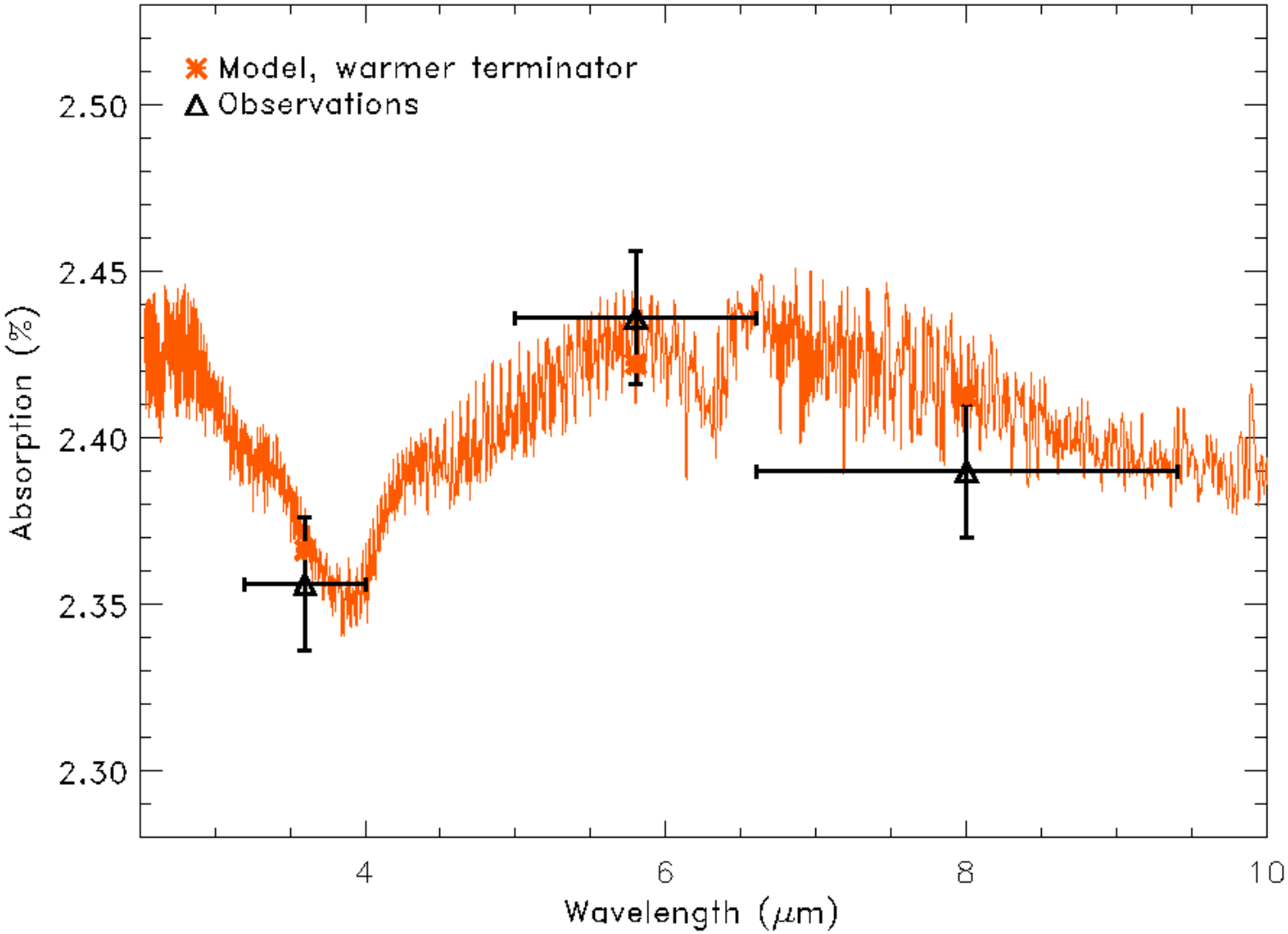

Tinetti *et al.*, Nature, 2007; Beaulieu et al. 2008

HD189733b, Water + Methane

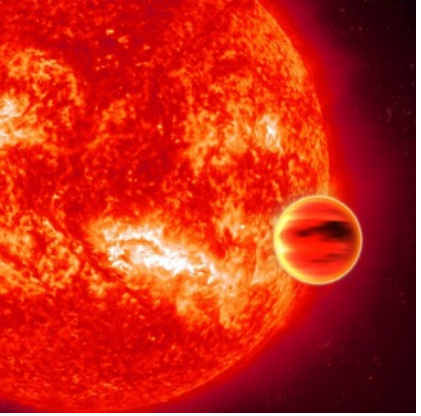

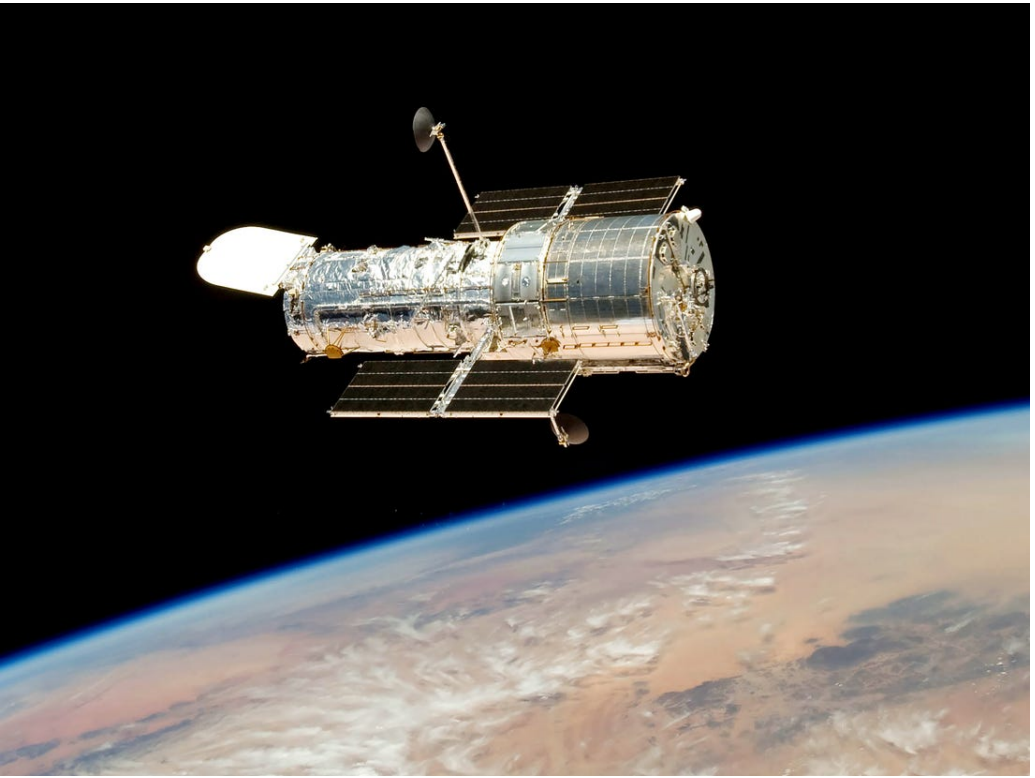

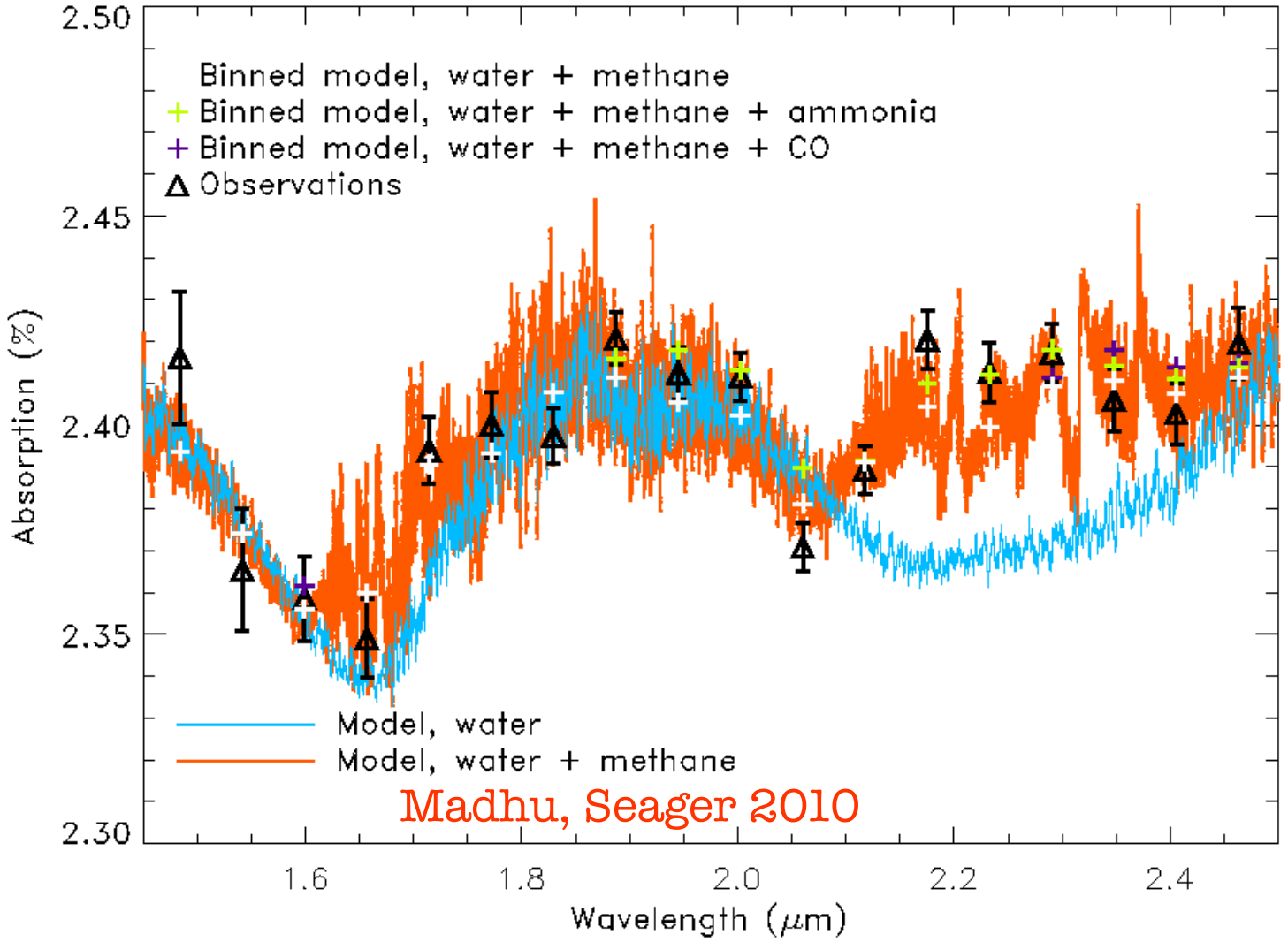

Madhu, Seager 2010

Swain, Vasisht, Tinetti, *Nature,* 2008

HD189733b, Water + Methane

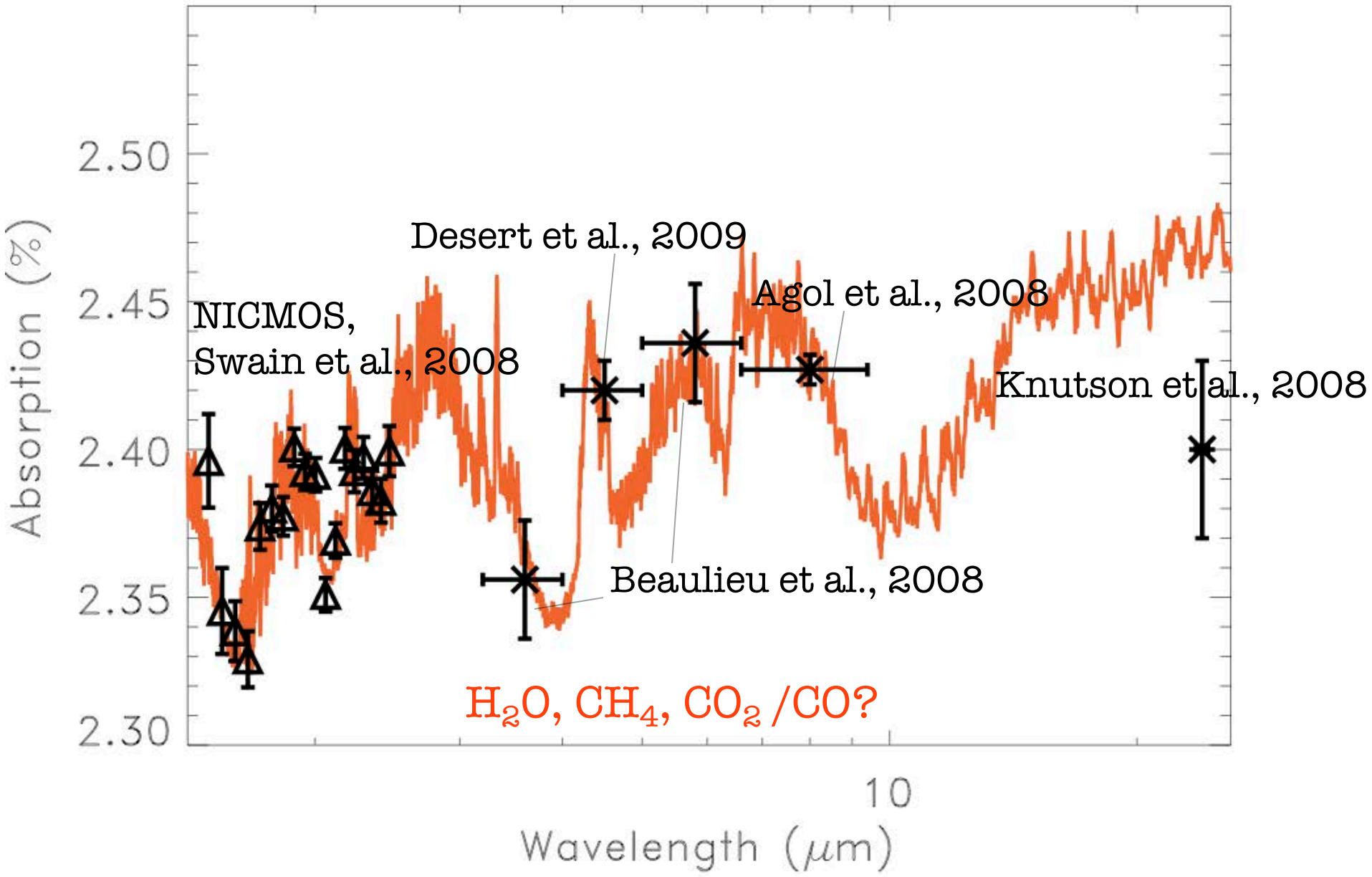

Water, CO on HD 189733b occultation obs: Spitzer

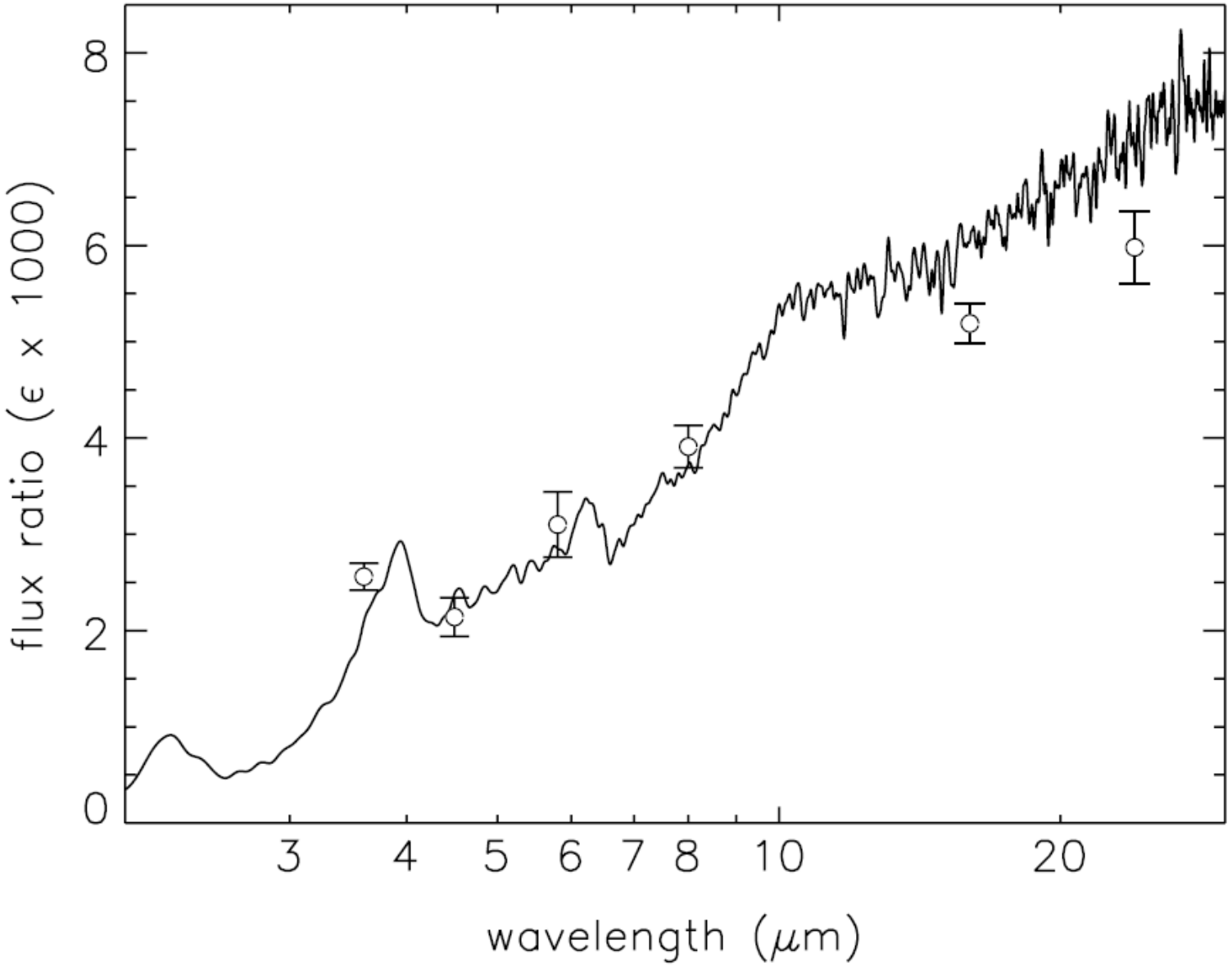

Charbonneau et al., *ApJ*, 2008; Barman, *ApJL*, 2008

HD209458b

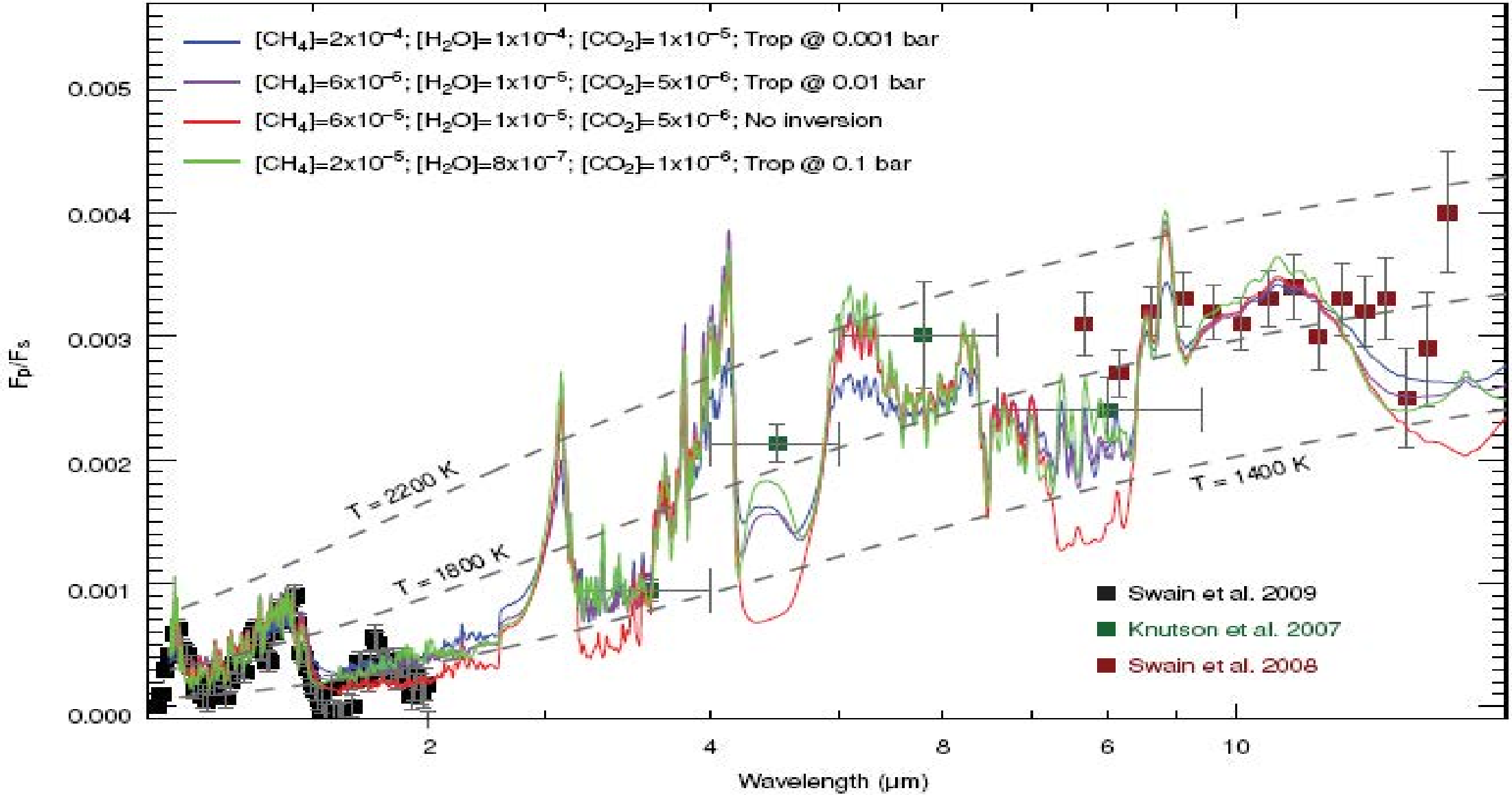
[CH4]=2x10−4; [H2O]=1x10−4; [CO2]=1x10−5; Trop @ 0.001 bar
[CH4]=6x10−5; [H2O]=1x10−5; [CO2]=5x10−6; Trop @ 0.01 bar
[CH4]=6x10−5; [H2O]=1x10−5; [CO2]=5x10−6; No inversion
[CH4]=2x10−5; [H2O]=8x10−7; [CO2]=1x10−6; Trop @ 0.1 bar
Fp/Fs
0.005
0.004
0.003
0.002
0.001
0.000
T = 2200 K
T = 1800 K
T = 1400 K
Swain et al. 2009
Knutson et al. 2007
Swain et al. 2008
2
4
8
6
10
Wavelength (μm)

GJ1214, super Earth ? Mini Neptunes ? With HST clouds are currently hid
Need to go further to the IR

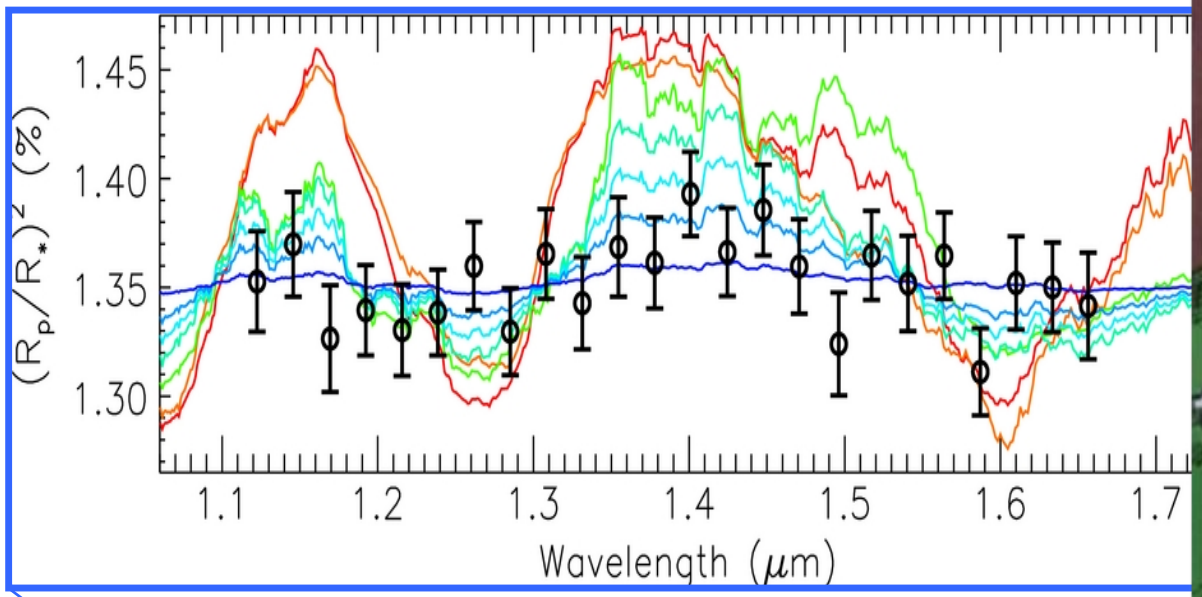

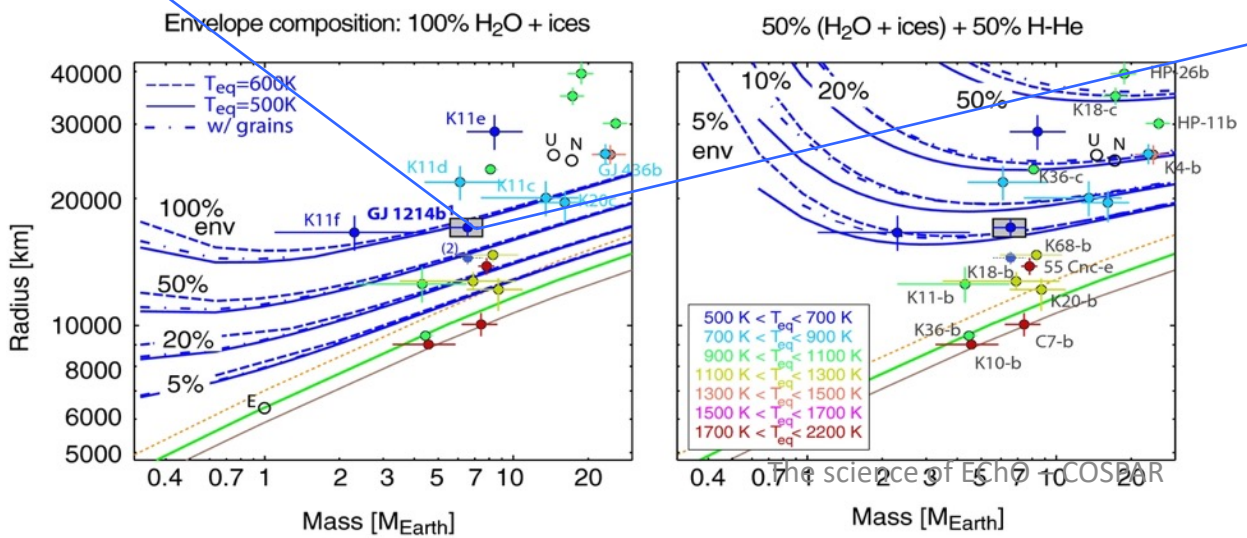

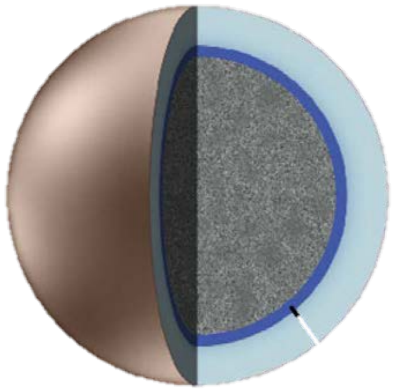

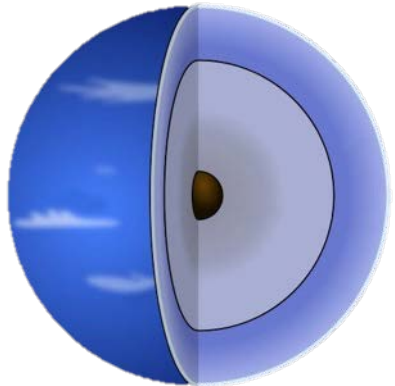

Analysing exoplanet data, Chef's cooking recipie

HST Archives

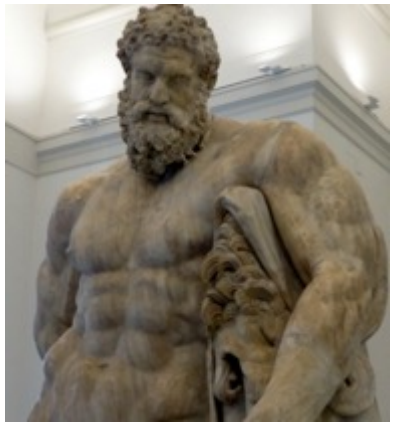

IRACLIS code

Tsiaras et al.

TauREX code

Waldmann, Al Refaie Changeat, Edwards, et al

Computing power

Ariel school 2019

In White light

We fit a transit model x systematics model

Models for systematics

$$n_w^{scan} = (1 - ra_1(t - T0))\ (1 - rb_1 e^{-rb2(t-to)})$$

Linear ramp

Exponential ramp

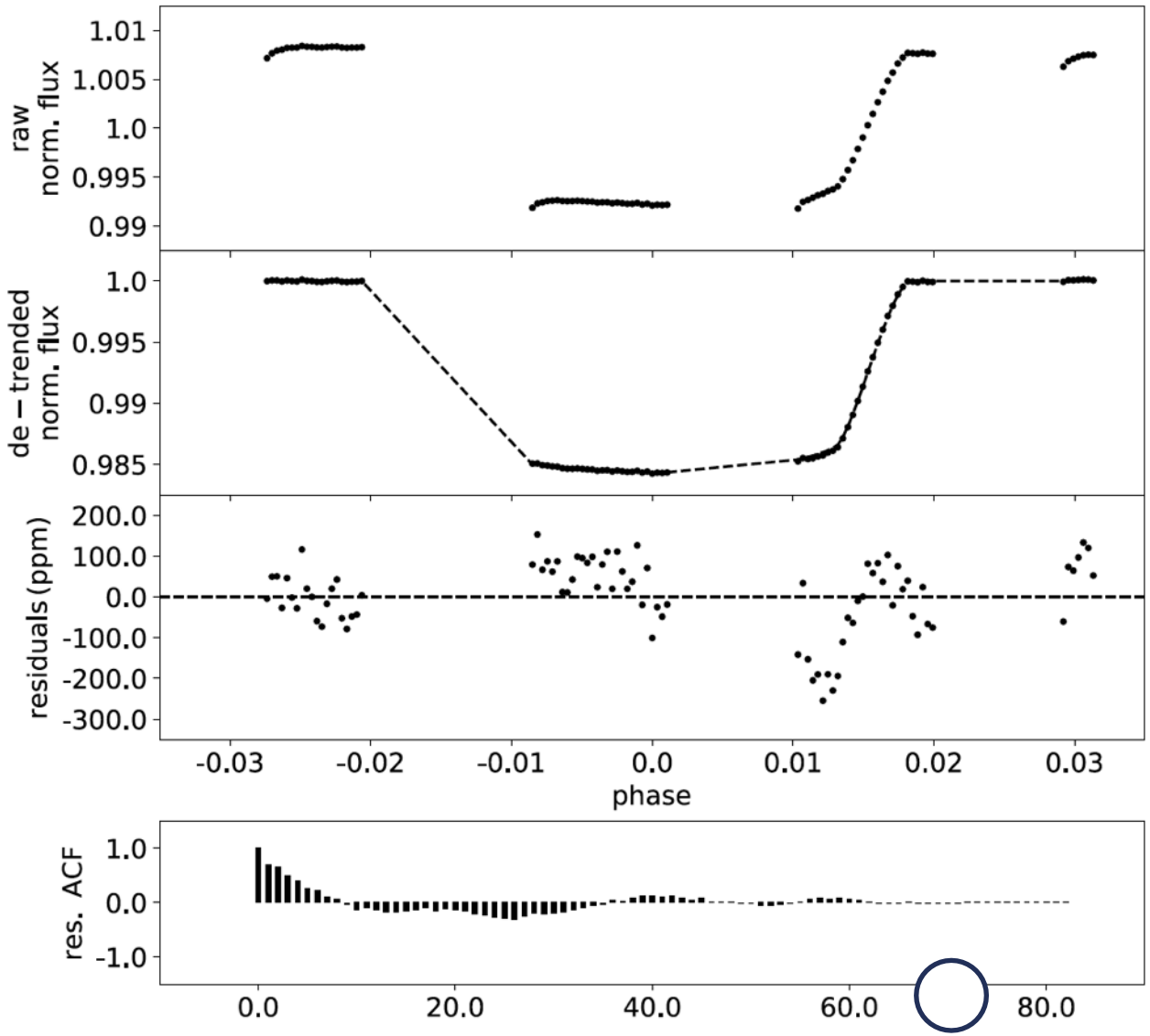

Figure 4.7: Results from the analysis of the white light-curve for the test case of HD 209458 b. Top panel: Normalised raw light-curve. Second panel: Light-curve divided by the best-fit model for the systematics. Third panel: Fitting residuals. Bottom panel: Autocorrelation function of the residuals.

In white light

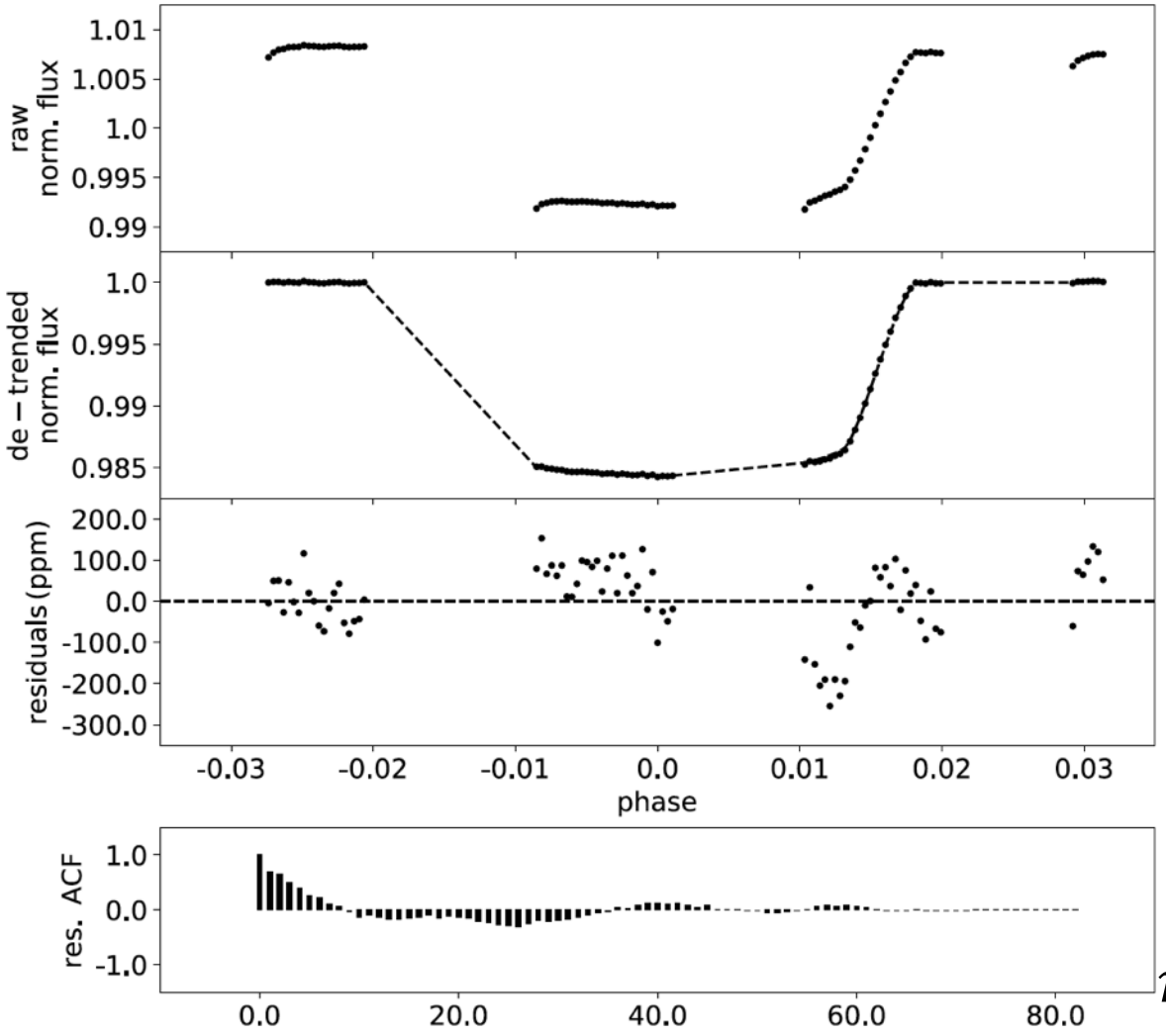

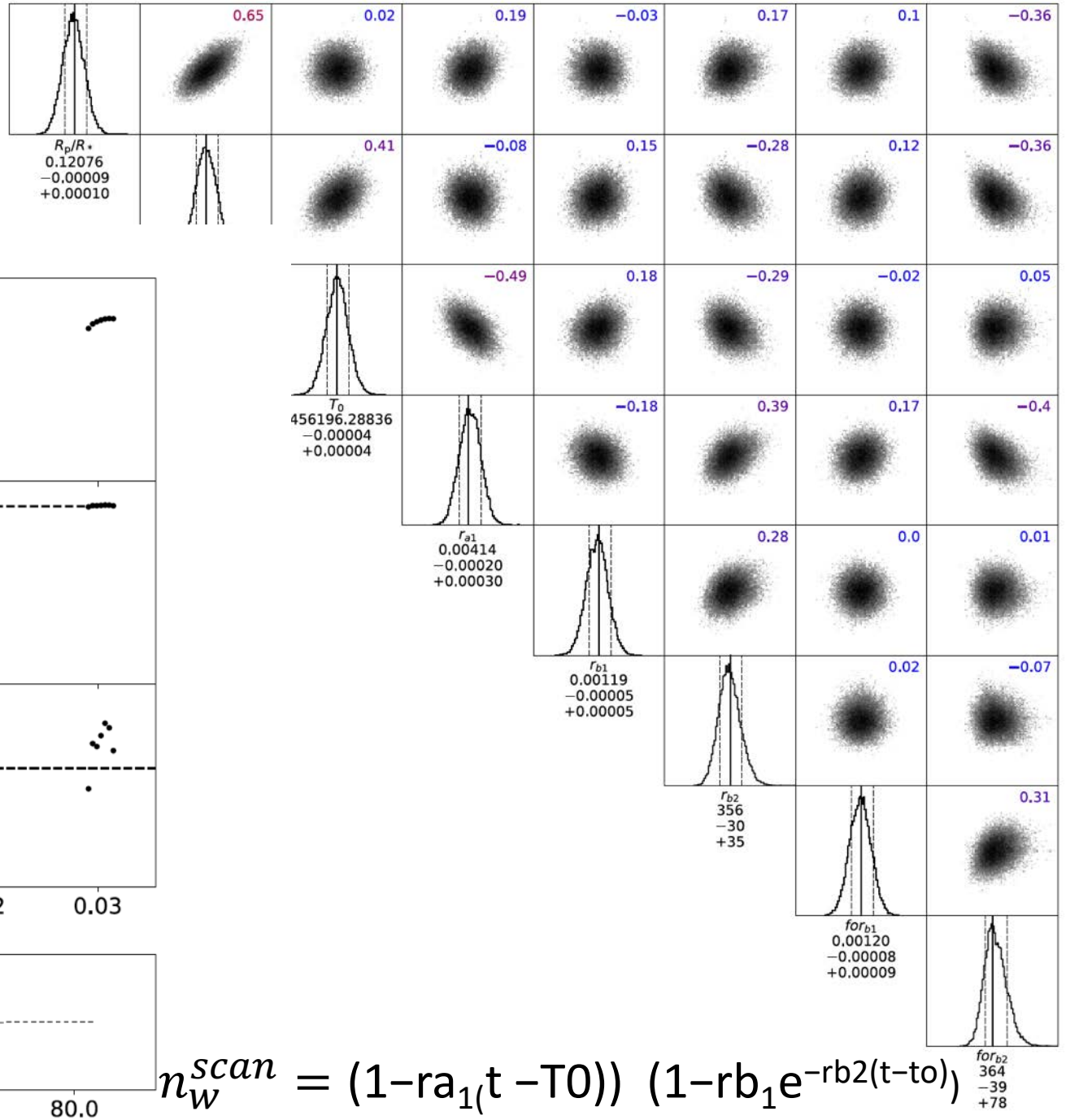

$$n_w^{scan} = (1-ra_1(t-T0))\ (1-rb_1 e^{-rb2(t-to)})$$

White light versus 1.3 microns

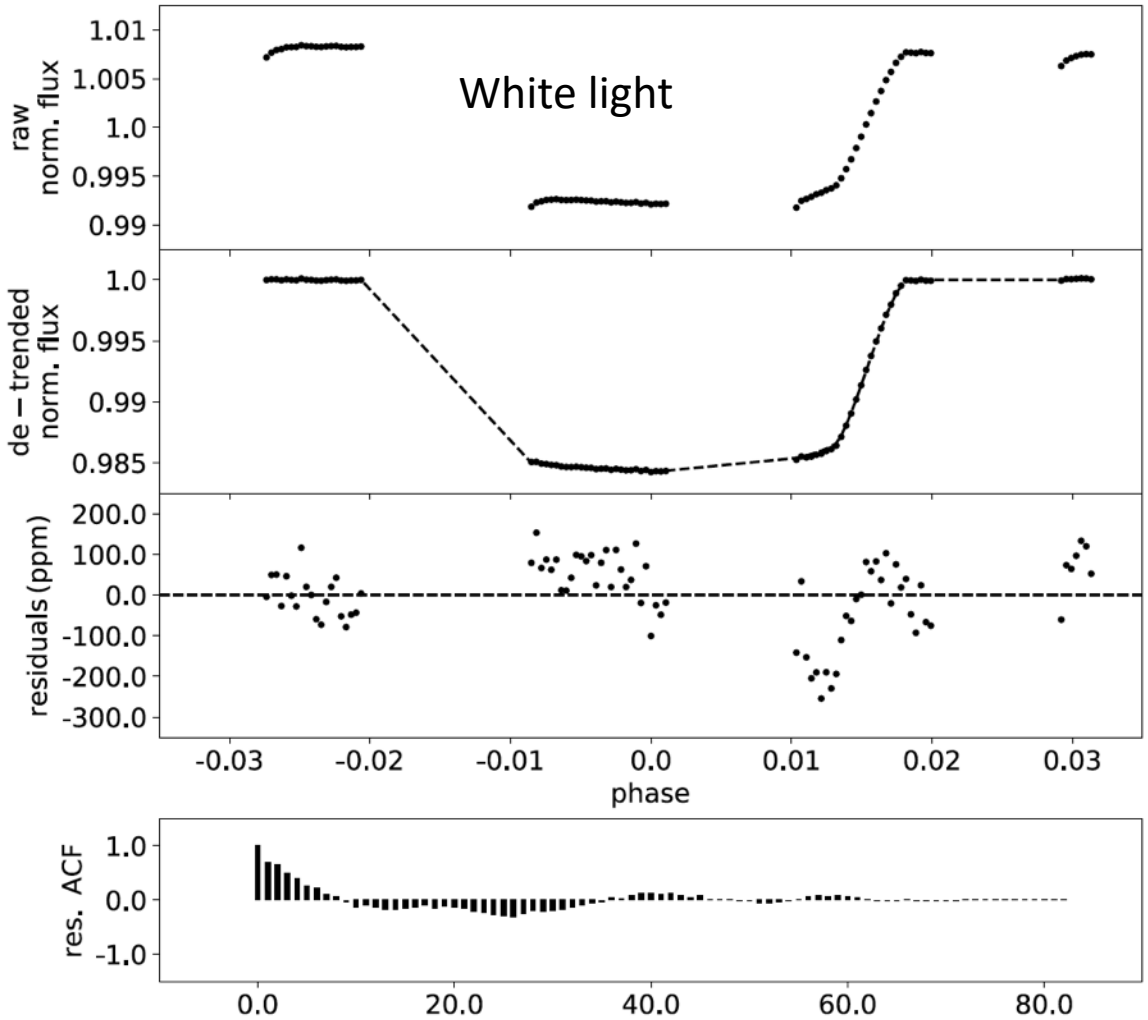

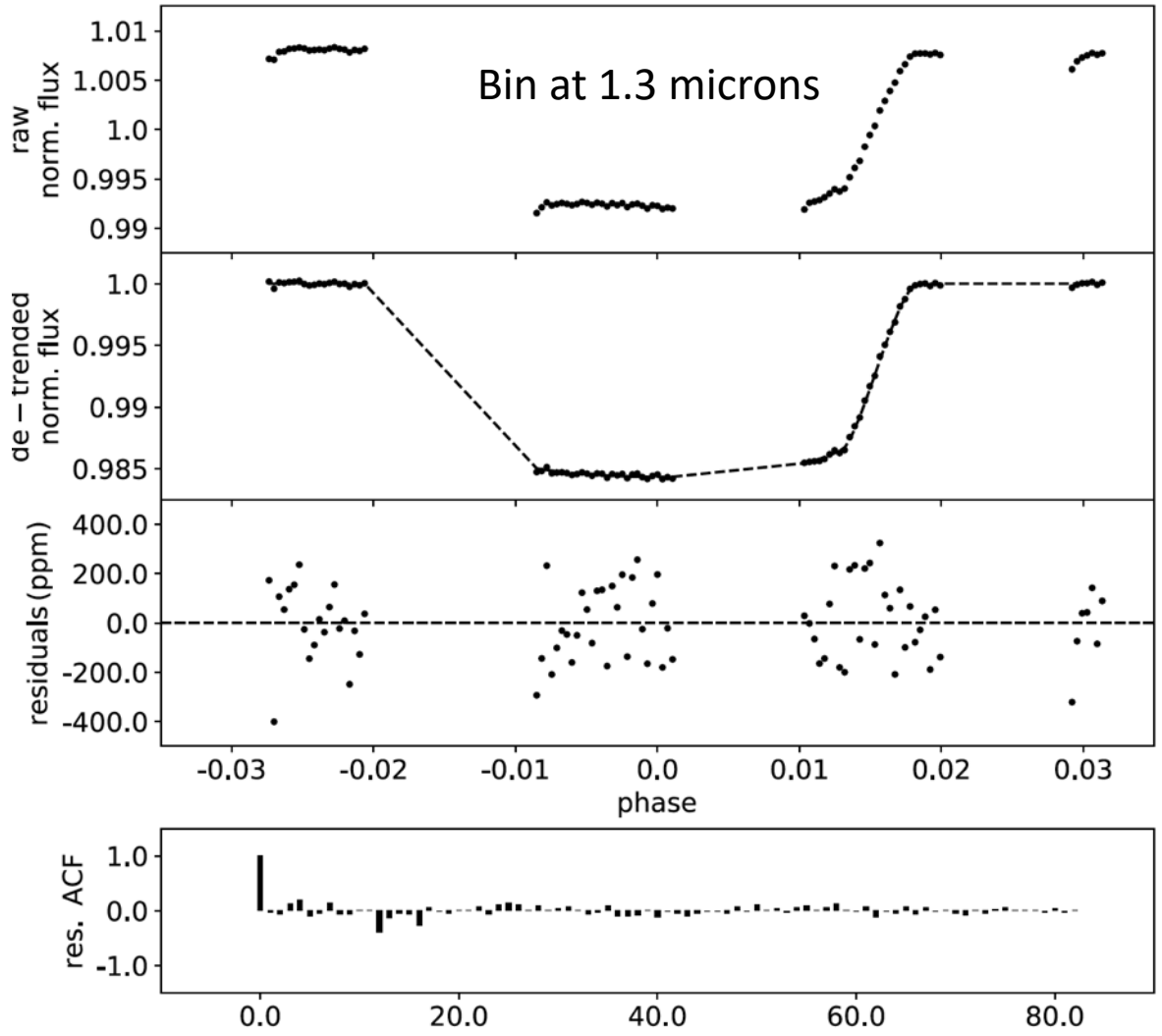

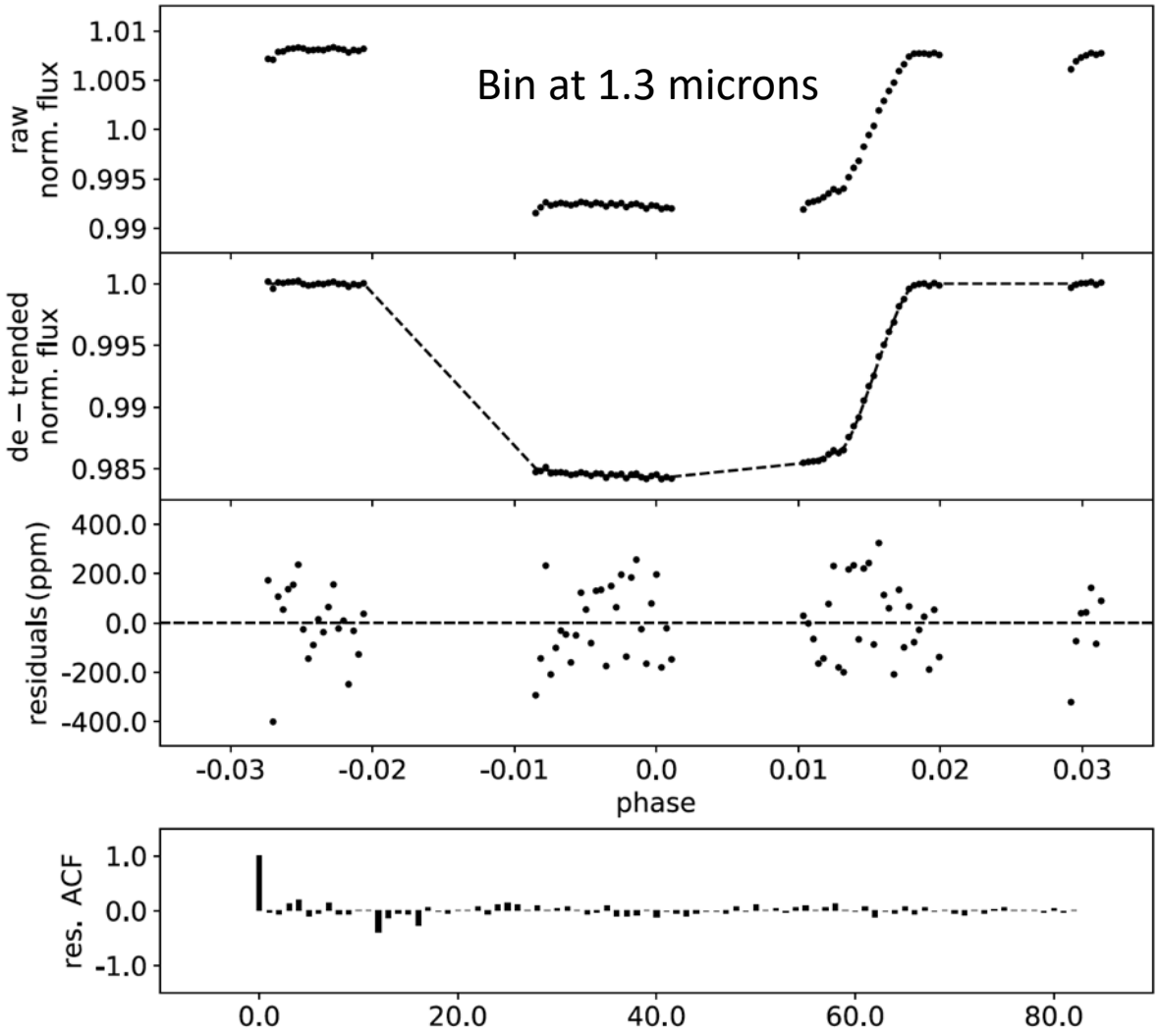

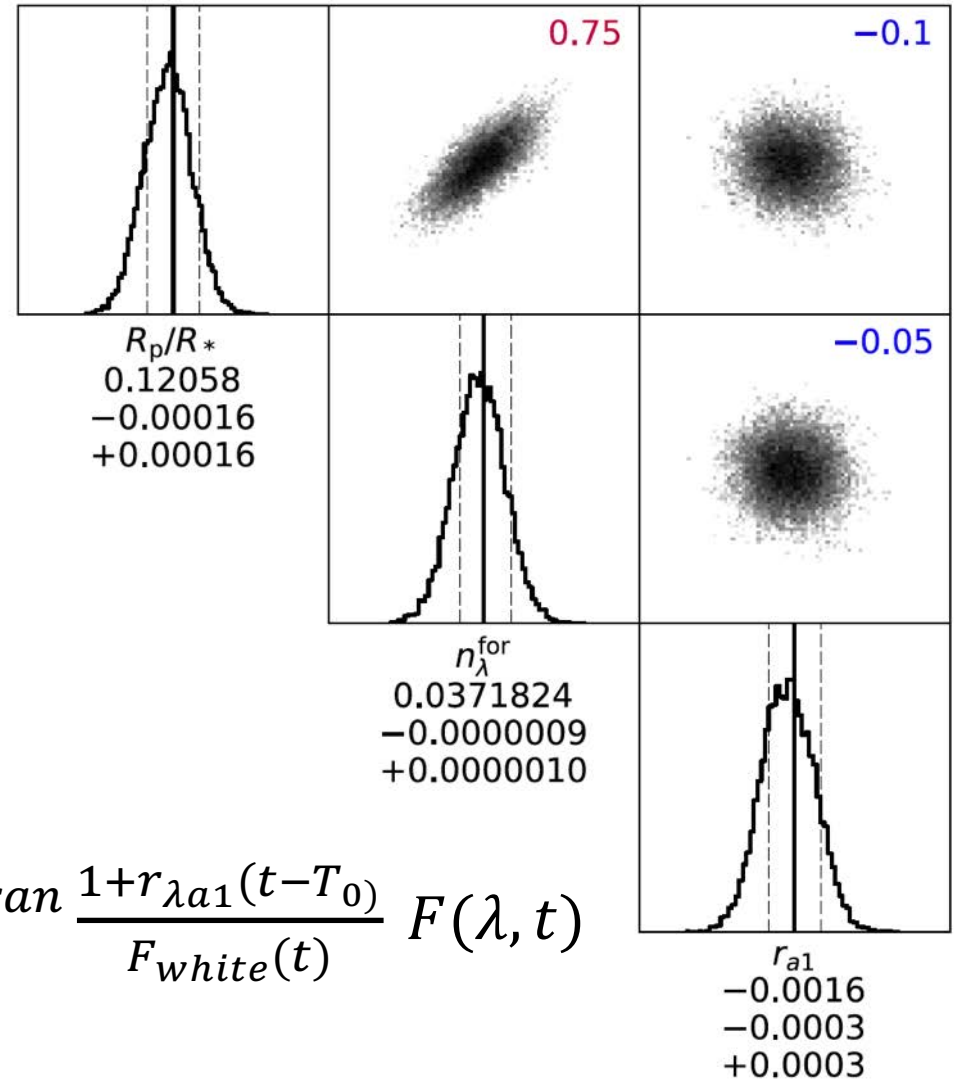

$$n_\lambda^{scan} \frac{1+r_{\lambda a1}(t-T_0)}{F_{white}(t)} F(\lambda,t)$$

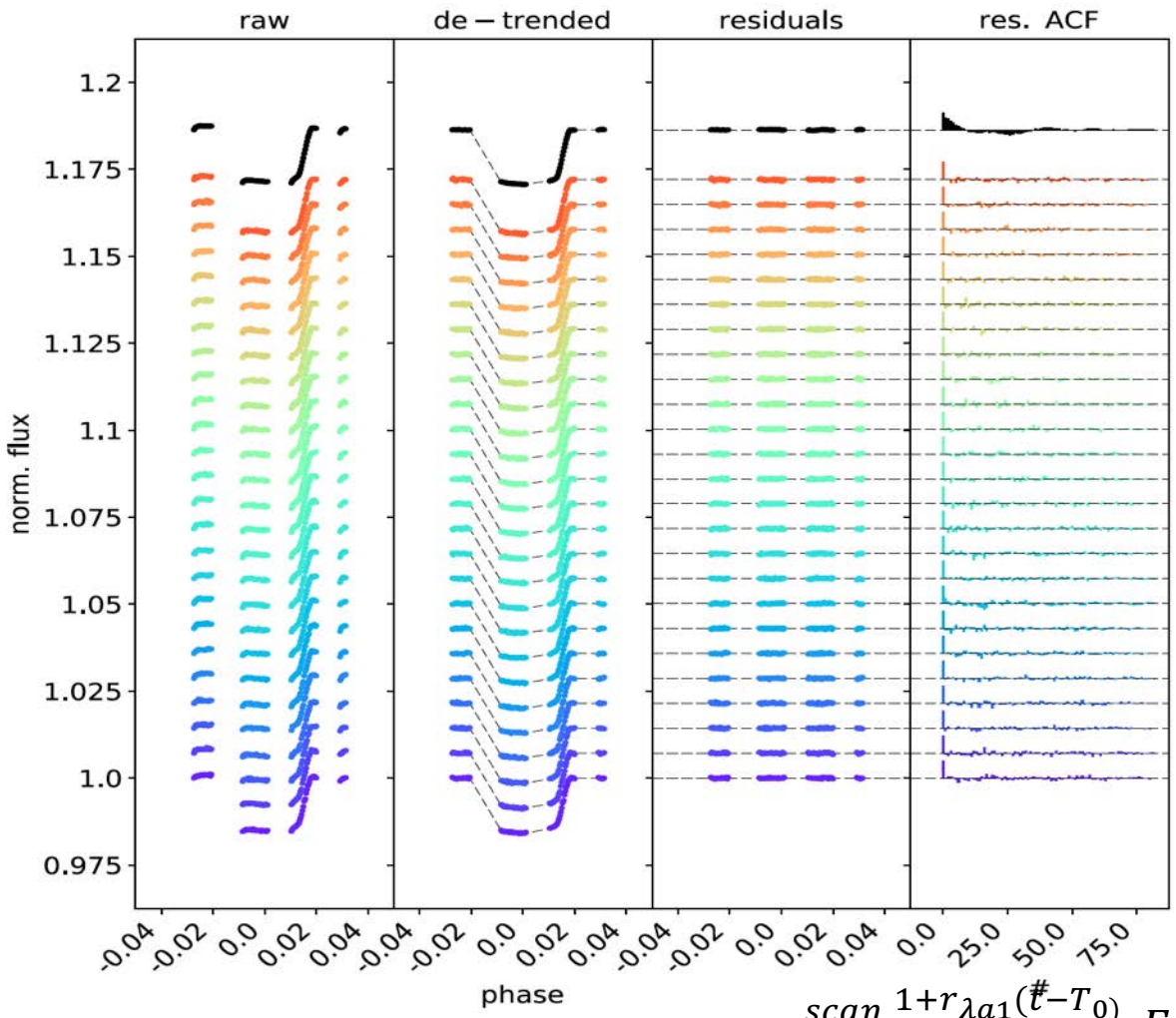

$$n_{\lambda}^{scan}\,\frac{1+r_{\lambda a1}(t-T_0)}{F_{white}(t)}\,F(\lambda,t)$$

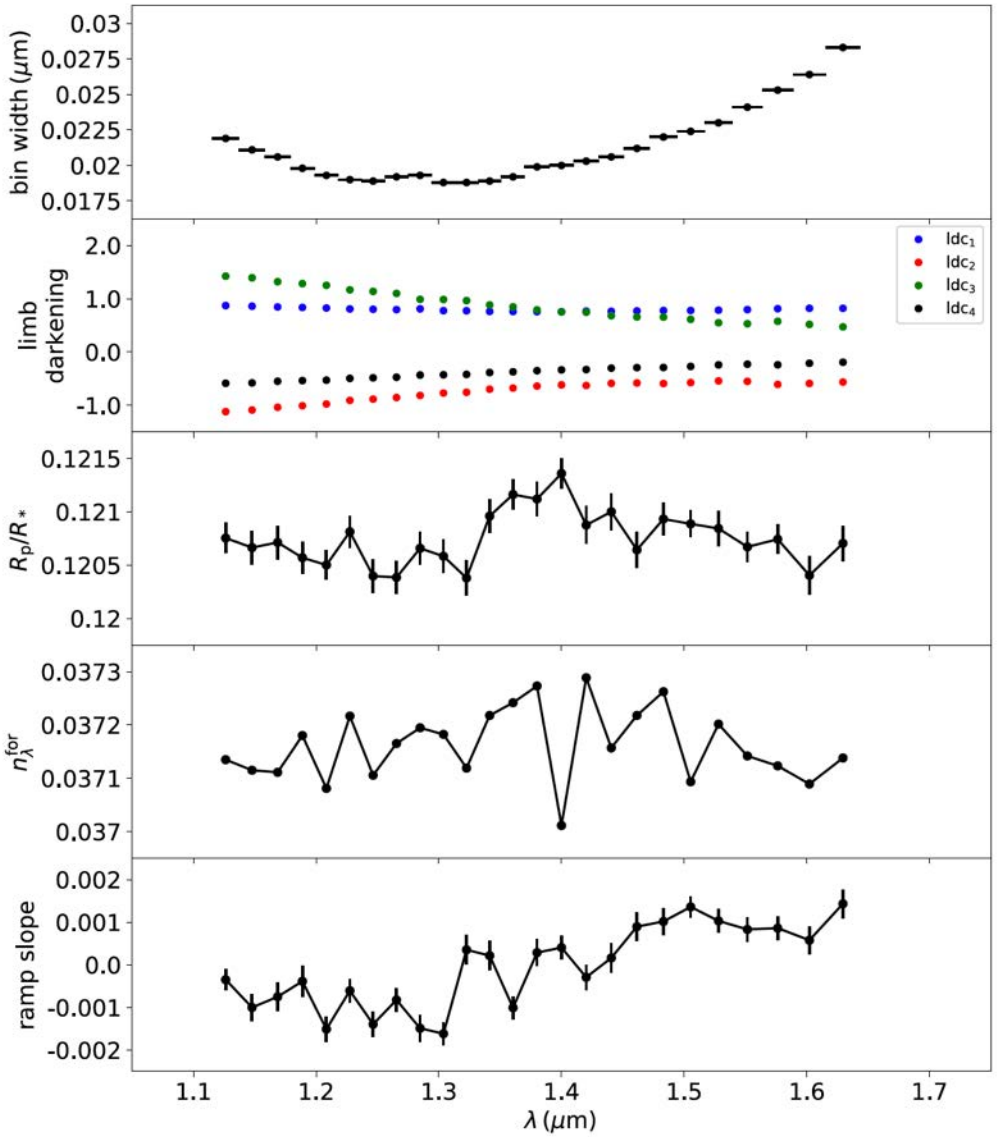

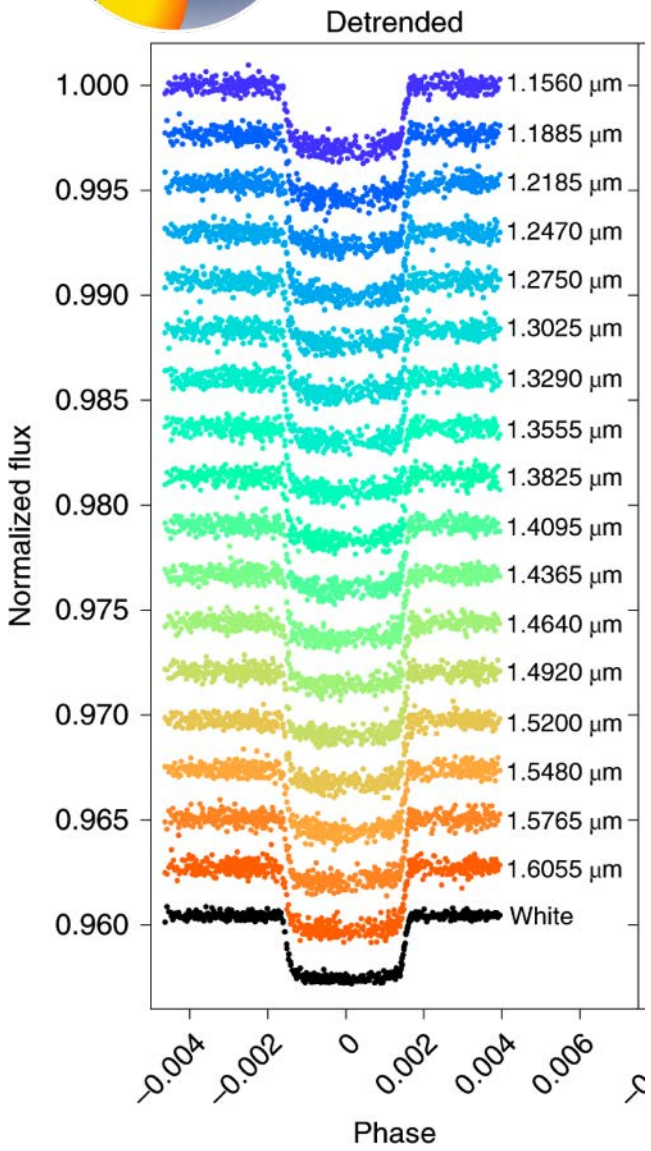

planet WASP-127b, Skaf et al. 2021
Ariel School)

1.1-1.7 microns
H20 dominated spectra

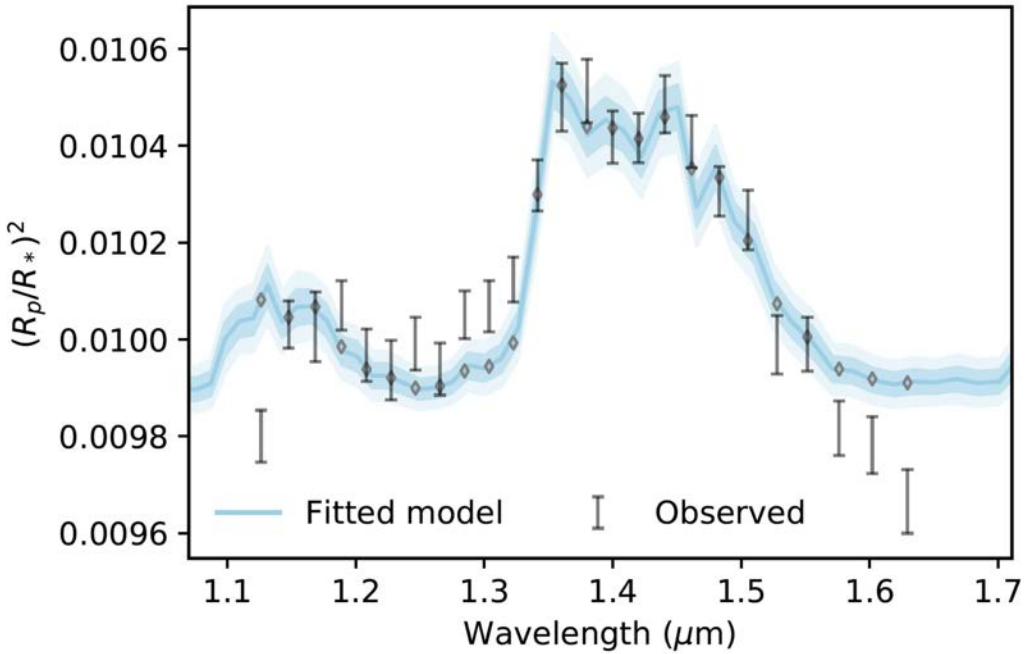

ARES I: CHARACTERISING HOT JUPITERS WASP-127 B, WASP-79 B AND WASP-62 B WITH HUBBLE WFC3 TRANSMISSION SPECTRA*

Nour Skaf,[1,2] Michelle Fabienne Bieger,[3] Billy Edwards,[2] Quentin Changeat,[2] Mario Morvan,[2] Flavien Kiefer,[4] Doriann Blain,[1] Tiziano Zingales,[5] Mathilde Poveda,[6,7] Ahmed Al-Refaie,[2] Robin Baeyens,[8] Amélie Gressier,[4,1,9] Gloria Giulluy,[10,11] Adam Yassin Jaziri,[5] Darius Modirrousta-Galian,[11] Lorenzo Mugnai,[12] William Pluriel,[5] Niall Whiteford,[13] Sam Wright,[2] Benjamin Charnay,[1] Angelos Tsiaras,[2] Ingo Waldmann,[2] and Jean-Philippe Beaulieu[14,4]

Table 1. Target Parameters

Parameter	WASP-127b	WASP-79b	WASP-62b
Stellar parameters			
Spectral type	G5	F5	F7
$T_{\rm eff}$ (K)	5750	6600	6230
$\log g$ (cgs)	3.9	4.06	4.45
[Fe/H]	-0.18	0.03	0.04
Planetary parameters			
P (d)	4.17807015	3.662387	4.411953
$T_{\rm mid}$ (BJD−2450000)	8138.670144	7815.89868	5855.39195
I_c (°)	87.88	83.3	88.3
$M_{\rm P}(M_J)$	0.18	0.9	0.57
$R_{\rm P}(R_J)$	1.37	2.09	1.39
$T_{\rm eq,A=0}$	1400	1900	1440
Derived parameters used for the Iraclis runs			
$R_{\rm P}/R_*$	0.09992	0.112606	0.1091
$a_{\rm pl}/R_*$	7.846	6.069	9.5253

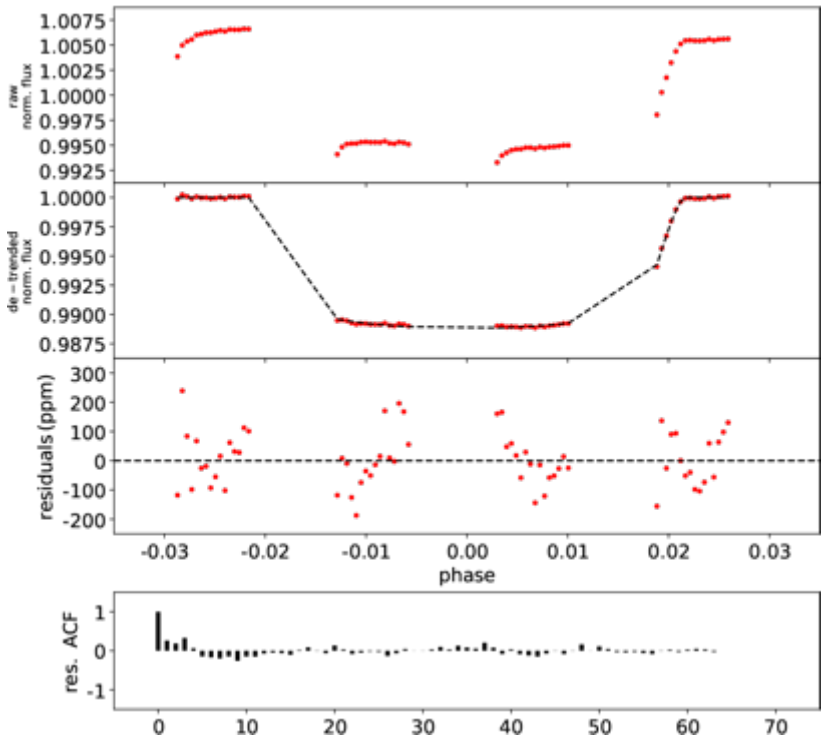

Skaf et al.

Table 4. Comparison of the Bayesian log evidence for different models. For WASP-79b and WASP-62b, the retrieved temperature is always significantly below the equilibrium temperature for the planet, particularly if FeH is not included as an opacity source.

WASP-127b (No Molecules Log Evidence: 1.73)			
Setup	Log Evidence	Retrieved Temperature [K]	Equilibrium Temperature [K]
H_2O	161.87	1027	~1400
H_2O, CH_4, CO, CO_2, NH3	161.27	1005	
H_2O, FeH	170.20	1305	
H_2O, CH_4, CO, CO_2, NH3, FeH	169.64	1304	
WASP-79 (No Molecules Log Evidence: 173.53)			
Setup	Log Evidence	Retrieved Temperature [K]	Equilibrium Temperature [K]
H_2O	188.34	621	~1800
H_2O, CH_4, CO, CO_2, NH3	187.98	603	
H_2O, FeH	190.87	888	
H_2O, CH_4, CO, CO_2, NH3, FeH	190.60	924	
WASP-62 (No Molecules Log Evidence: 184.49)			
Setup	Log Evidence	Retrieved Temperature [K]	Equilibrium Temperature [K]
H_2O	191.65	607	~1450
H_2O, CH_4, CO, CO_2, NH3	190.92	597	
H_2O, FeH	193.40	842	
H_2O, CH_4, CO, CO_2, NH3, FeH	193.11	894	

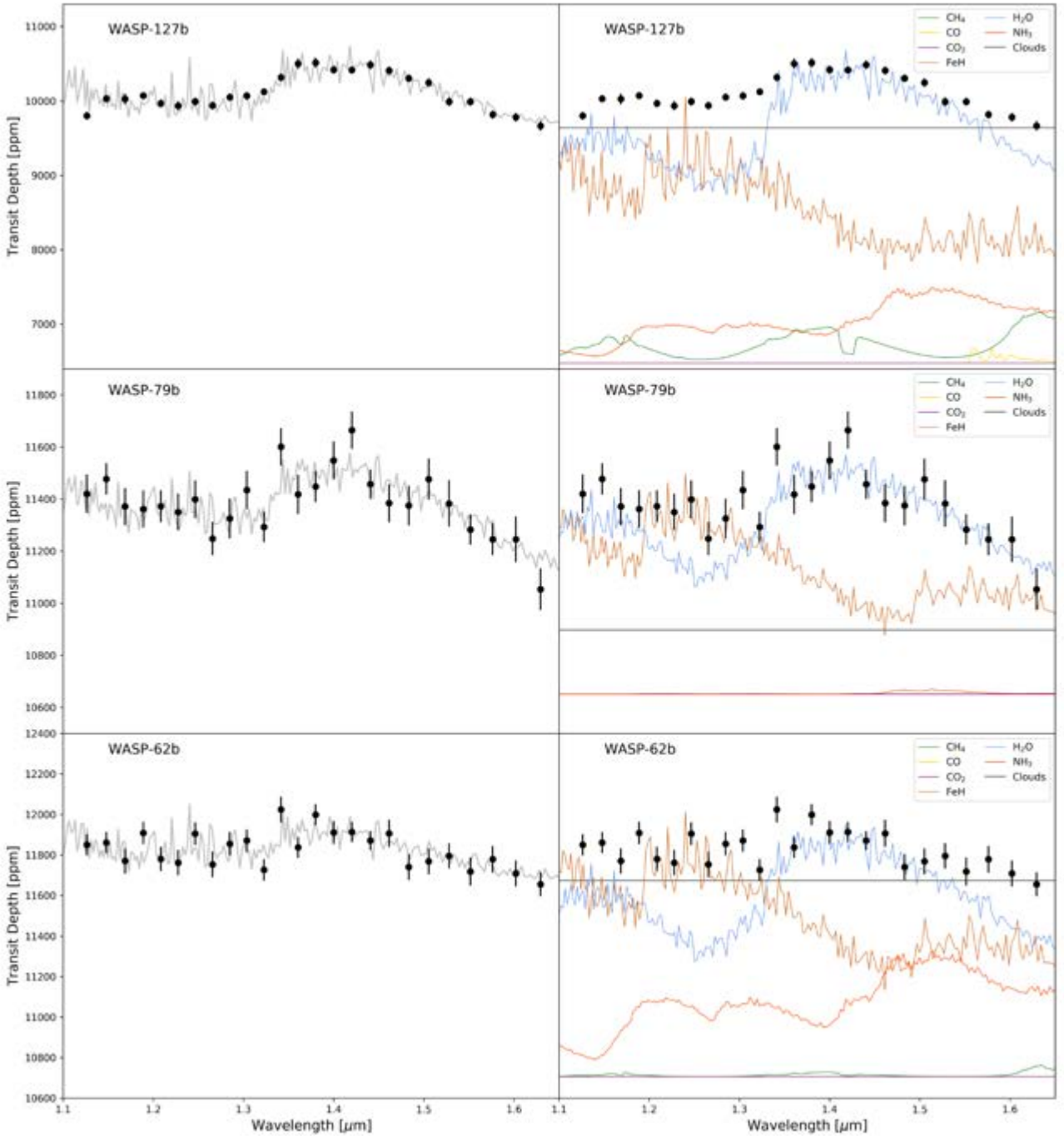

Table 3. Table of fitted parameters for the retrievals performed on our targets

Retrieved Parameters	bounds	**WASP-127b**	**WASP-79b**	**WASP-62b**
$\log[H_2O]$	1e-12 - 1e-1	$-2.71^{+0.78}_{-1.05}$	$-2.34^{+0.51}_{-0.72}$	$-2.56^{+0.76}_{-1.17}$
$\log[FeH]$	1e-12 - 1e-1	$-5.25^{+0.88}_{-1.10}$	$-4.39^{+0.88}_{-1.12}$	$-4.10^{+1.26}_{-1.82}$
$\log[CH_4]$	1e-12 - 1e-1	< -5	< -5	< -5
$\log[CO]$	1e-12 - 1e-1	< -3	< -3	< -3
$\log[CO_2]$	1e-12 - 1e-1	< -3	< -3	< -3
$\log[NH3]$	1e-12 - 1e-1	< -5	< -5	< -5
T_p (K)	400-2500	1304^{+185}_{-175}	924^{+242}_{-204}	894^{+248}_{-239}
R_p (R_{jup})	$\pm$ 50%	$1.15^{+0.04}_{-0.04}$	$1.69^{+0.02}_{-0.02}$	$1.34^{+0.02}_{-0.02}$
$\log P_{clouds}$	1e-2 - 1e6	$1.7^{+0.93}_{-0.66}$	> 3	$2.5^{+1.1}_{-0.88}$
μ (derived)		$2.34^{+0.20}_{-0.03}$	$2.38^{+0.33}_{-0.07}$	$2.46^{+0.32}_{-0.04}$
ADI	-	167.9	17.1	8.6
σ-level	-	$> 5\sigma$	$> 5\sigma$	$3 - 5\sigma$

Analysis of Hubble near-IR observations

Method: HST WFC3 G141 Data analysis

TRAPPIST-1 h observations as an example (Gressier et al. 2022)

M-dwarf
0.11 $R_\odot$
2566K
39 light years

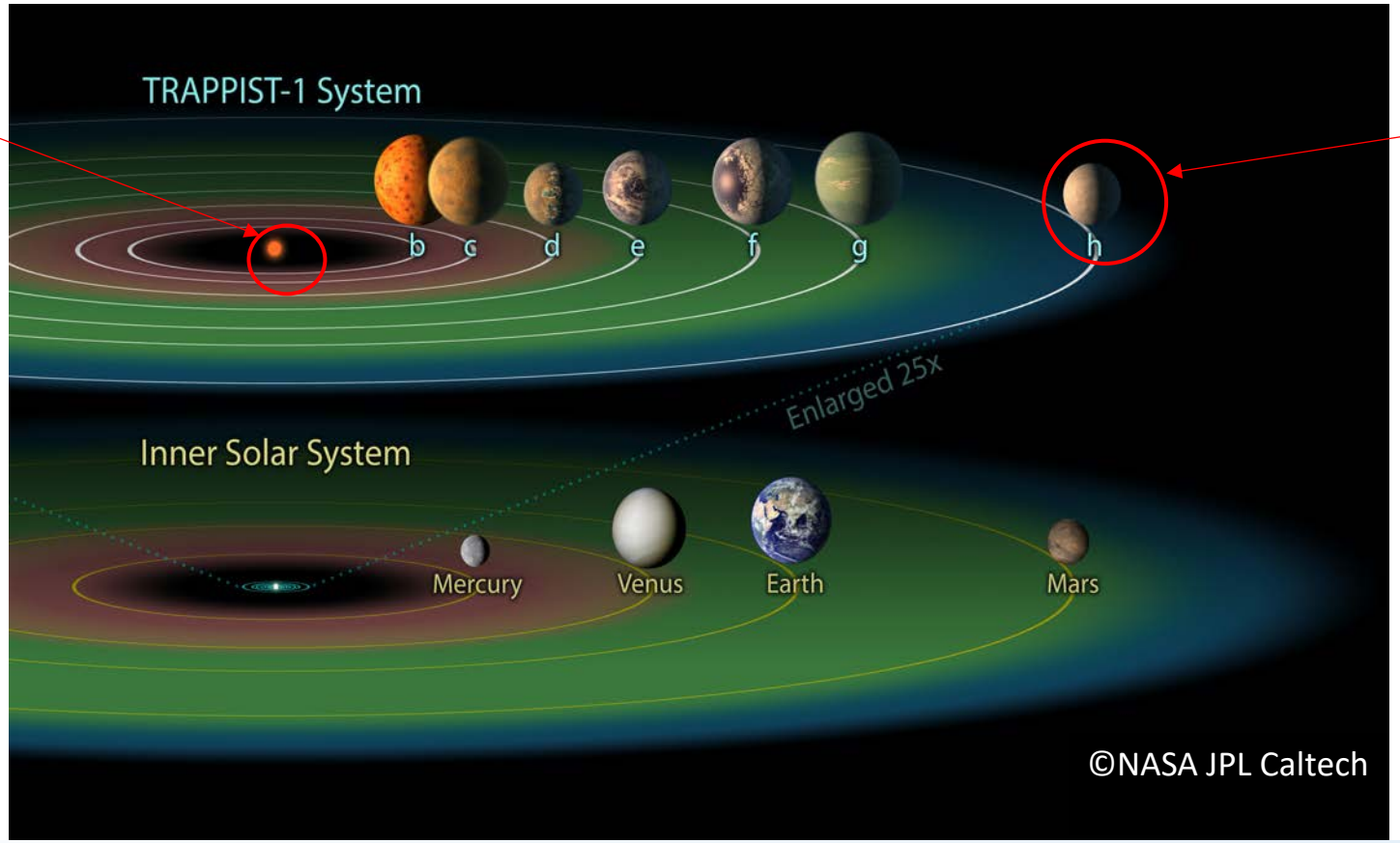

0.7 $R_\oplus$, 0.3 $M_\oplus$
173 K
~4000 kg/m^3
similar to Mars

Analysis of Hubble near-IR observations of Trappist-1h

tion

21)

TRAPPIST-1 h

- No proof of an atmosphere
- No molecular absorption features
- **Rule out a clear H- dominated atmosphere**

Gressier et al. 2022

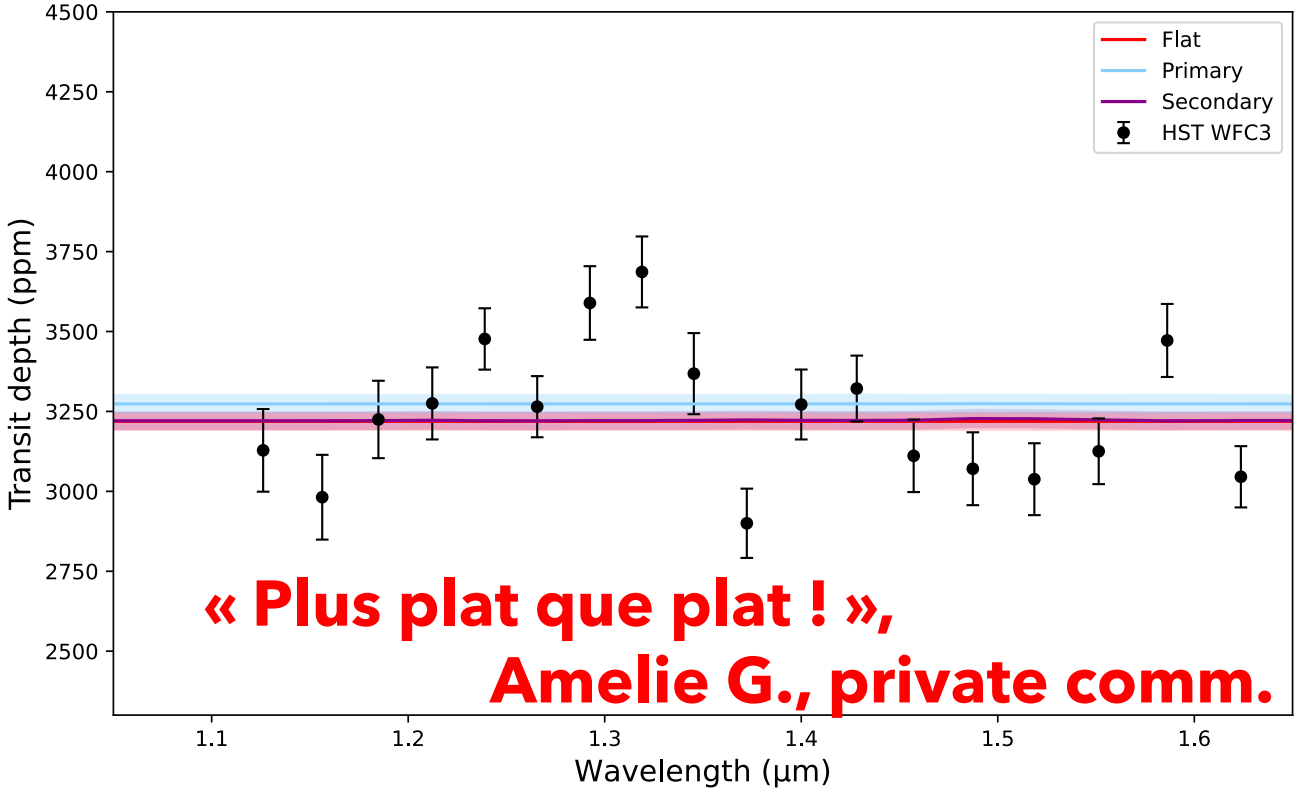

TRAPPIST-1 h transmission spectrum in the NIR (1.1-1.7 μm) and best fit for a light and a heavy atmospheric model

Population study, 26 planets < 6 Rearth

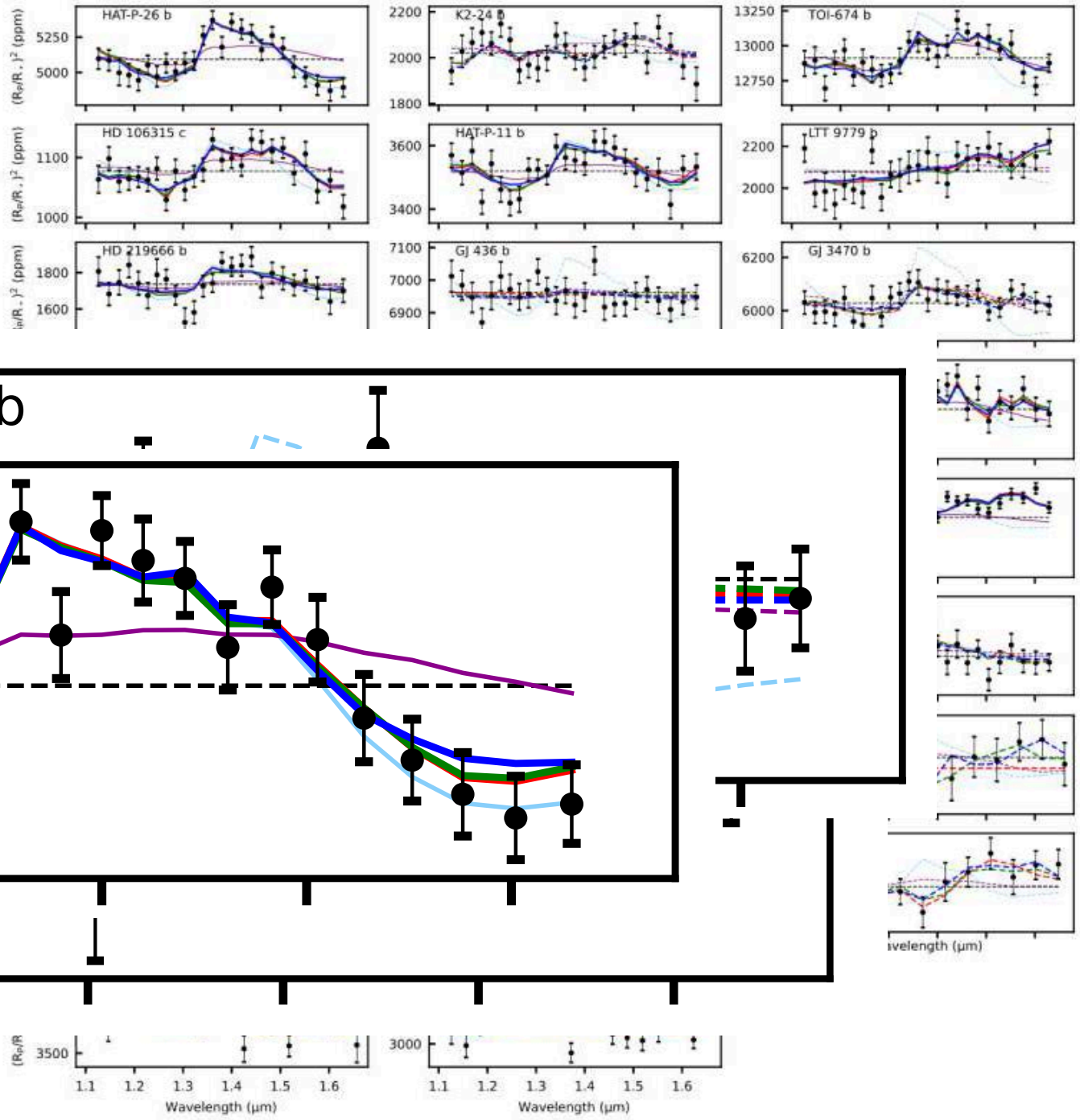

Gress
2023 submitte

Planet	H_2O	CH_4	CO	CO_2	NH_3	HCN	N_2	references
55 Cancri e								T16a
GJ 436 b								
GJ 1132 b								
GJ 1214 b								
GJ 3470 b								B19a, E22
HAT-P-11 b								F14,E22
HAT-P-26 b								W17, MD19, E22
HD 3167 c								G20, ME20, E22
HD 97658 b								E22
HD 106315 c								G20, K20, E22
HD 219666 b								
HIP 41378 b								
K2-18 b								T19, B19b, E22
K2-24 b								
LHS 1140 b								E22
LTT 9779 b								
TOI-270 c								
TOI-270 d								E22
TOI-674 b								B22, E22
TRAPPIST-1 b								
TRAPPIST-1 c								
TRAPPIST-1 d								
TRAPPIST-1 e								
TRAPPIST-1 f								
TRAPPIST-1 g								
TRAPPIST-1 h								

Population study, 26 planets < 6 Rearth

- Atmosphere detected for 50% of planets
- 9/26 strong H2O detection
- No hint of CH4 due to bias because of overlapping H20 line
- No detection below 1.7$R_\oplus$
- Flat transmission spectra for Sub-Neptunes

Gressier, Changeat, Edwards et al. 2023 submitted

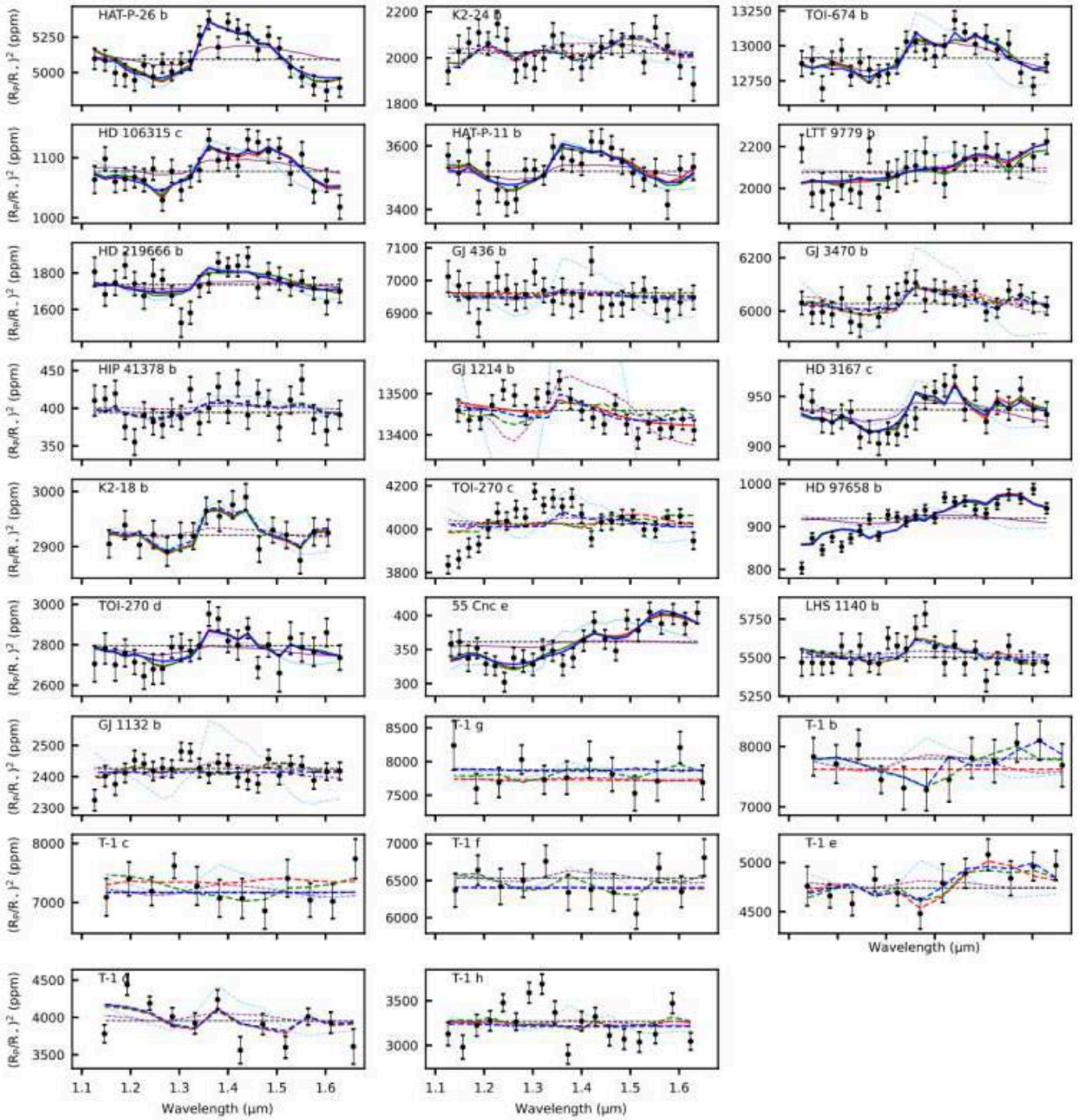

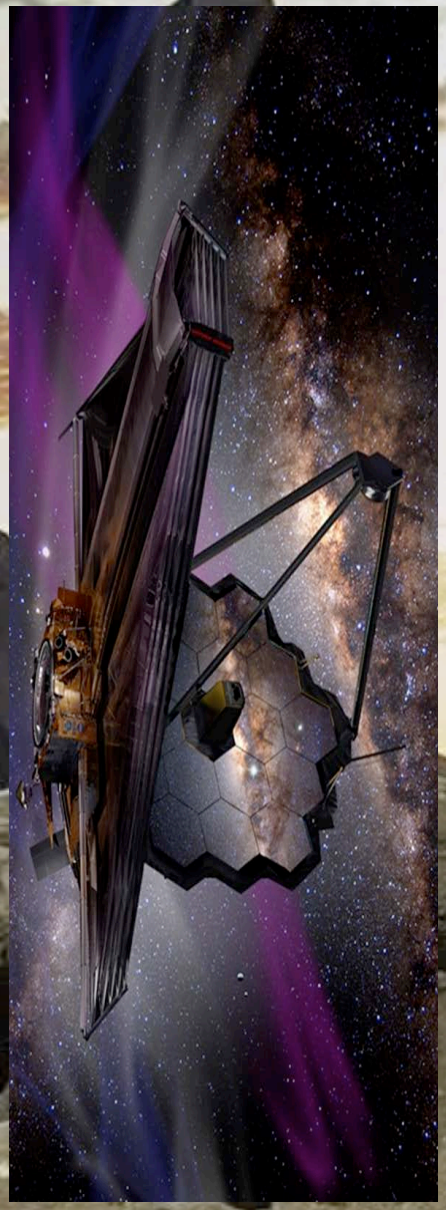


NASA

Four instruments

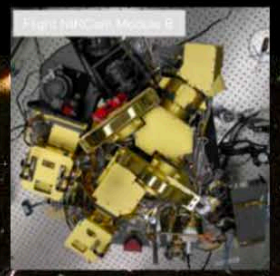

0.6-28 microns
25 m^2

It is the largest and most complex telescope ever launched in space

17 observing modes,
including 10 modes dedicated to exoplanet observations

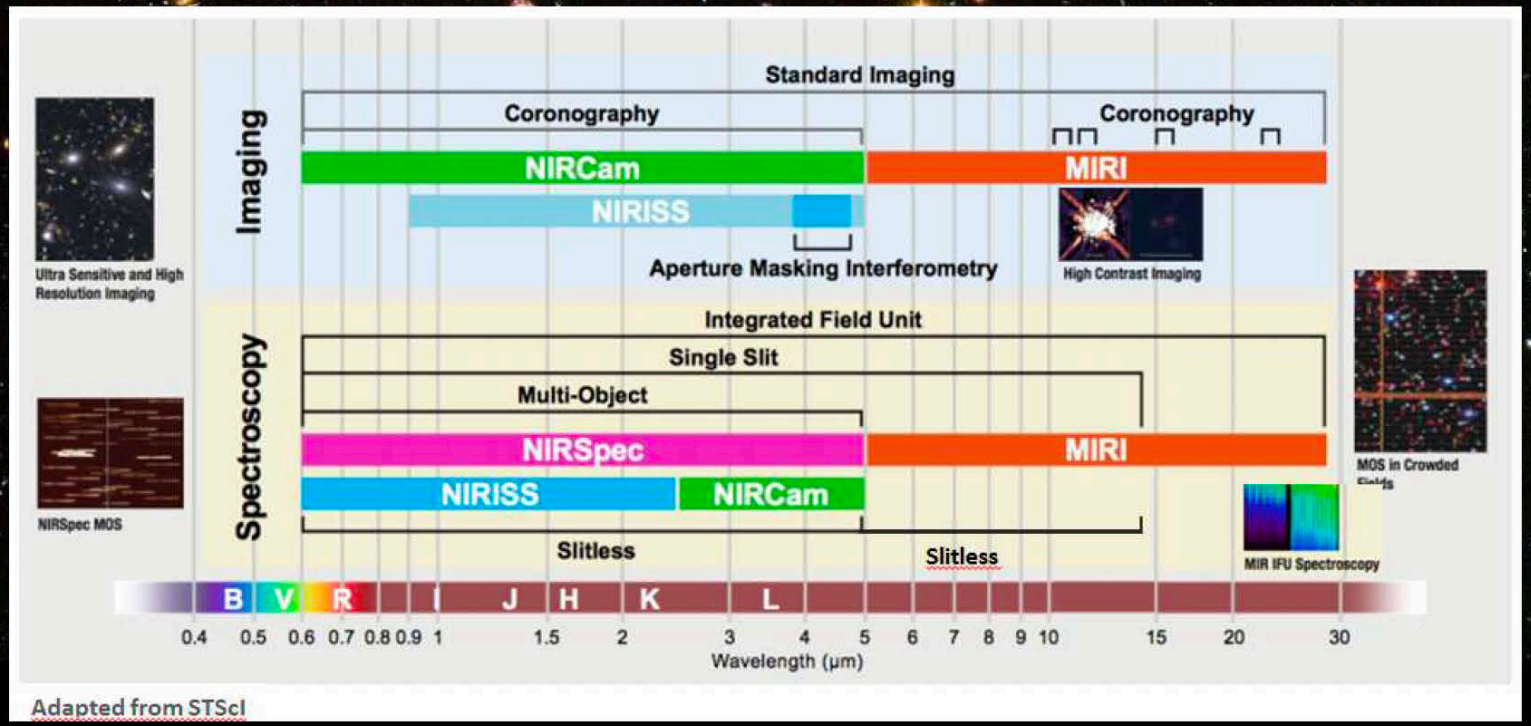

Adapted from STScI

JWST Cycle-2

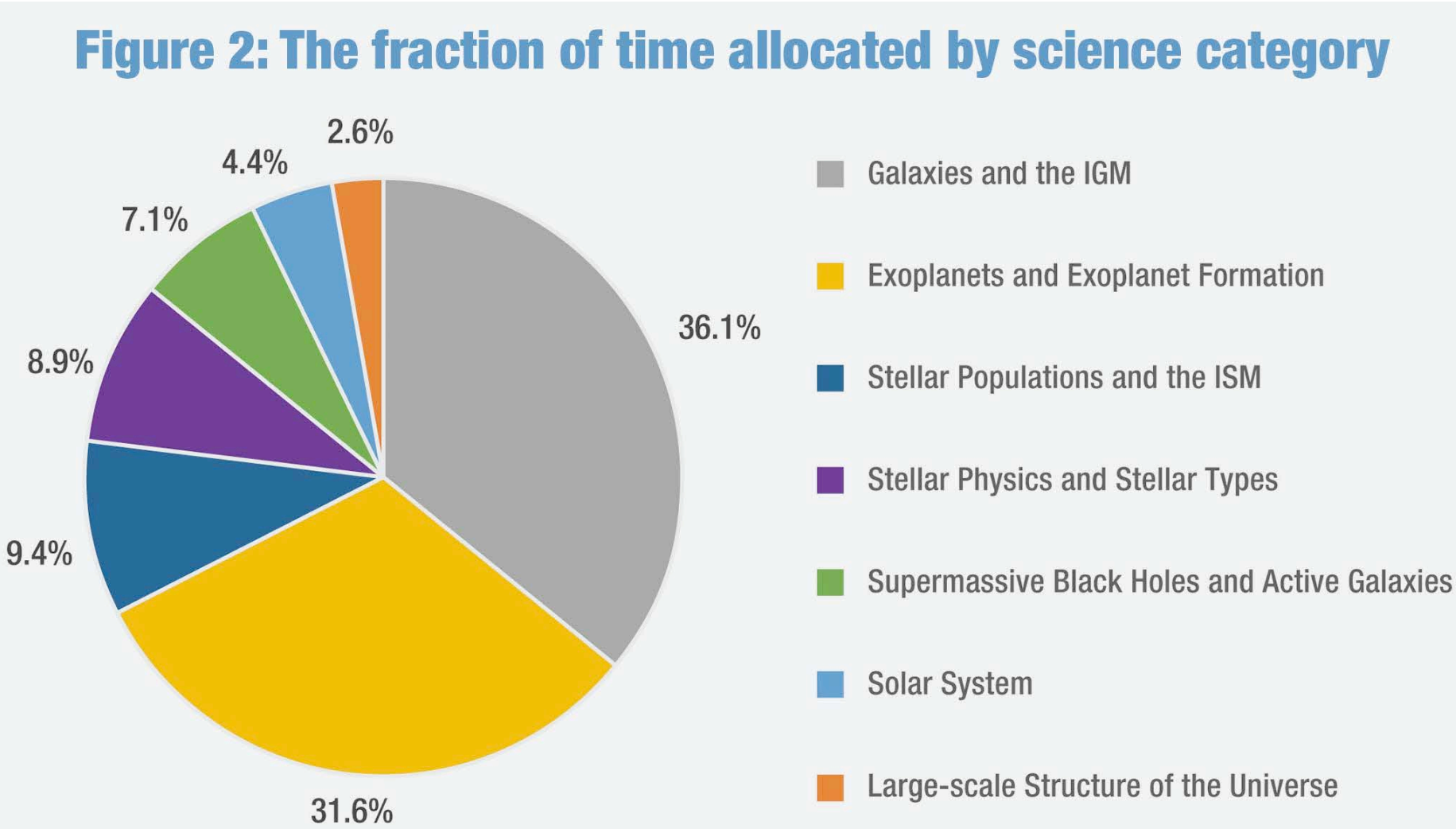
Figure 2: The fraction of time allocated by science category
2.6%
4.4%
7.1%
8.9%
9.4%
36.1%
31.6%
Galaxies and the IGM
Exoplanets and Exoplanet Formation
Stellar Populations and the ISM
Stellar Physics and Stellar Types
Supermassive Black Holes and Active Galaxies
Solar System
Large-scale Structure of the Universe

Figure 3: Cycle 1 – 3 Proposal Timeline

Beginning in Cycle 3, STScI plans to release the annual JWST General Observer (GO)/Archival (AR) Call for Proposals in mid-August and to support the annual proposal deadline in late October.

Cycle 3 is the last cycle in which Guaranteed Time Observers (GTOs) can submit GTO Programs

Hot saturn WASP-39b

- Orbit a G7 star in 4.05 days
- 0.28 Mjup and 1.28 Rjup
- Temperature 1170 K

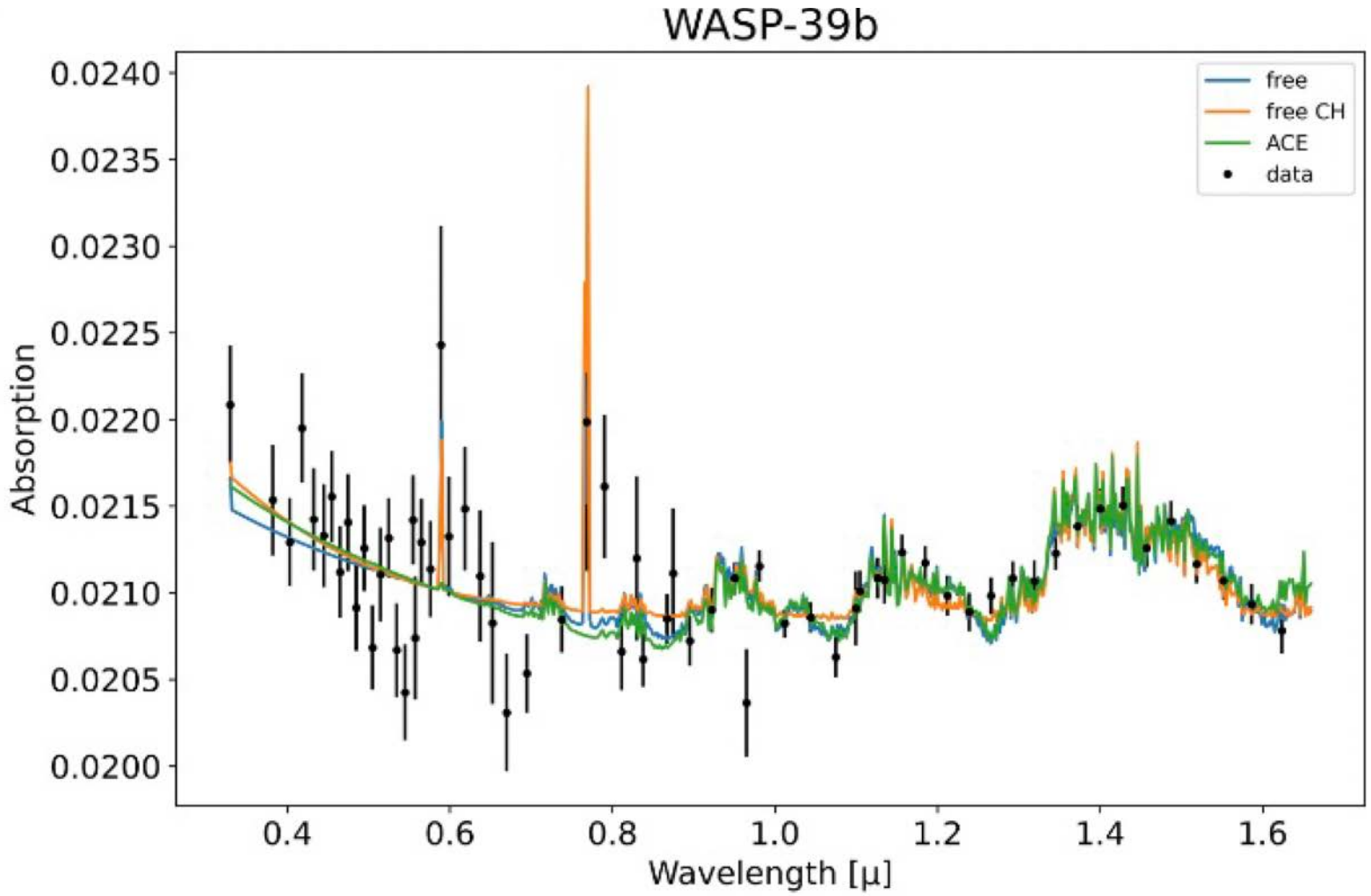

Panek et al., 2023

Hot saturn WASP-39b

Notice the two Spitzer points 3.6 and 4.5 microns

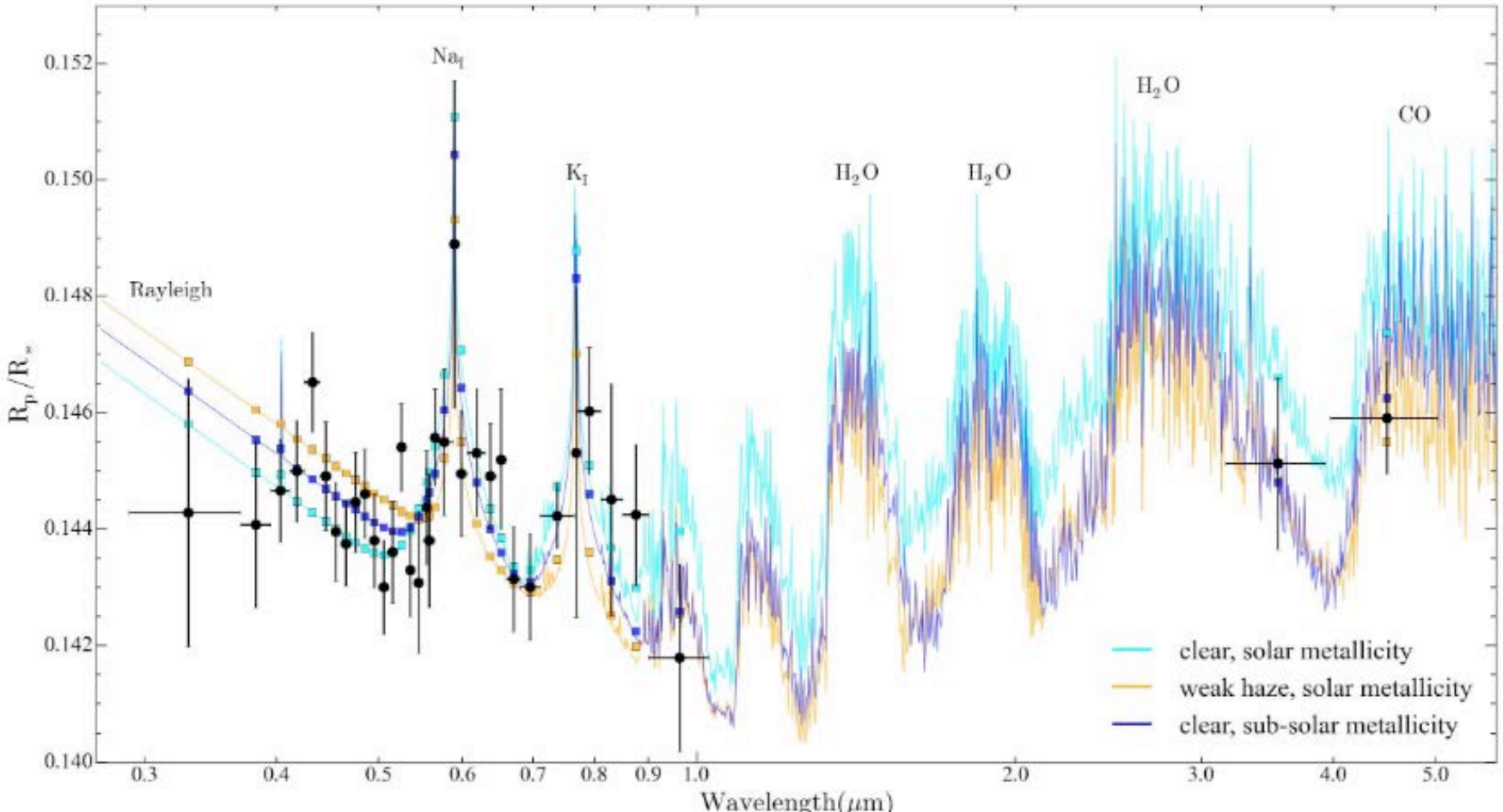

WASP-39b, first hot-Saturn with JWST

- Orbit a G7 star in 4.05 days
- 0.28 Mjup and 1.28 Rjup
- Temperature 1170 K

- Observation 10 July 2022
- Nature paper 25 august 2022

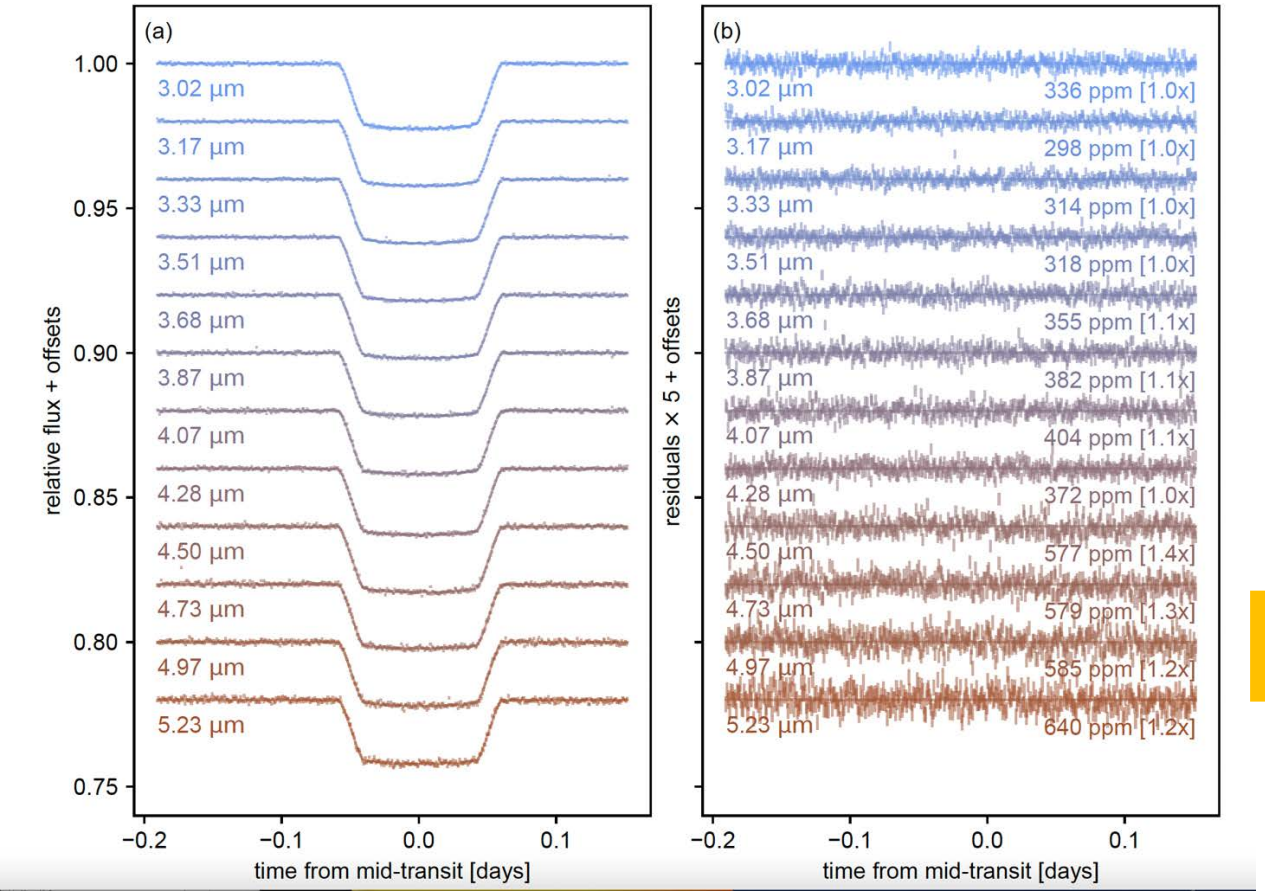

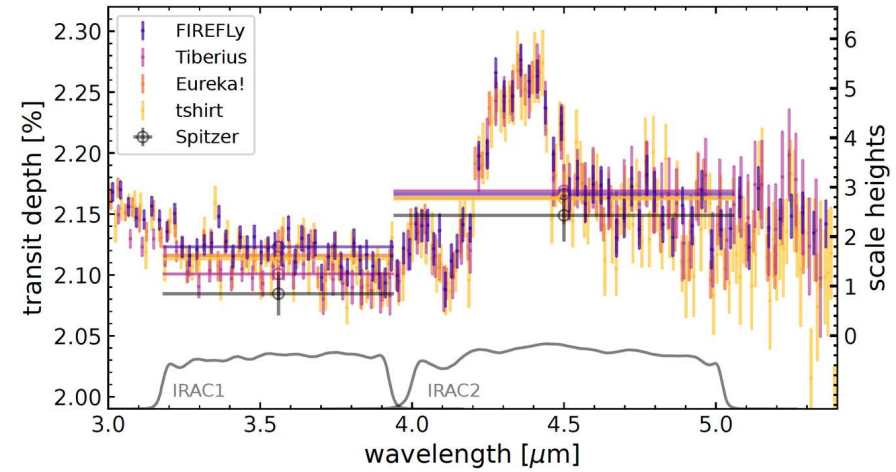

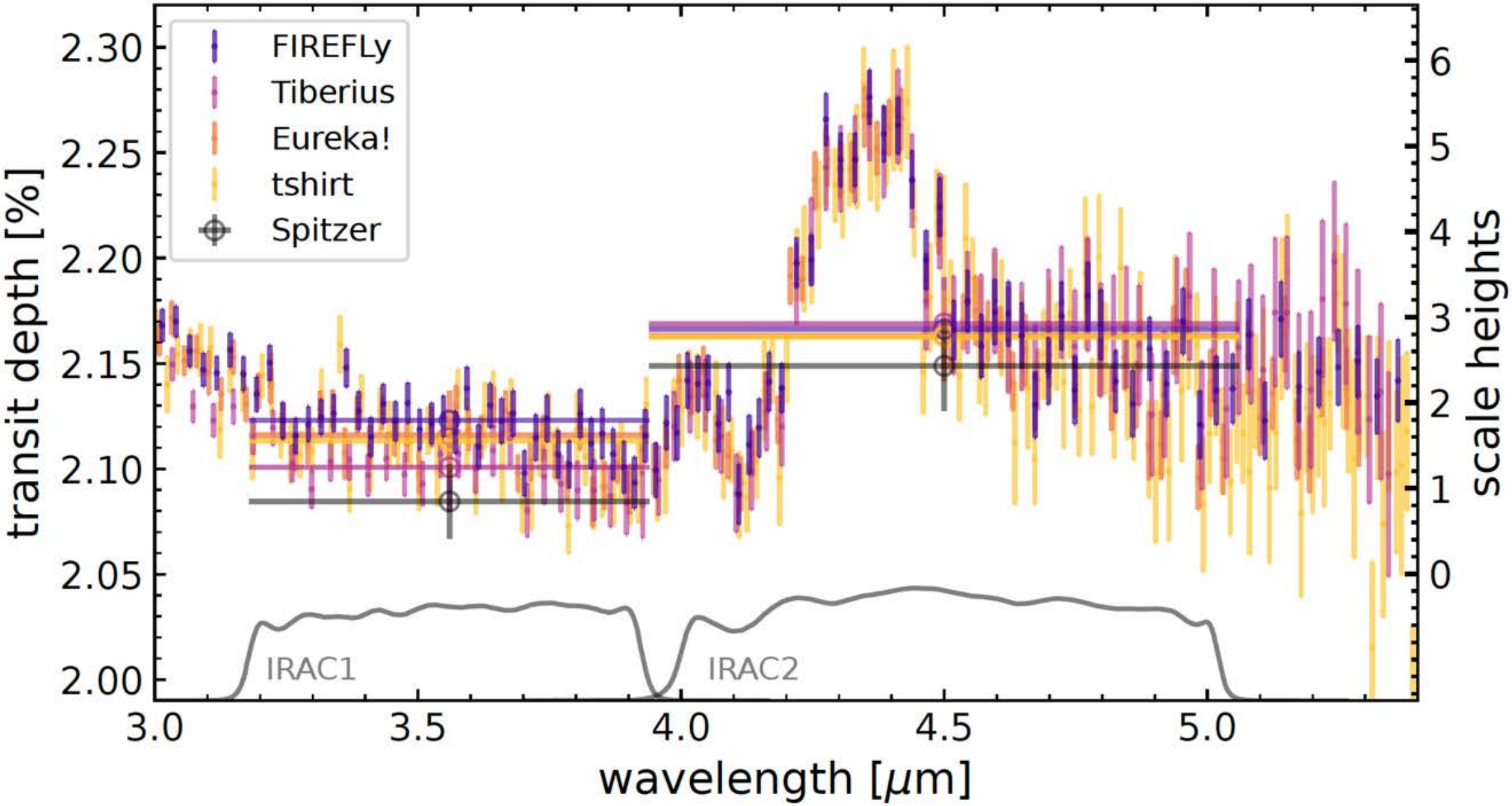
FIREFLy
Tiberius
Eureka!
tshirt
Spitzer
IRAC1
IRAC2
transit depth [%]
scale heights
wavelength [μm]
2.30
2.25
2.20
2.15
2.10
2.05
2.00
6
5
4
3
2
1
0
3.0
3.5
4.0
4.5
5.0

Early Release Science of the exoplanet WASP-39b with JWST NIRSpec PRISM

Z. Rustamkulov et al., 2023, Nature 664 February 2023

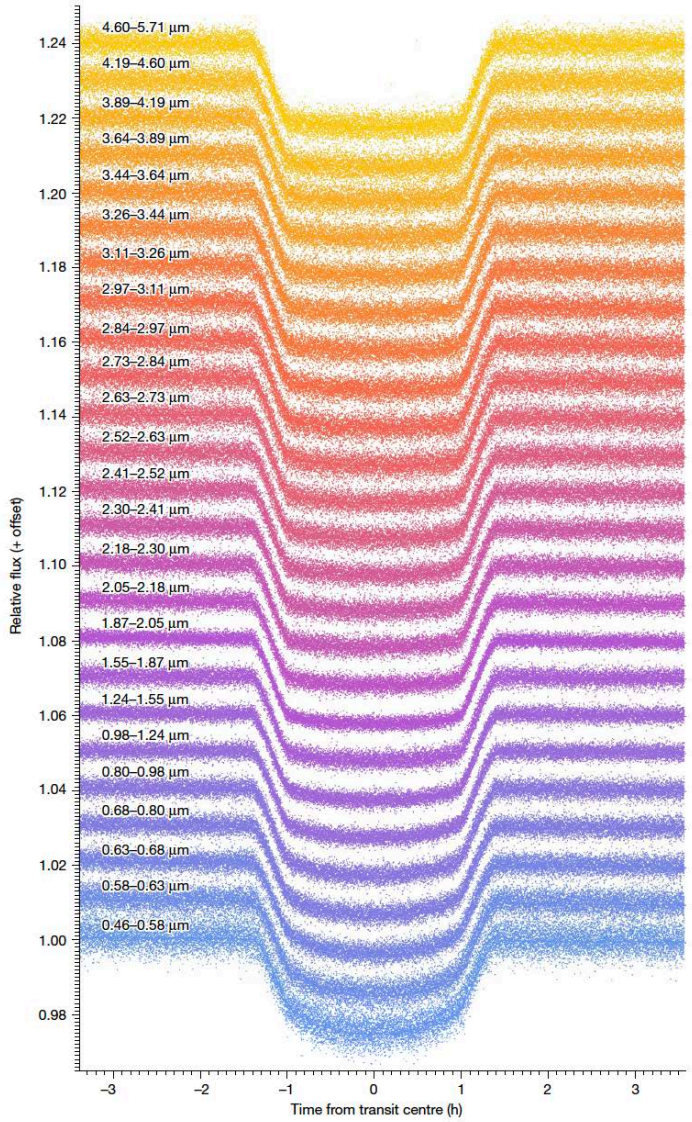

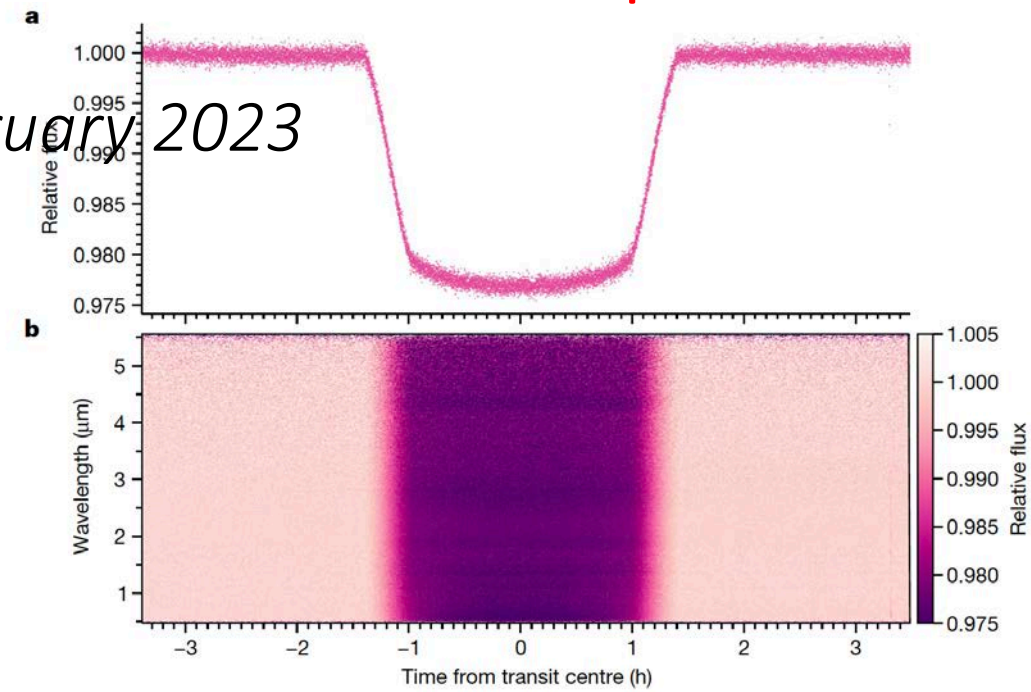

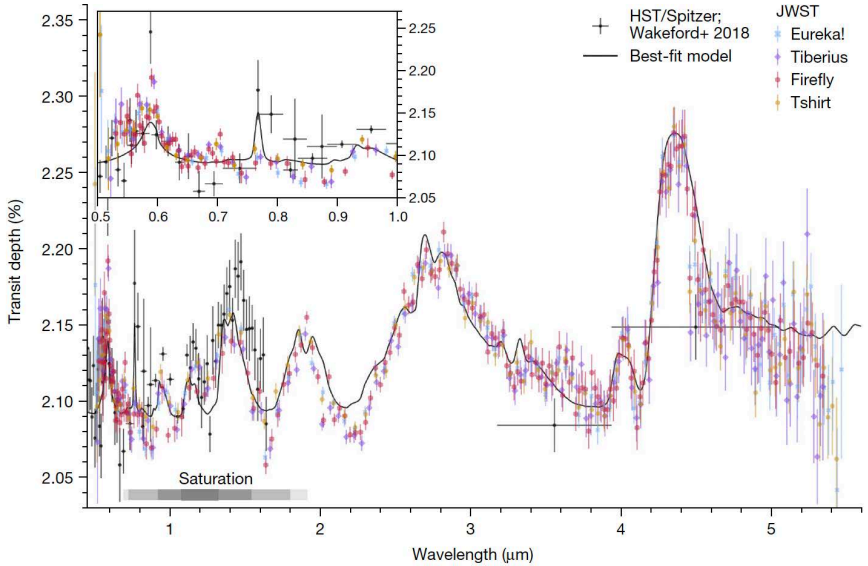

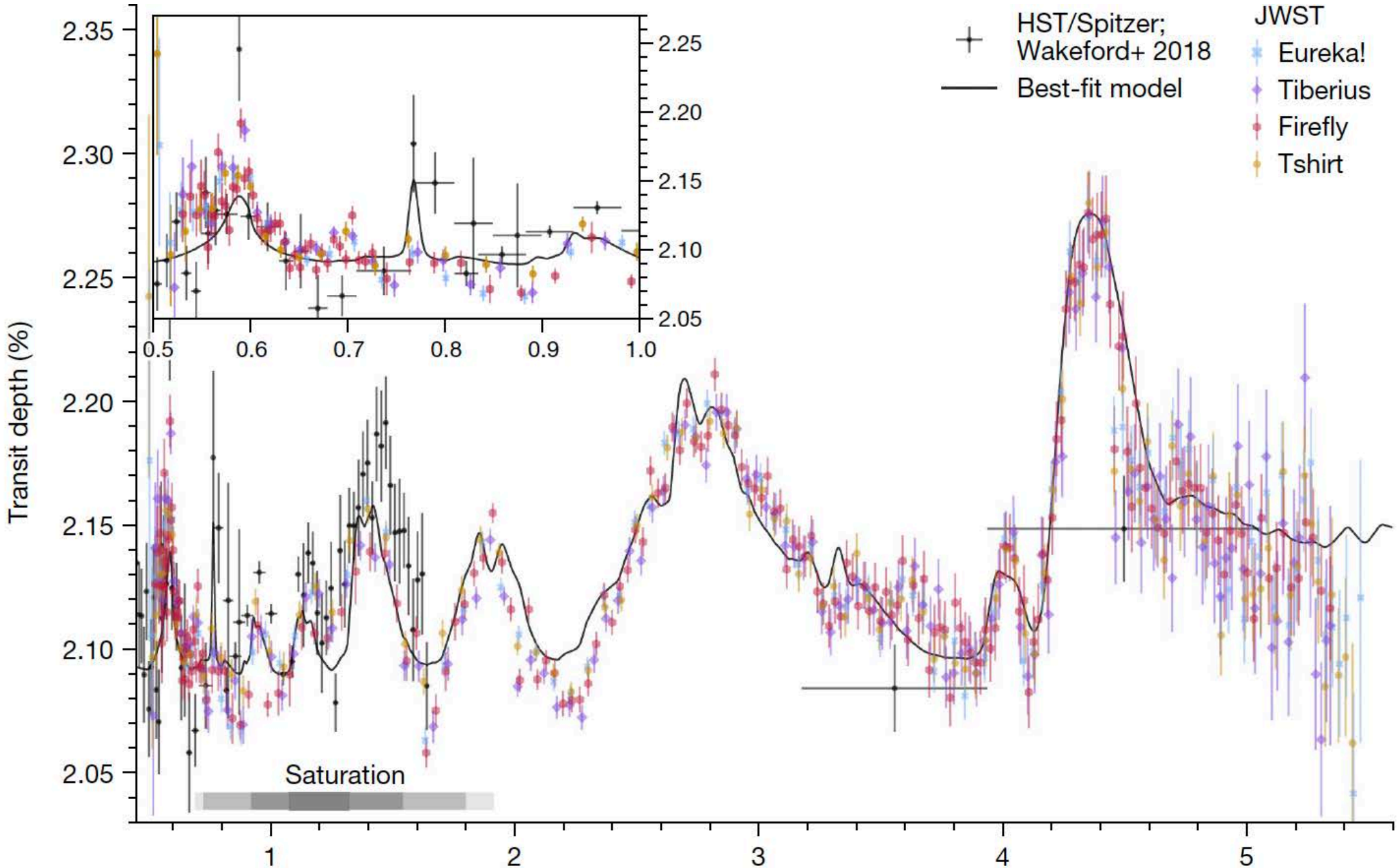
HST/Spitzer;
Wakeford+ 2018
Best-fit model
JWST
Eureka!
Tiberius
Firefly
Tshirt
Transit depth (%)
Saturation
2.35
2.30
2.25
2.20
2.15
2.10
2.05
1
2
3
4
5
0.5
0.6
0.7
0.8
0.9
1.0
2.25
2.20
2.15
2.10
2.05

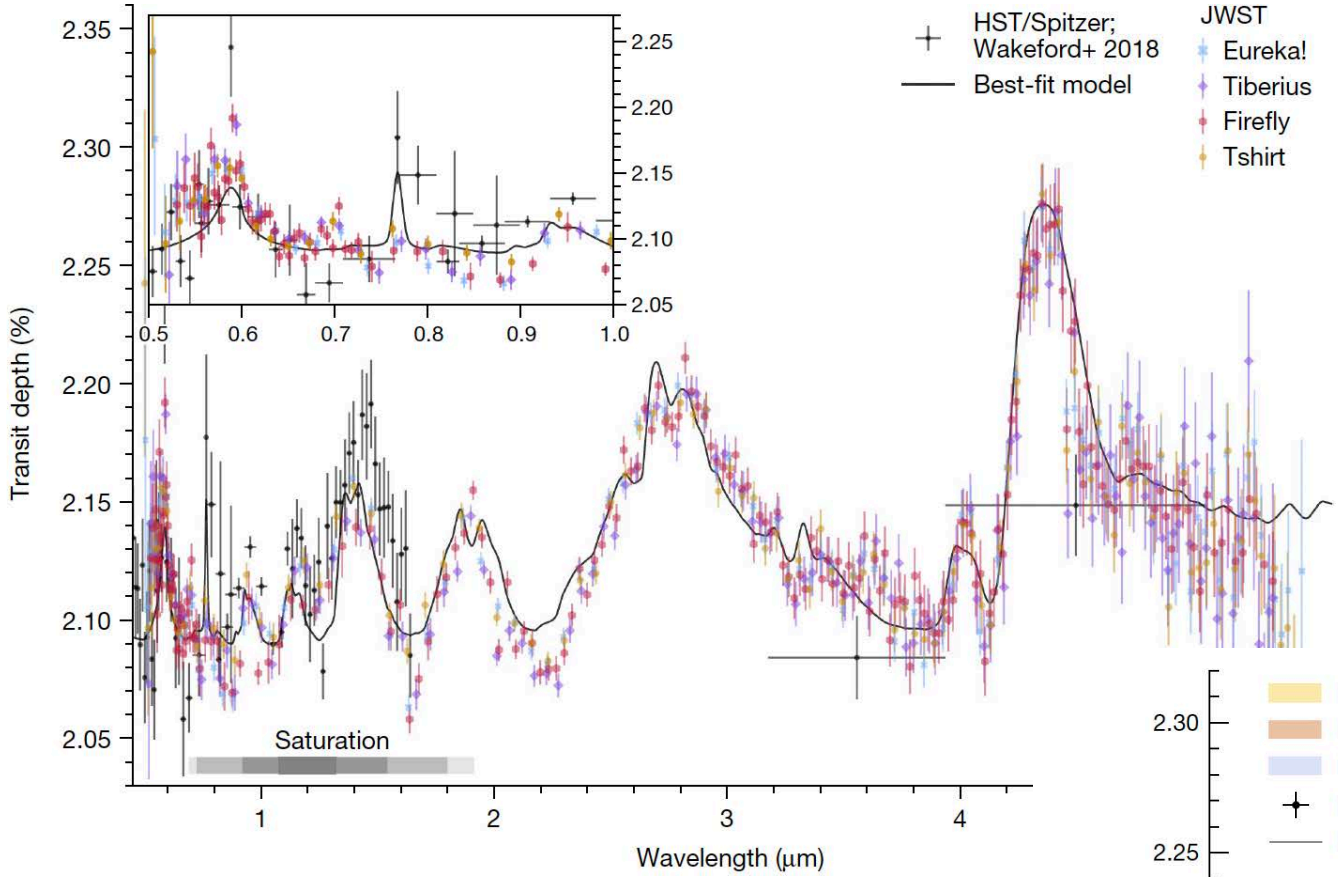
HST/Spitzer;
Wakeford+ 2018
Best-fit model
JWST
Eureka!
Tiberius
Firefly
Tshirt
Saturation
Transit depth (%)
Wavelength (μm)

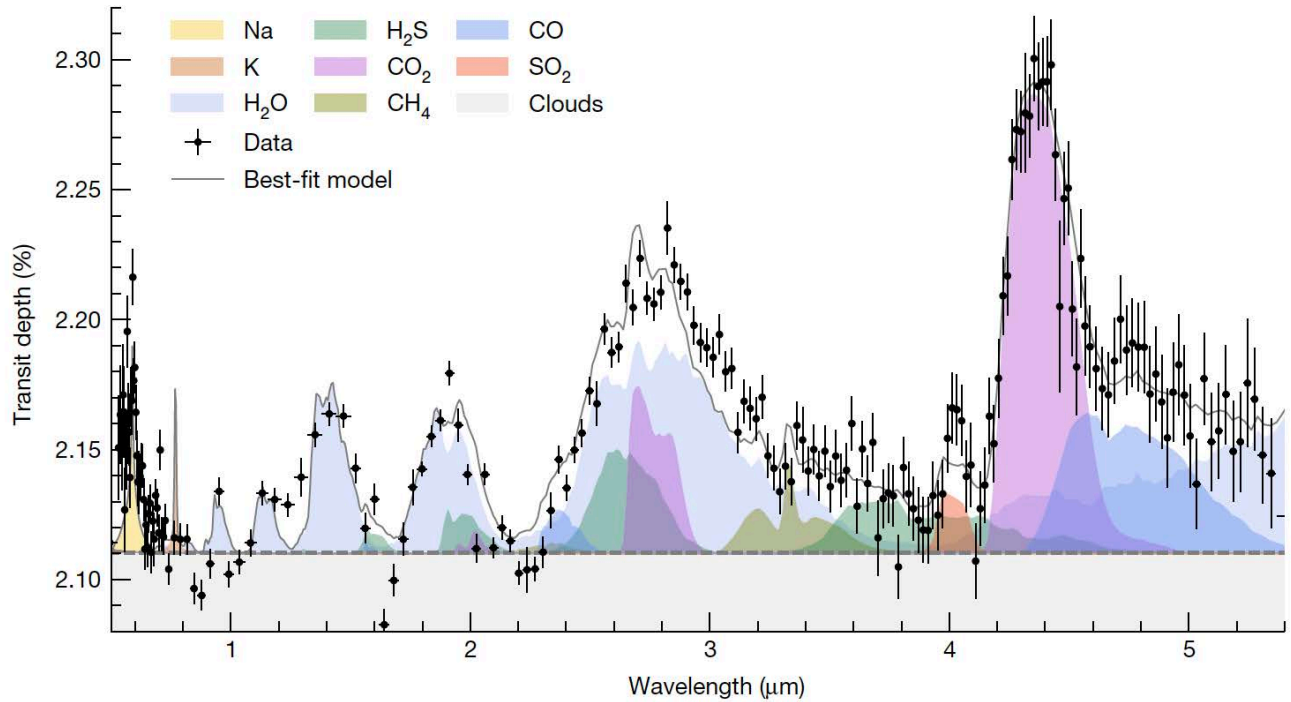
Na
K
H2O
H2S
CO2
CH4
CO
SO2
Clouds
Data
Best-fit model
Transit depth (%)
Wavelength (μm)

WASP-39b WITH NIRSPEC PRISM

Z. Rustamkulov et al., 2023

- Resolution of 20-300, over 0.5-5.5 microns
- Detection of Na (19σ), H2O (33σ), CO2 (28σ) and CO (7σ).
- Non-detection of CH4, combined with a strong CO2 feature, favours atmospheric models with a super-solar atmospheric metallicity.
- 4 µm is best explained by SO2 (2.7σ),

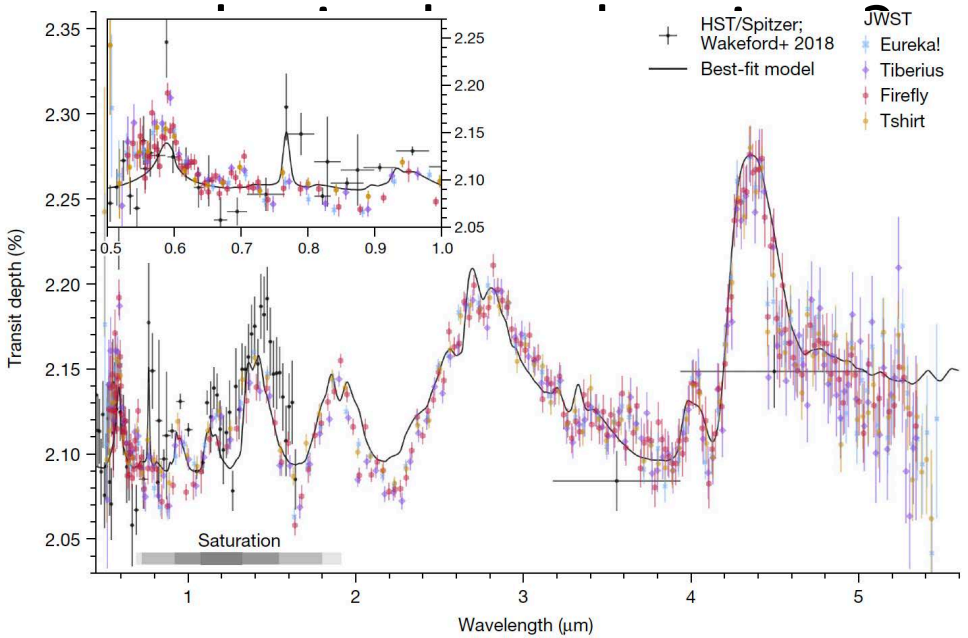

Early Release Science of the exoplanet WASP-39b with JWST NIRSpec G395H

Lili, Alderson et al., 2023, Nature 664 February 2023

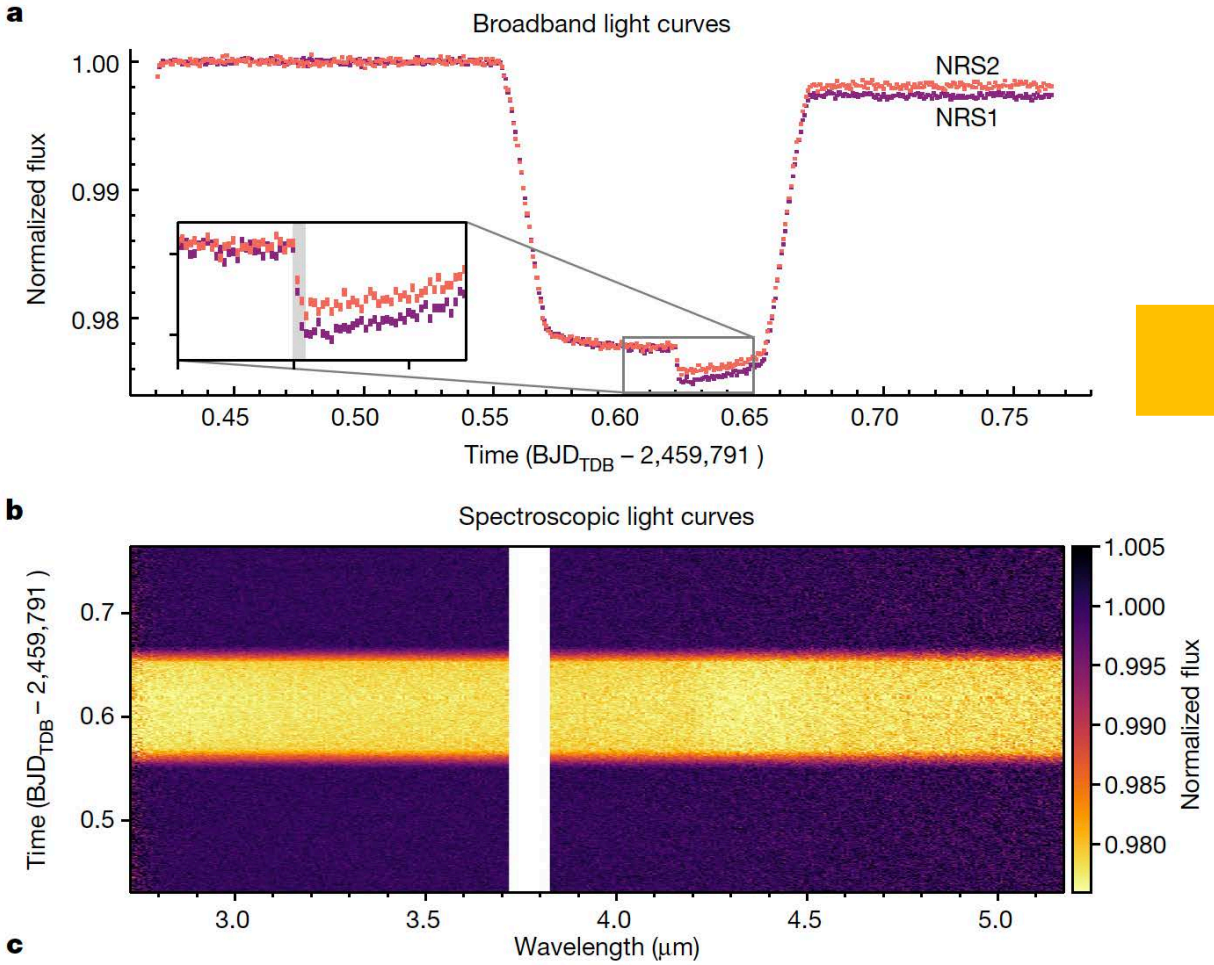

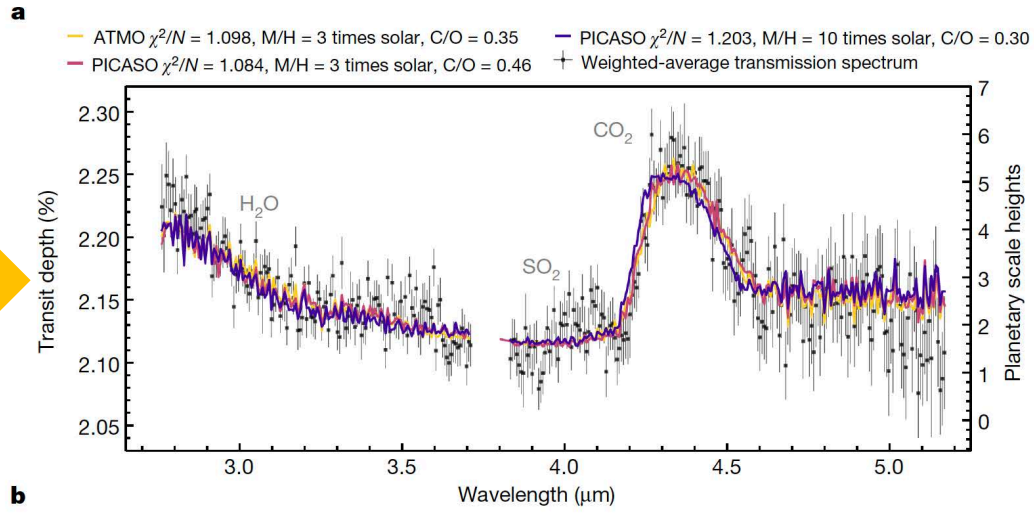

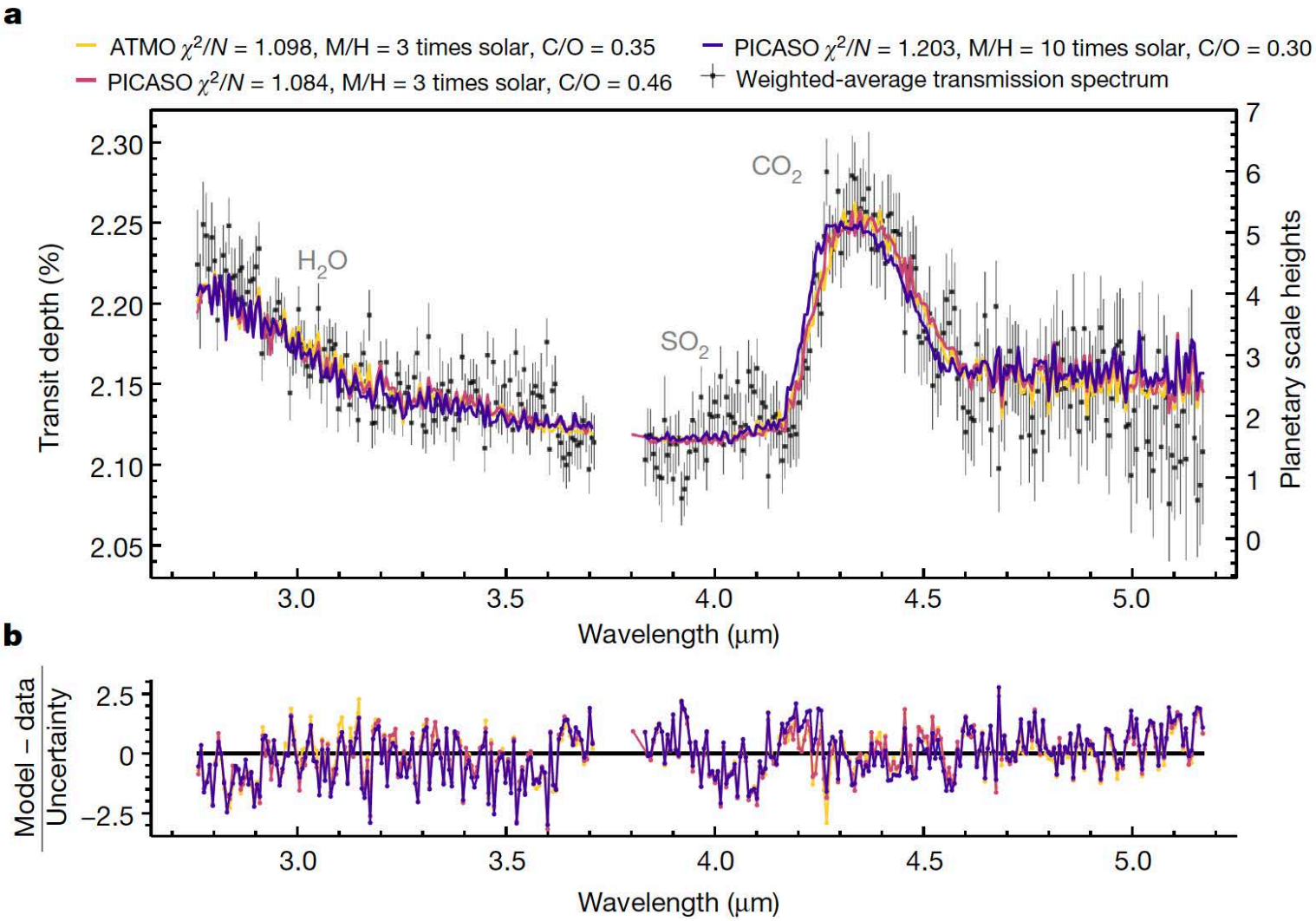

Fig. 3 | Spectra from three independent 1D RCTE models and their residuals, fit to the weighted-average WASP-39b G395H transmission spectrum. **a**, Spectra from the three models. **b**, Their residuals. The models are dominated by absorption from H_2O and CO_2 with a grey-cloud-top pressure corresponding to ≈1 mbar. The models find that the data are best explained by 3–10 times solar metallicity (M/H) and sub-solar to solar C/O (C/O = 0.30–0.46). The extra absorption owing to SO_2, seen in the spectrum around 4.1 μm, is not included in the RCTE model grids and causes a marked impact on the χ^2/N (see Fig. 4).

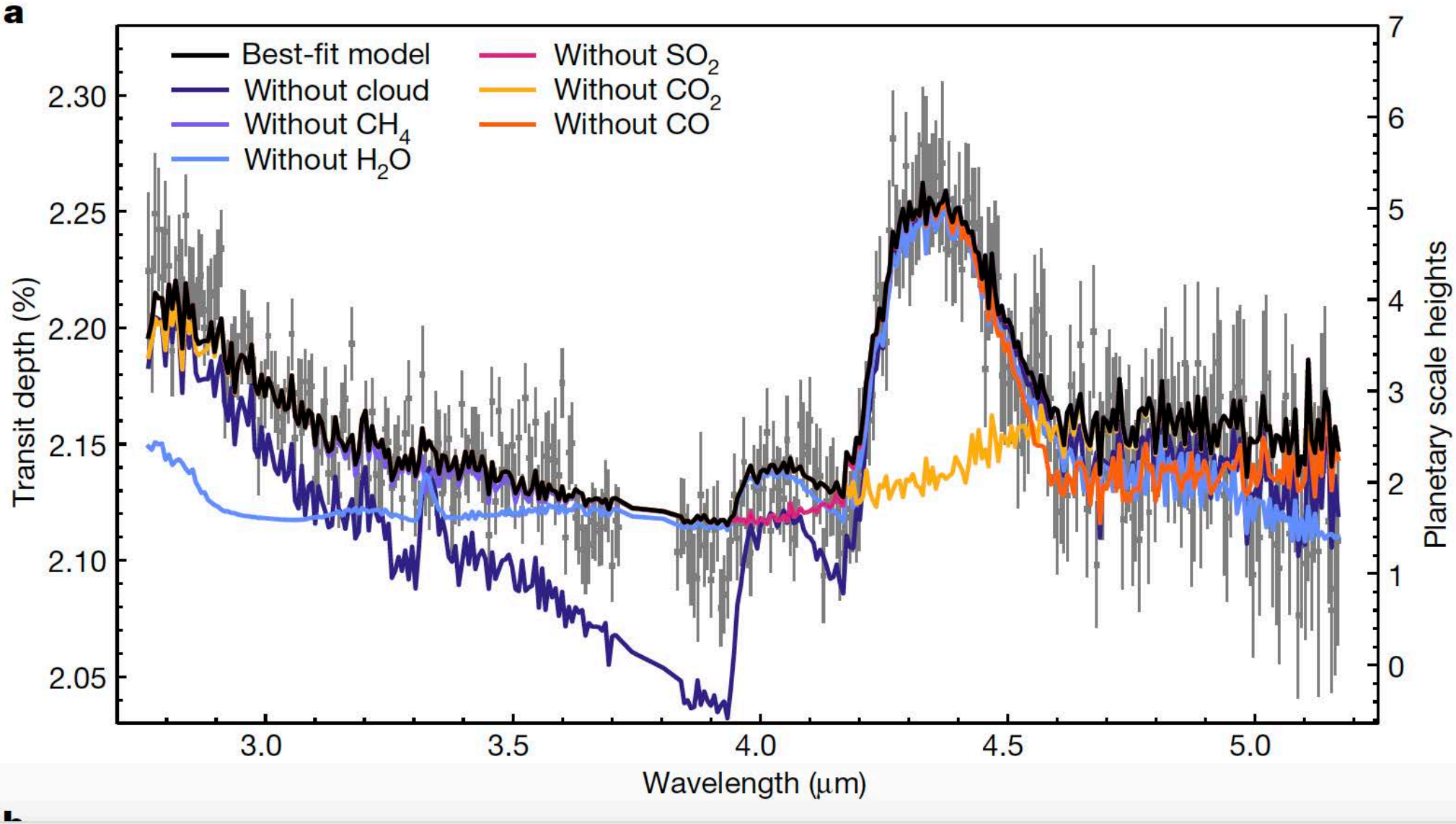
a
Best-fit model
Without cloud
Without CH_4
Without H_2O
Without SO_2
Without CO_2
Without CO
Transit depth (%)
2.30
2.25
2.20
2.15
2.10
2.05
3.0
3.5
4.0
4.5
5.0
Wavelength (μm)
Planetary scale heights
7
6
5
4
3
2
1
0

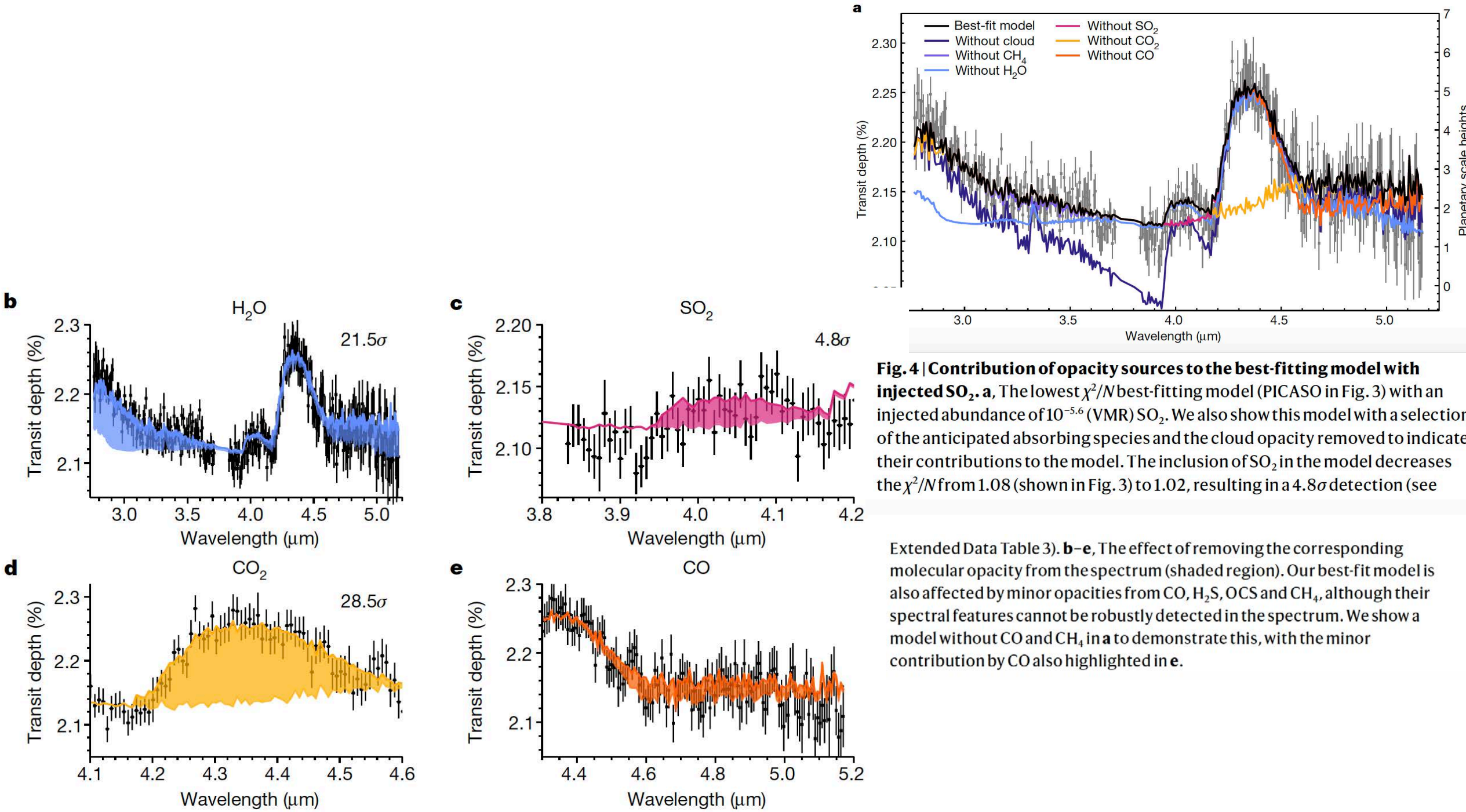

Fig. 4 | Contribution of opacity sources to the best-fitting model with injected SO_2. a, The lowest χ^2/N best-fitting model (PICASO in Fig. 3) with an injected abundance of $10^{-5.6}$ (VMR) SO_2. We also show this model with a selection of the anticipated absorbing species and the cloud opacity removed to indicate their contributions to the model. The inclusion of SO_2 in the model decreases the χ^2/N from 1.08 (shown in Fig. 3) to 1.02, resulting in a 4.8σ detection (see Extended Data Table 3). **b**–**e**, The effect of removing the corresponding molecular opacity from the spectrum (shaded region). Our best-fit model is also affected by minor opacities from CO, H_2S, OCS and CH_4, although their spectral features cannot be robustly detected in the spectrum. We show a model without CO and CH_4 in **a** to demonstrate this, with the minor contribution by CO also highlighted in **e**.

WASP-39b WITH NIRSPEC G395H

Lili, Alderson et al., 2023

- ***Medium resolution specta R=600 3-5 microns, 146 x above photon noise***
- ***CO2 (28.5σ), H20 (21.5 σ), SO2 (4.1σ)***
- ***3-10 time solar solar metallicity, sub-solar C/0***

Early Release Science of the exoplanet WASP-39b with JWST NIRISS,

Adina D. Feinstein et al., 2023, Nature, February 2023

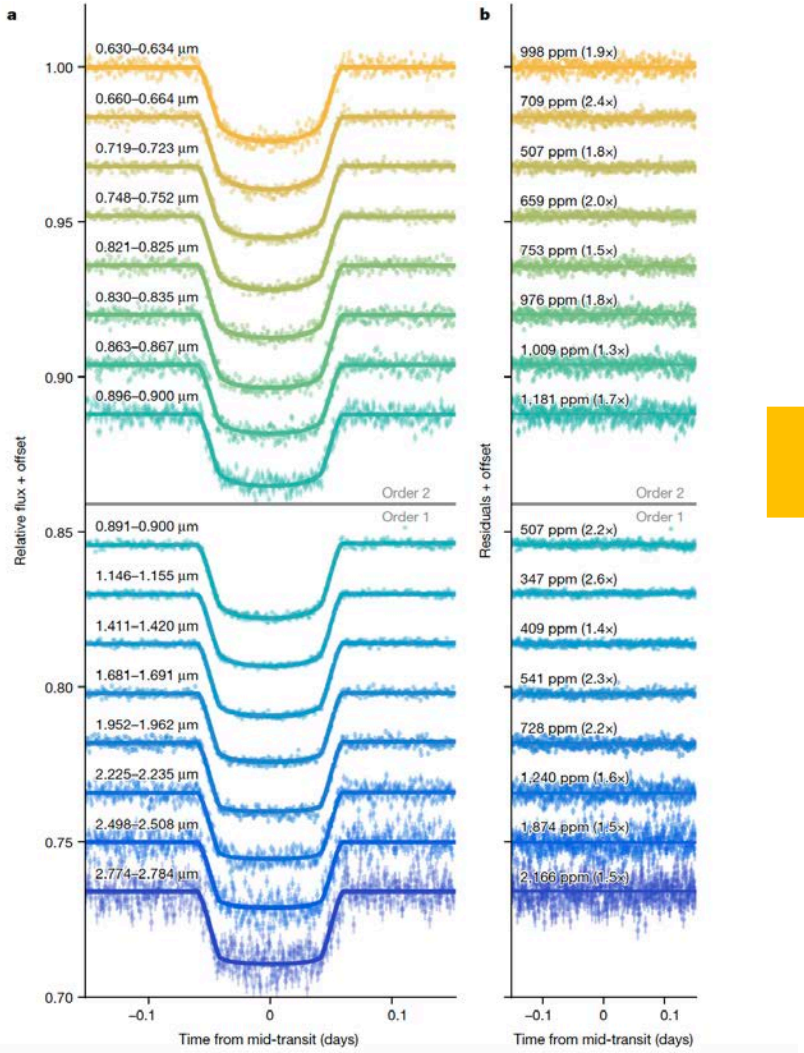

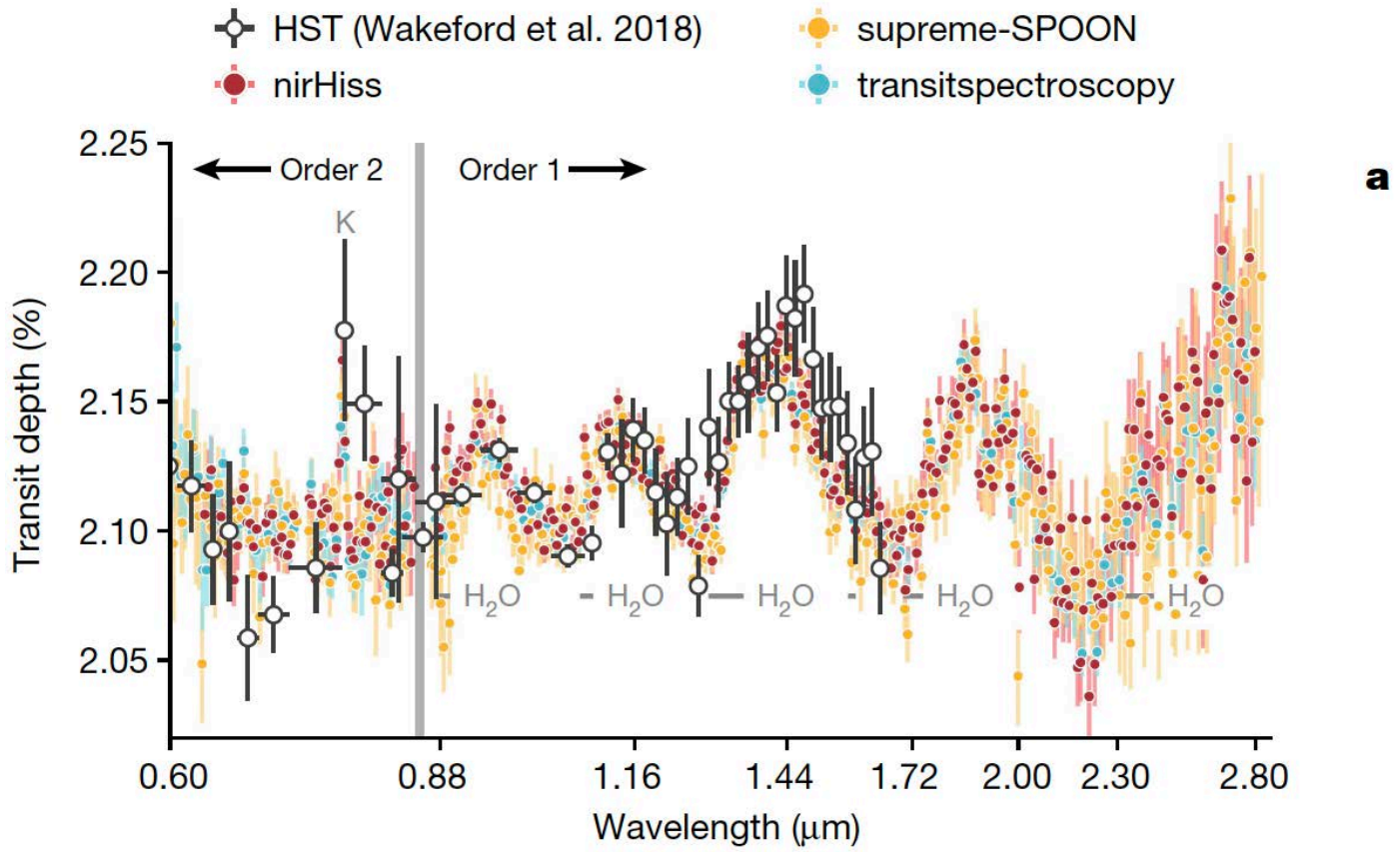

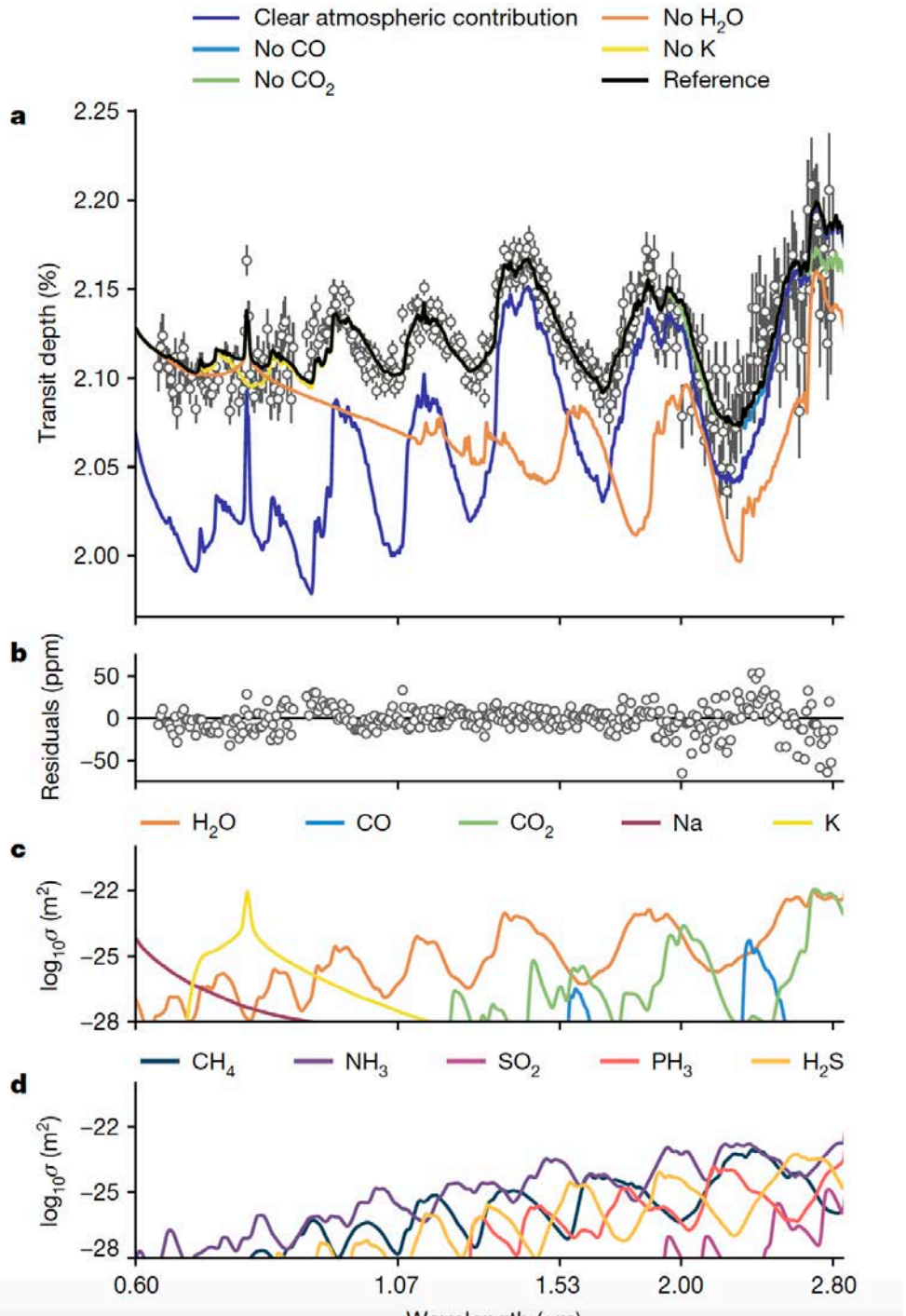
Clear atmospheric contribution
No CO
No CO_2
No H_2O
No K
Reference
a
Transit depth (%)
2.25
2.20
2.15
2.10
2.05
2.00
b
Residuals (ppm)
50
0
−50
H_2O
CO
CO_2
Na
K
c
$\log_{10}\sigma$ (m^2)
−22
−25
−28
CH_4
NH_3
SO_2
PH_3
H_2S
d
$\log_{10}\sigma$ (m^2)
−22
−25
−28
0.60
1.07
1.53
2.00
2.80

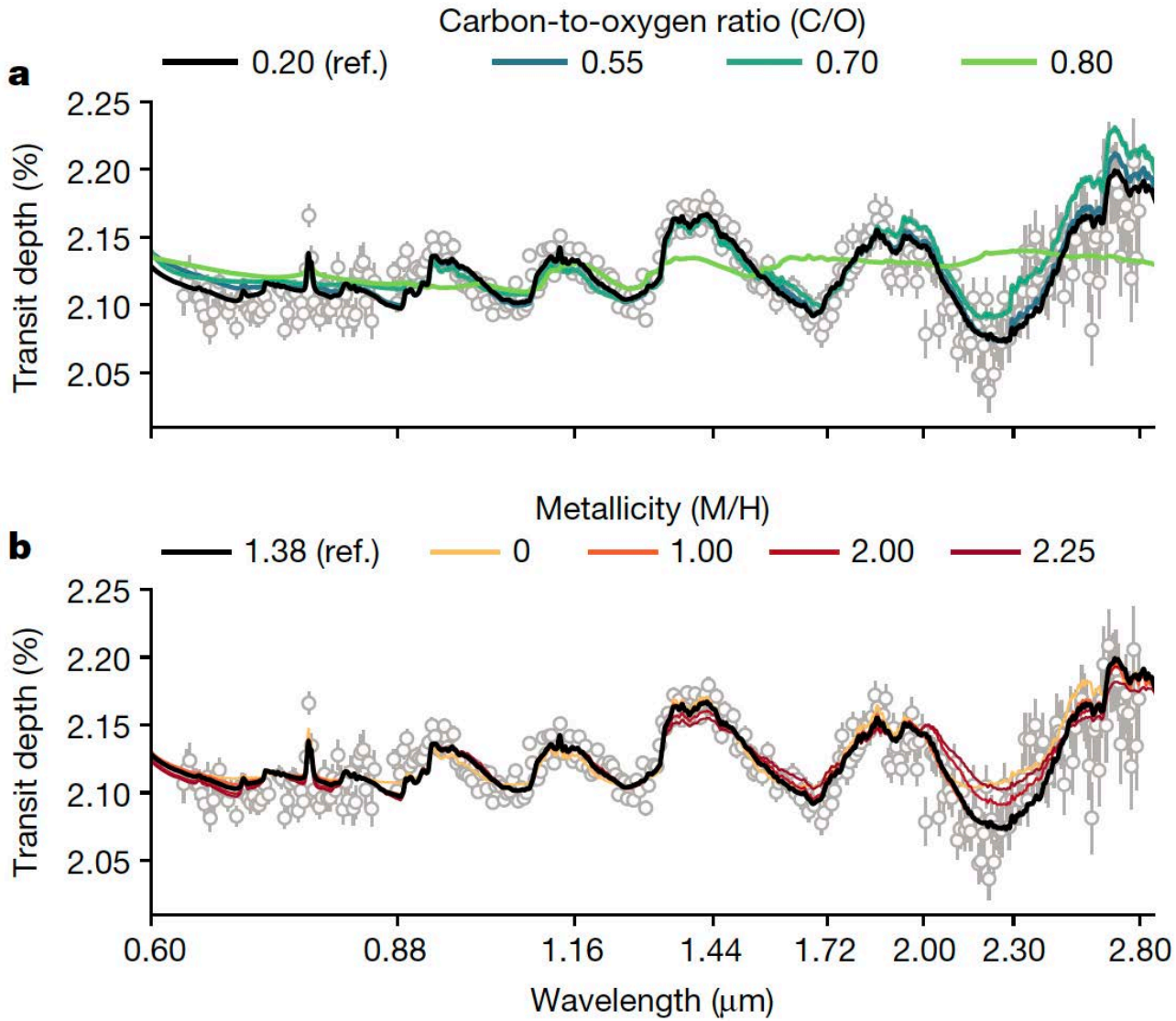

Fig. 4 | Impact of the C/O ratio and metallicity on the JWST-NIRISS spectrum of WASP-39b. a, Variation of the C/O ratio in the best-fit reference model while

WASP-39b WITH NIRISS SOS

Lili, Alderson et al., 2023

- ***Medium resolution specta R ~ 300 0.6-2.8 microns***
- ***H20 (30 σ), K at 6.8σ and CO at 3.6σ, but no notable detections of Na, CH4, CO2, HCN and H2S.***
- ***10-30 time solar solar metallicity, sub-solar C/0, solar to super solar K/0***
- ***Non-grey clouds with inhomogenous coverage of planet terminator***

WASP-39b WITH NIRISS SOS
Lili, Alderson et al., 2023

- ***Medium resolution specta R ~ 300 0.6-2.8 microns***
- ***H20 (30 σ), K at 6.8σ and CO at 3.6σ, but no notable detections of Na, CH4, CO2, HCN and H2S.***
- ***10-30 time solar solar metallicity, sub-solar C/0, solar to super solar K/0***
- ***Non-grey clouds with inhomogenous coverage of planet terminator***

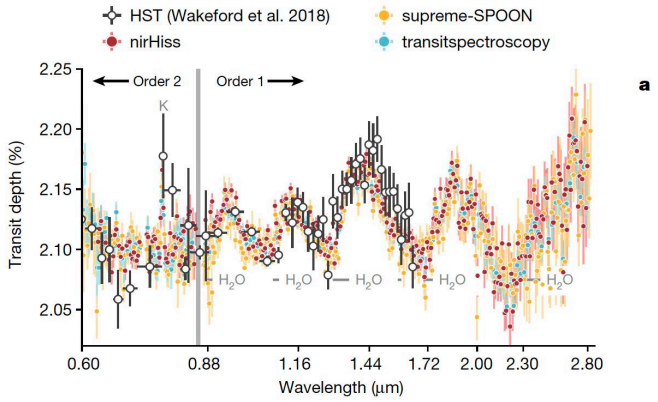

WASP-39b WITH NIRSPEC G395H
Lili, Alderson et al., 2023

- ***Medium resolution specta R=600 3-5 microns, 1.46 x above photon noise***
- ***CO2 (28.5σ), H20 (21.5 σ), SO2 (4.1σ)***
- ***3-10 time solar solar metallicity, sub-solar C/0***

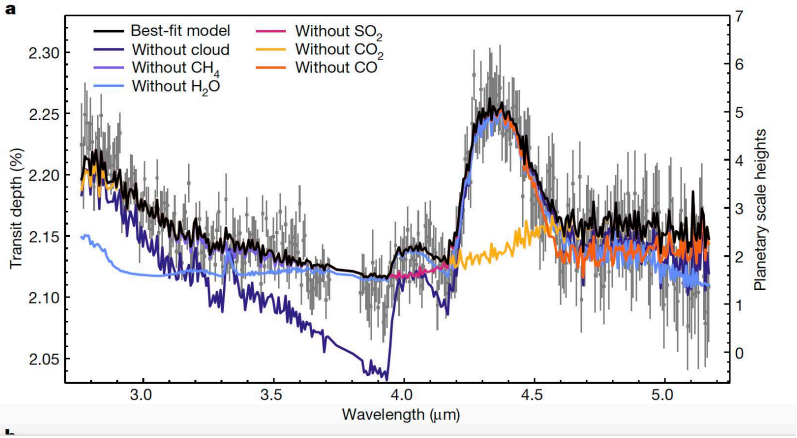

WASP-39b WITH NIRSPEC PRISM
Z. Rustamkulov et al., 2023

- **Resolution of 20-300, over 0.5-5.5 microns**
- **Detection of Na (19σ), H2O (33σ), CO2 (28σ) and CO (7σ).**
- **Non-detection of CH4, combined with a strong CO2 feature, favours atmospheric models with a super-solar atmospheric metallicity.**
- **4 μm is best explained by SO2 (2.7σ), atmospheric photochemistry?**

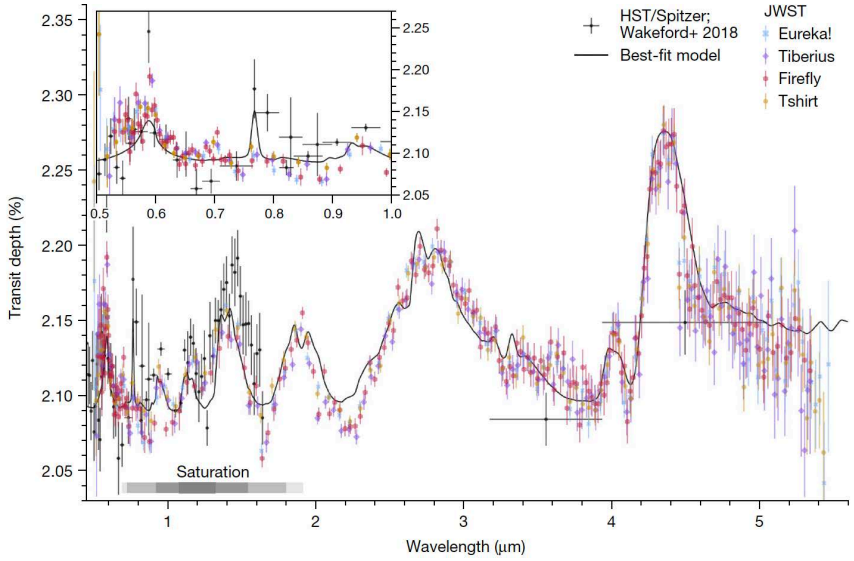

Prediction in the MIRI wavelength range

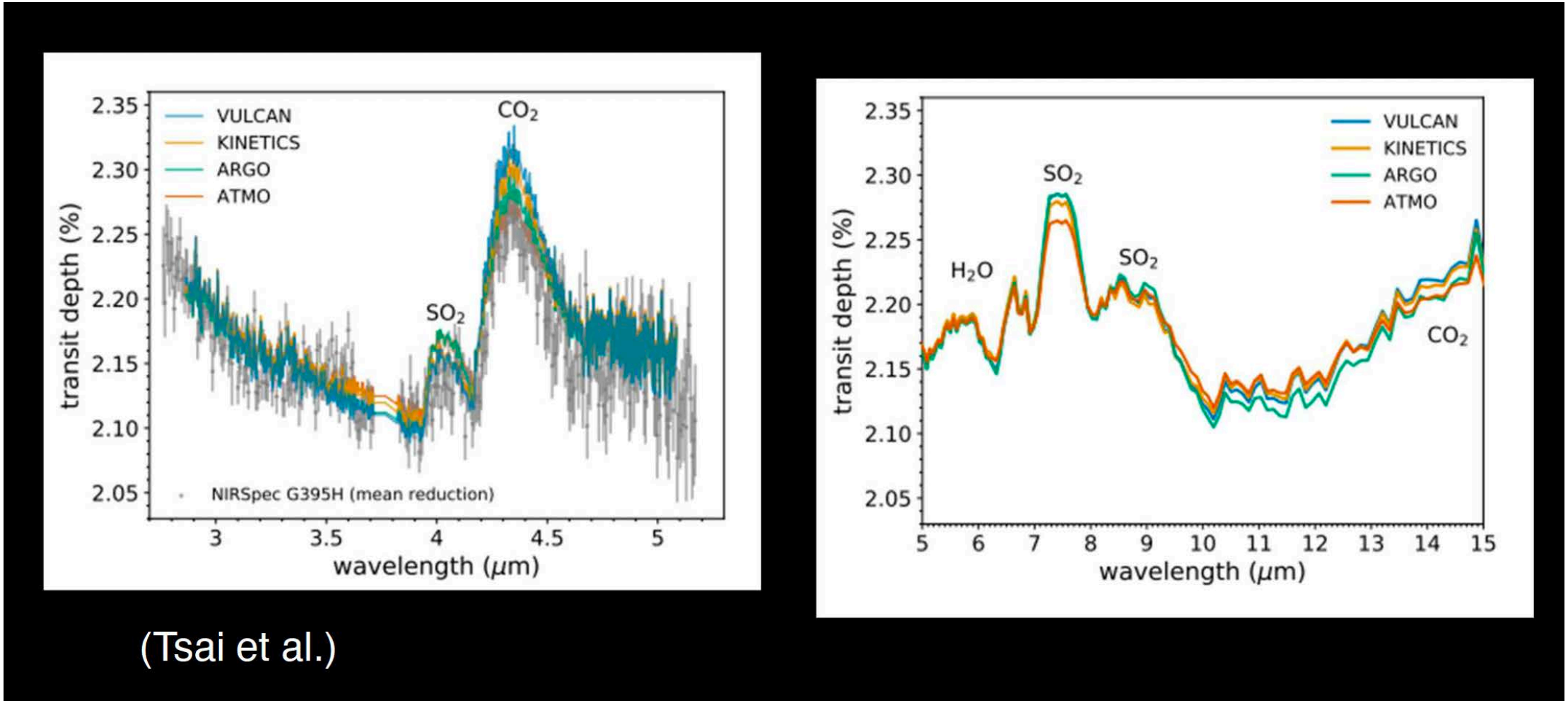

(Tsai et al.)

Tsai et al., 2023, Photochemically-produced SO2 in the atmosphere of WASP-39b, Nature Mars 2023

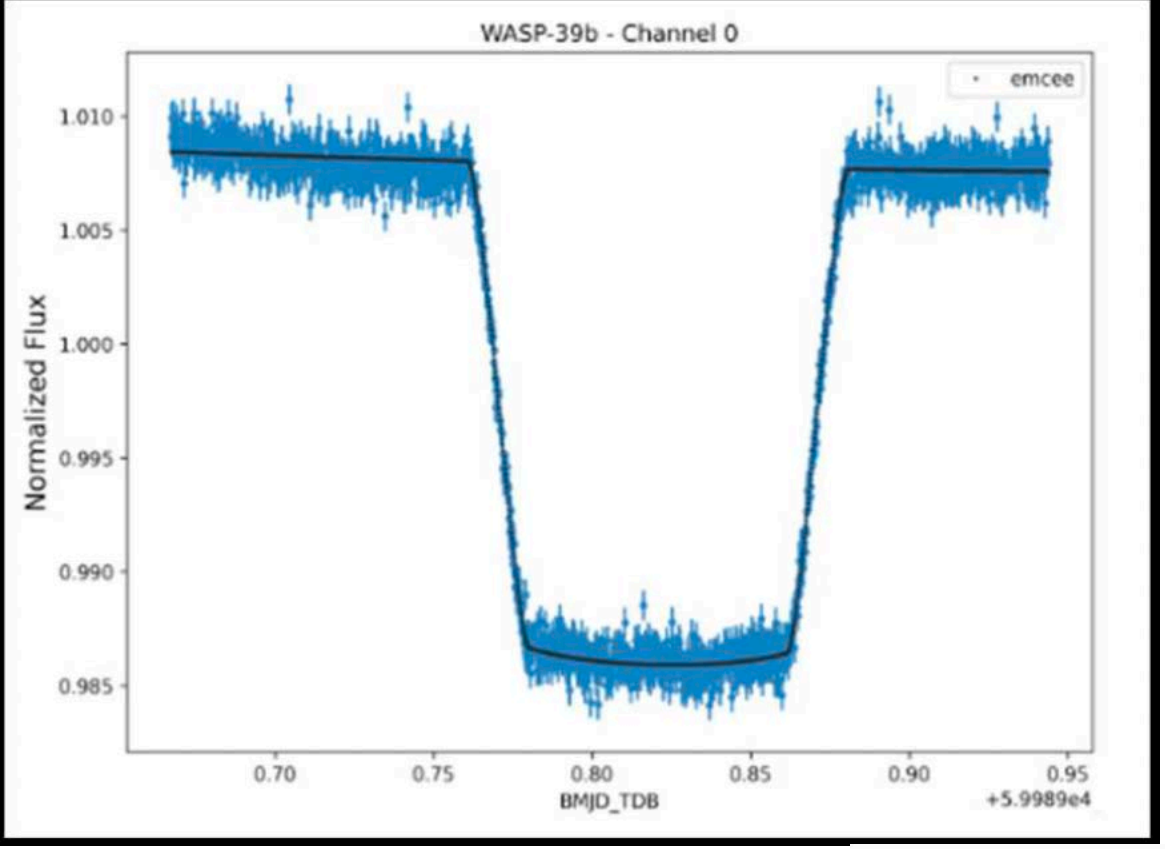

exquisite temporal stability of the telescope, less than 1 mas (requirement 4 mas)

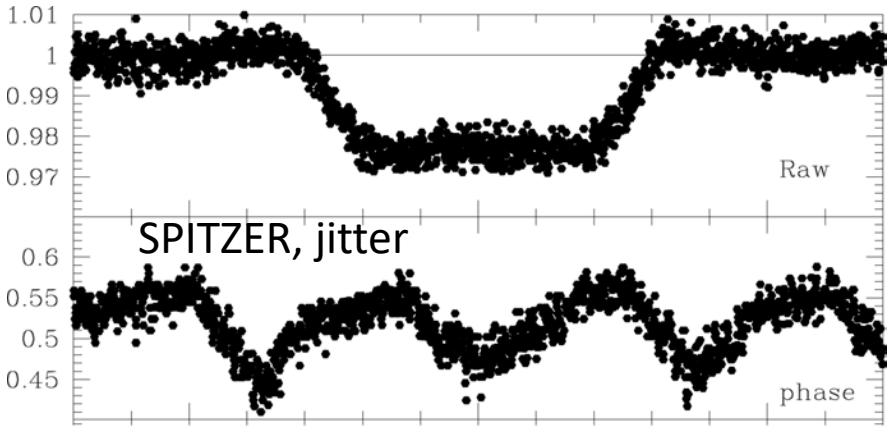

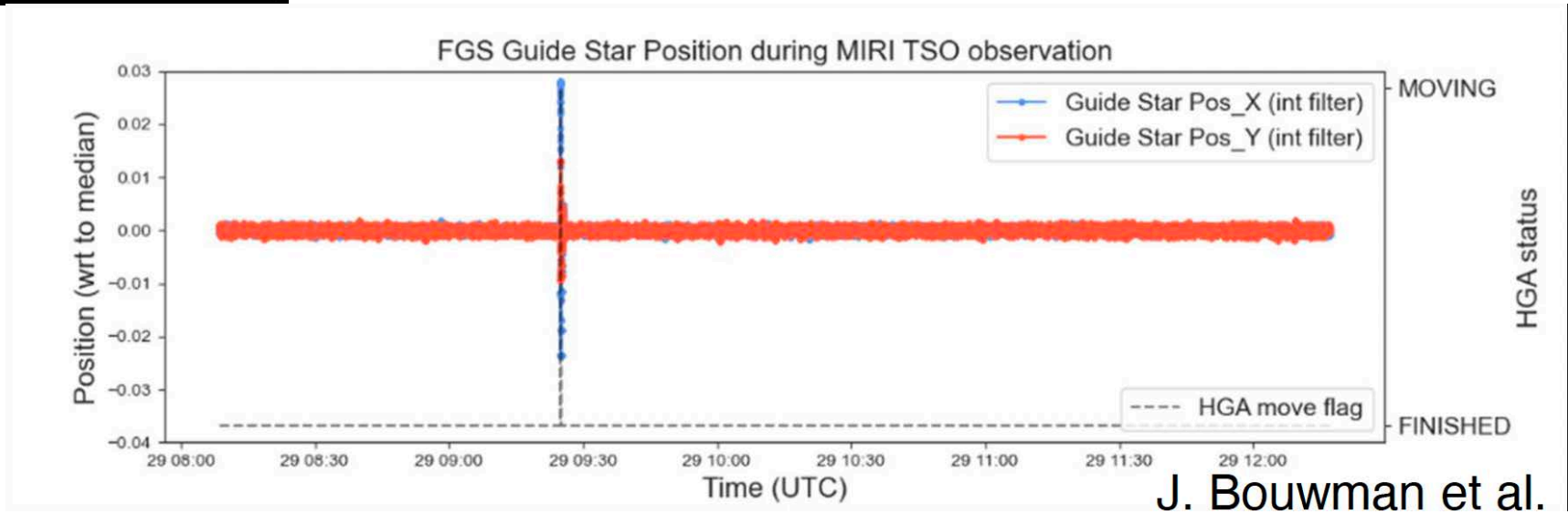

J. Bouwman et al.

First JWST direct imaging of HIP 65426b, NIRCAM+MIRI

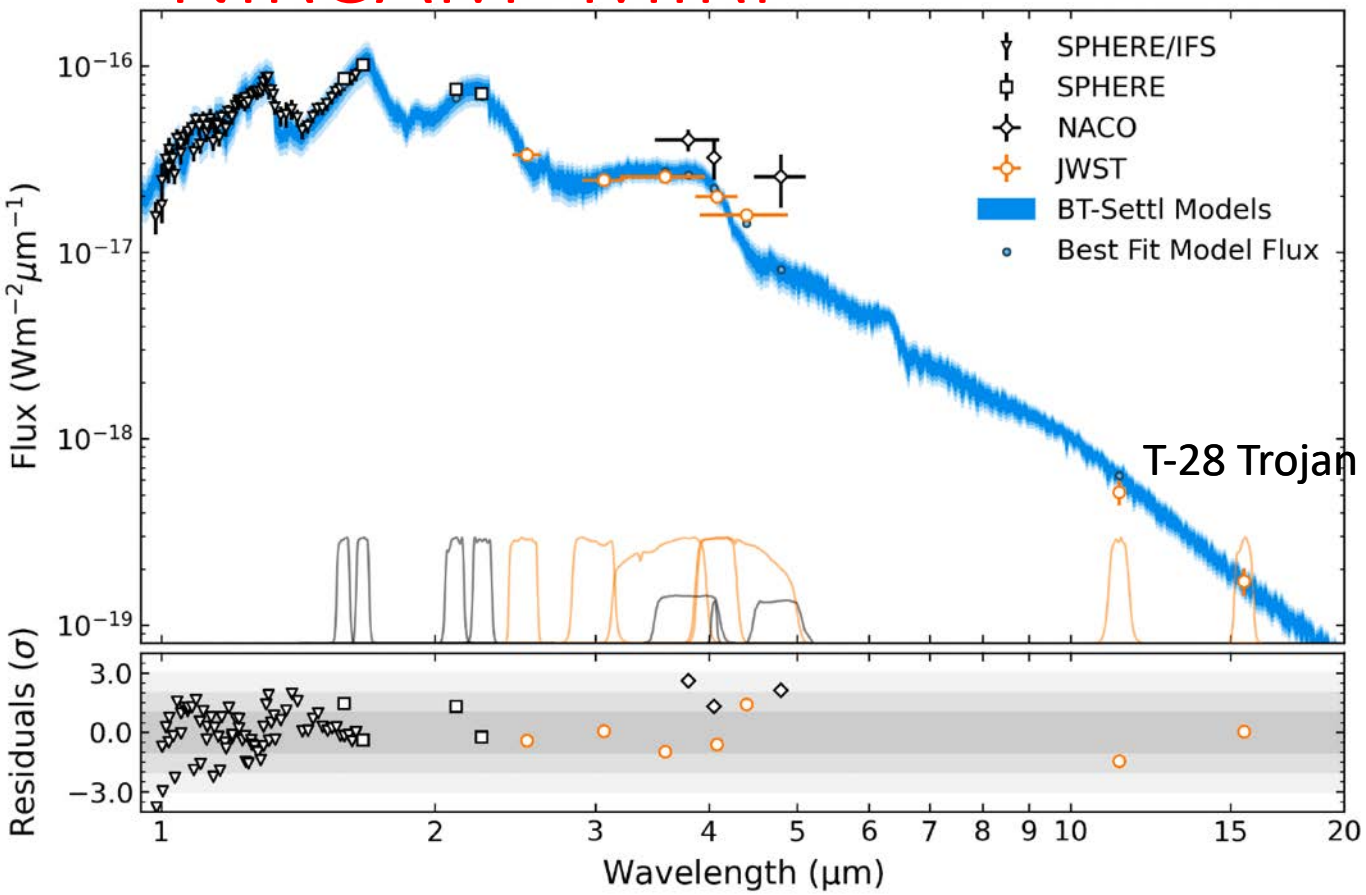

Figure 9. All existing spectroscopic and photometric observations of HIP 65426 b as obtained from SPHERE/IFS (triangles), SPHERE/IRDIS (squares), NaCo (diamonds), and *JWST* (circles). ***Top:*** Data are plotted alongside the 1, 2, and 3σ confidence intervals obtained from fitting to a collection of `BT-SETTL` atmospheric forward models (blue shaded regions), and the model values in the photometric bandpasses (small blue circles). At 3σ, the best fit models occupy parameter ranges of $T_{\rm eff} = 1673^{+27}_{-25}$ K, $\log(g) = 4.10^{+0.20}_{-0.17}$ dex, and $R = 0.90^{+0.04}_{-0.04}$ $R_{\rm Jup}$. The NaCo data have not been included in the model fitting process. Also plotted are the normalised filter throughput profiles for all photometric observations, with the NaCo throughputs scaled by a factor of 2 to improve clarity. ***Bottom:*** Residuals of each data point relative to the best fit model in addition to 1, 2, and 3σ regions (grey shading).

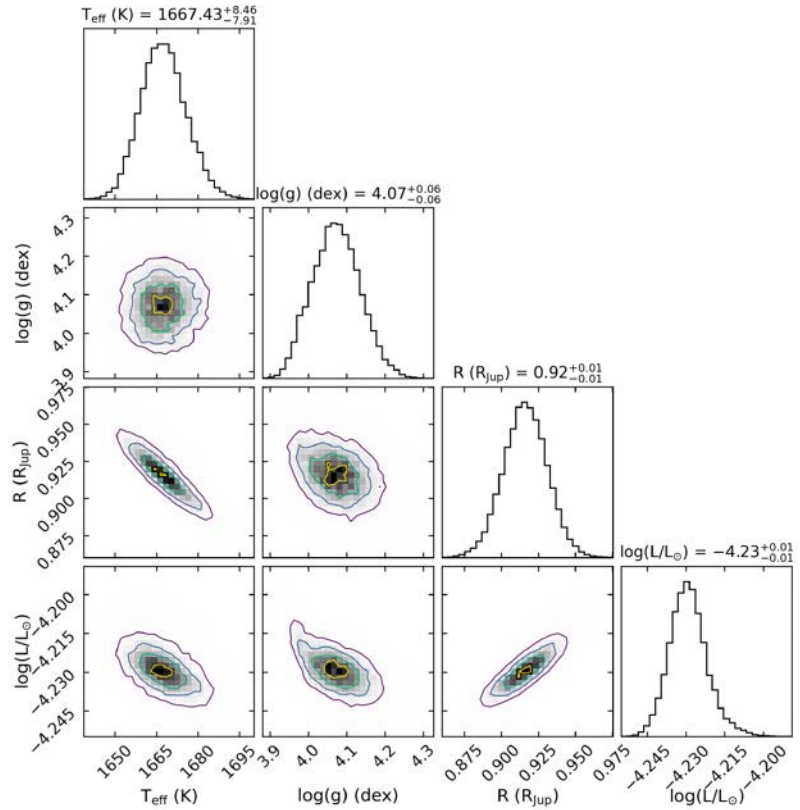

Figure 11. Posterior distributions for the BT−Settl atmospheric model fitting to both *JWST* and *VLT*/SPHERE observations of HIP 65426 b. Best fit values and 1σ uncertainties are indicated, however, these should be interpreted as the model phase space that fits these data, and not the precision to which these properties can be empirically measured.

ROCKY EXOPLANET LHS 475 b

TRANSIT LIGHT CURVE

NIRSpec | Bright Object Time-Series Spectroscopy

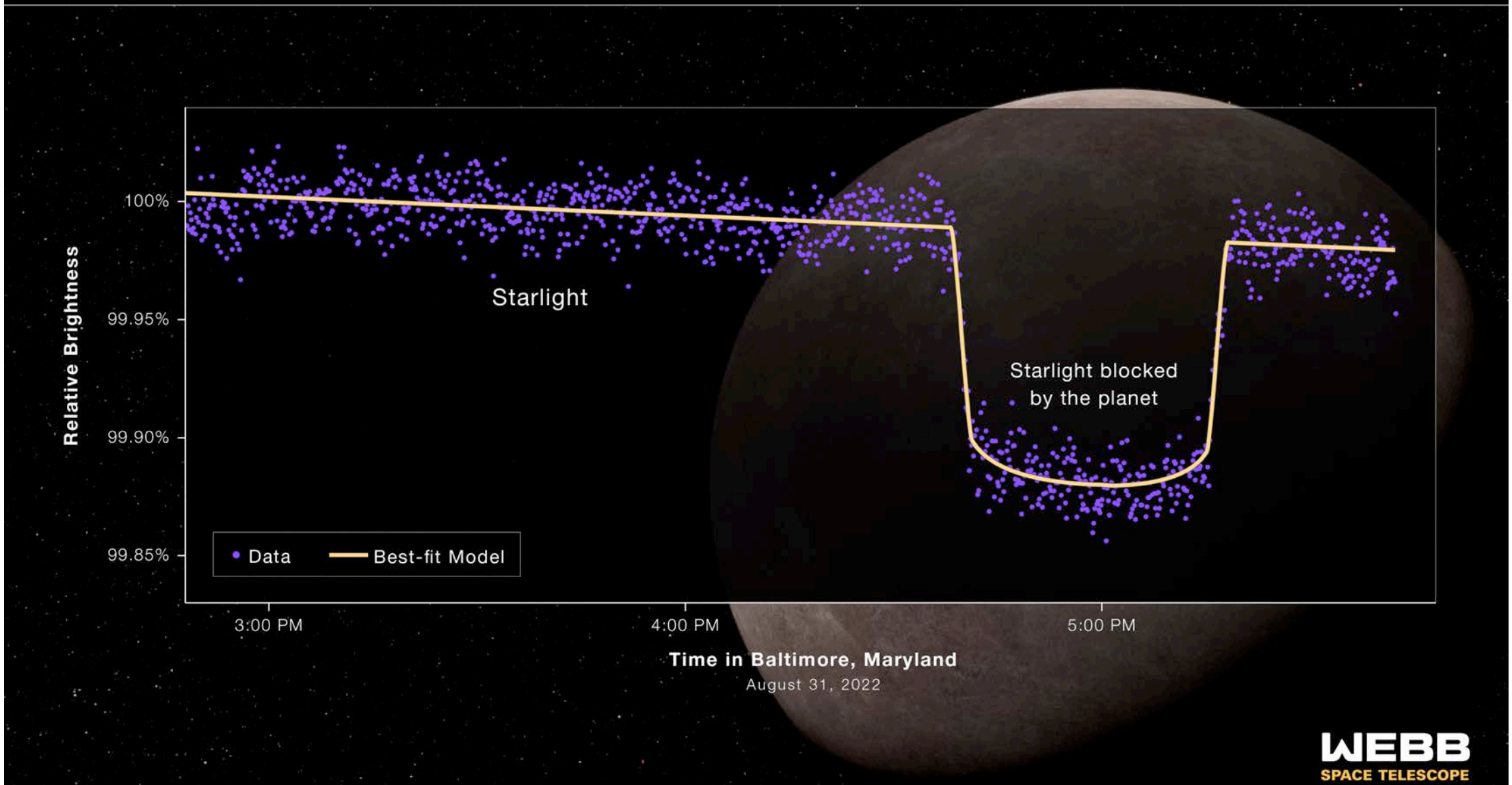

WEBB SPACE TELESCOPE

ROCKY EXOPLANET LHS 475 b

TRANSMISSION SPECTRUM

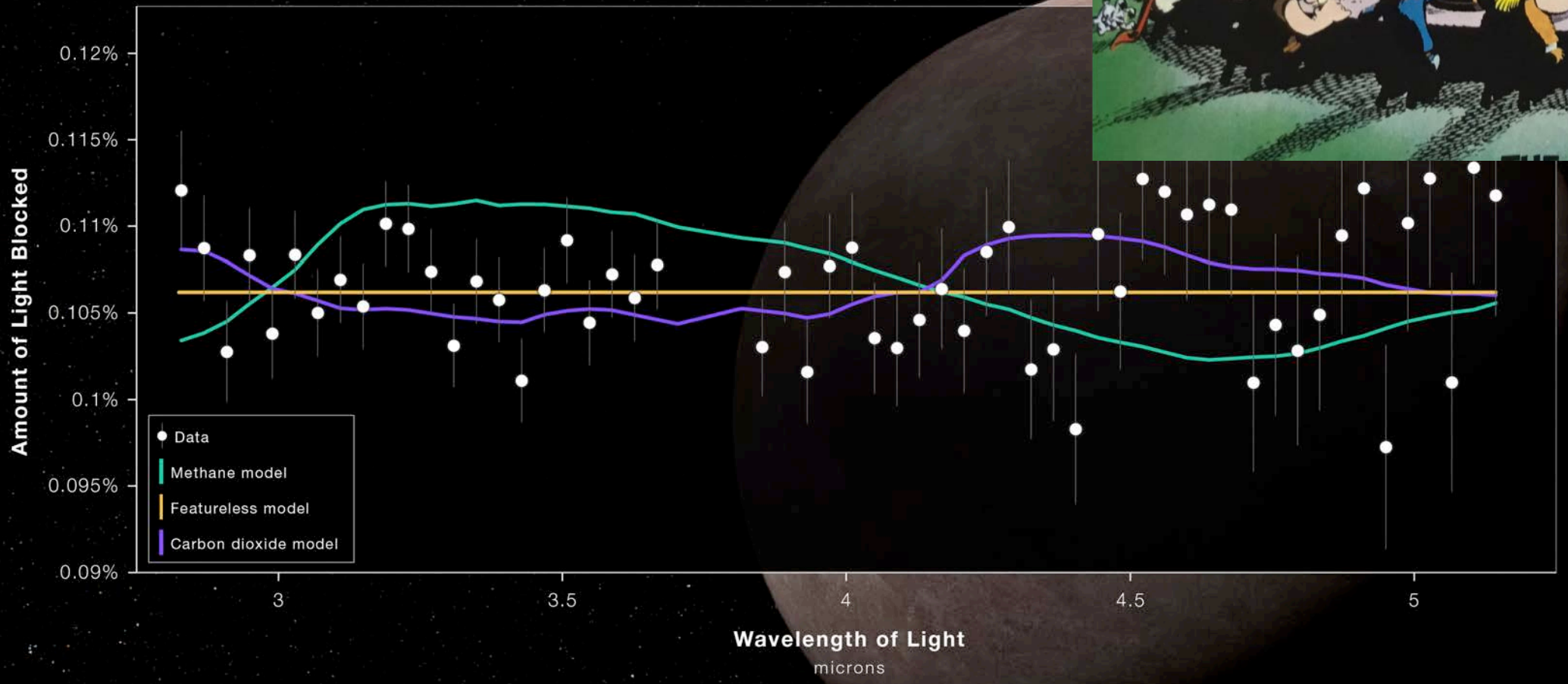

WEBB
SPACE TELESCOPE

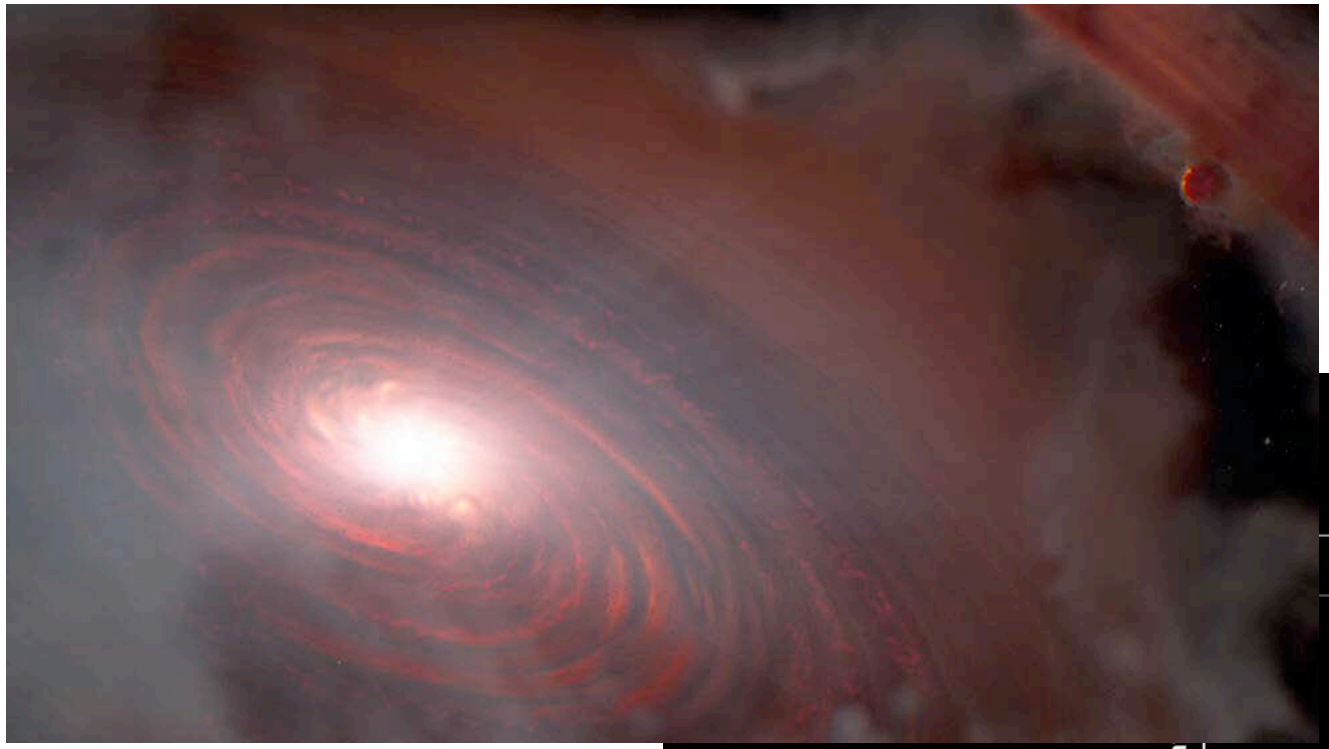

Water detection in protoplanetary disk PDS 70

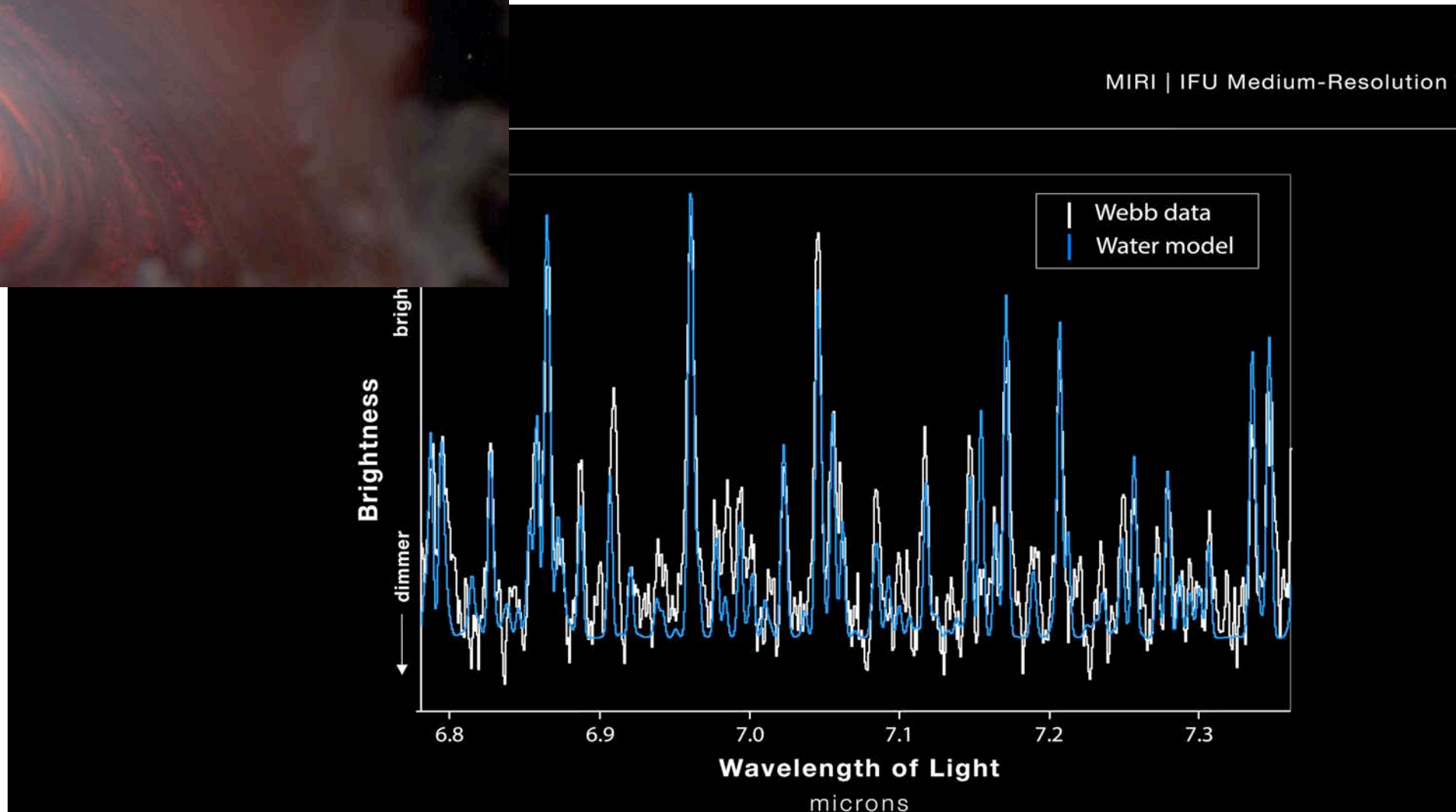

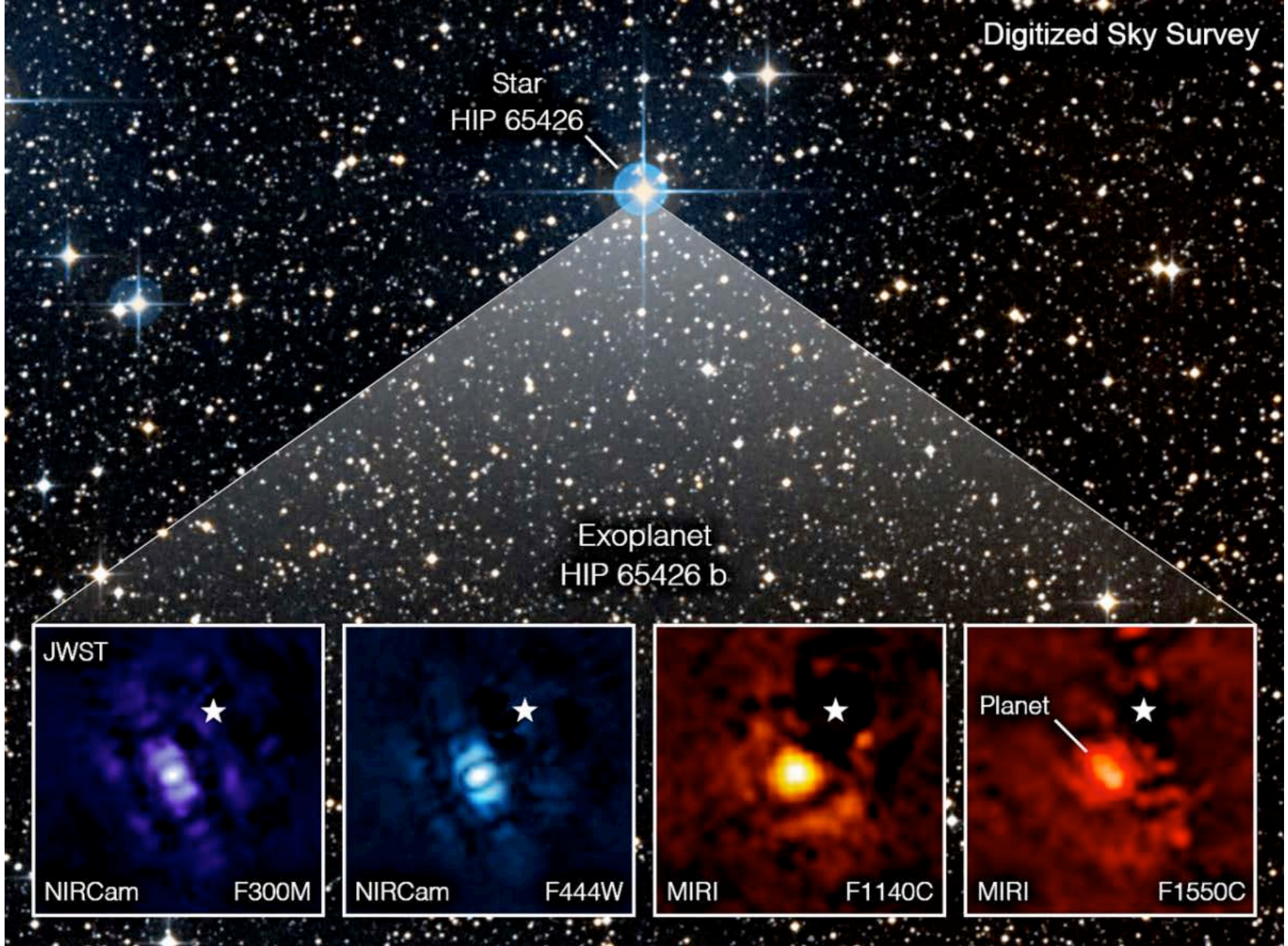
Digitized Sky Survey
Star
HIP 65426
Exoplanet
HIP 65426 b
JWST
NIRCam F300M
NIRCam F444W
MIRI F1140C
Planet
MIRI F1550C

First JWST direct imaging of HIP 65426b, NIRCAM+MIRI

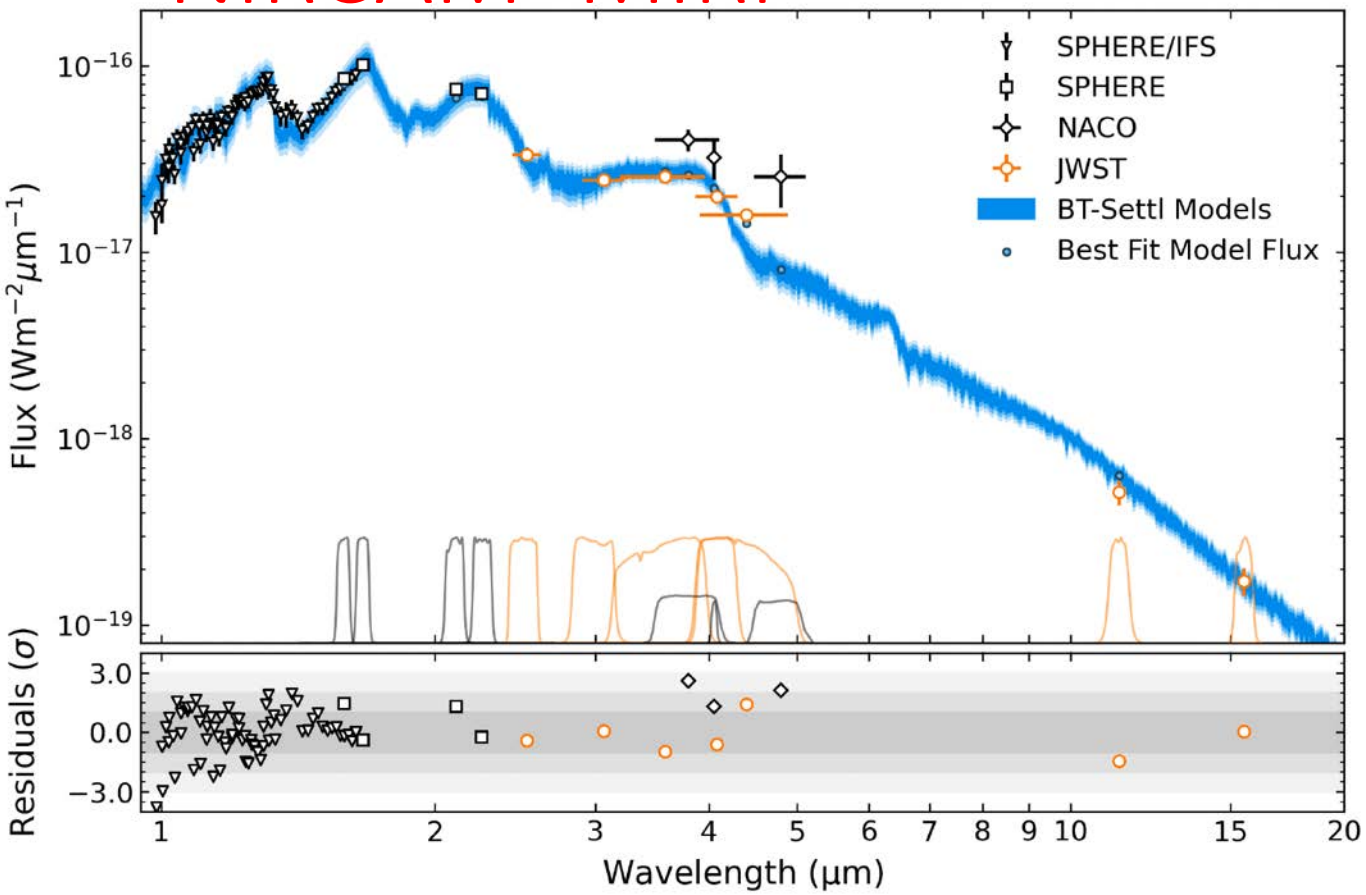

Figure 9. All existing spectroscopic and photometric observations of HIP 65426 b as obtained from SPHERE/IFS (triangles), SPHERE/IRDIS (squares), NaCo (diamonds), and *JWST* (circles). ***Top:*** Data are plotted alongside the 1, 2, and 3σ confidence intervals obtained from fitting to a collection of `BT-SETTL` atmospheric forward models (blue shaded regions), and the model values in the photometric bandpasses (small blue circles). At 3σ, the best fit models occupy parameter ranges of $T_{\rm eff} = 1673^{+27}_{-25}$ K, $\log(g) = 4.10^{+0.20}_{-0.17}$ dex, and $R = 0.90^{+0.04}_{-0.04}$ $R_{\rm Jup}$. The NaCo data have not been included in the model fitting process. Also plotted are the normalised filter throughput profiles for all photometric observations, with the NaCo throughputs scaled by a factor of 2 to improve clarity. ***Bottom:*** Residuals of each data point relative to the best fit model in addition to 1, 2, and 3σ regions (grey shading).

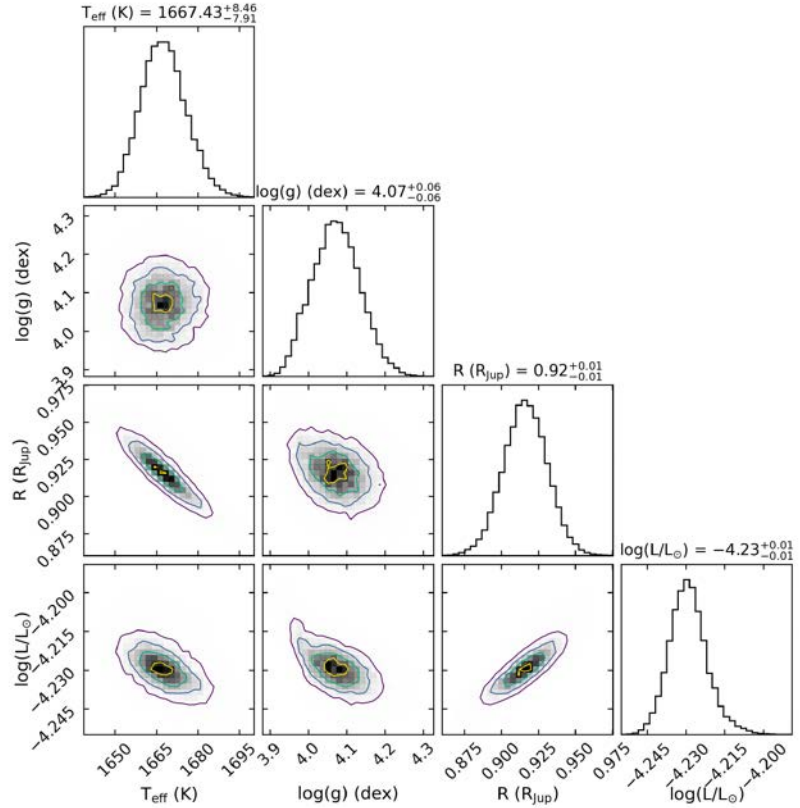

Figure 11. Posterior distributions for the BT−Settl atmospheric model fitting to both *JWST* and *VLT*/SPHERE observations of HIP 65426 b. Best fit values and 1σ uncertainties are indicated, however, these should be interpreted as the model phase space that fits these data, and not the precision to which these properties can be empirically measured.

Back to Trappist system, Trappist-1b and 1c

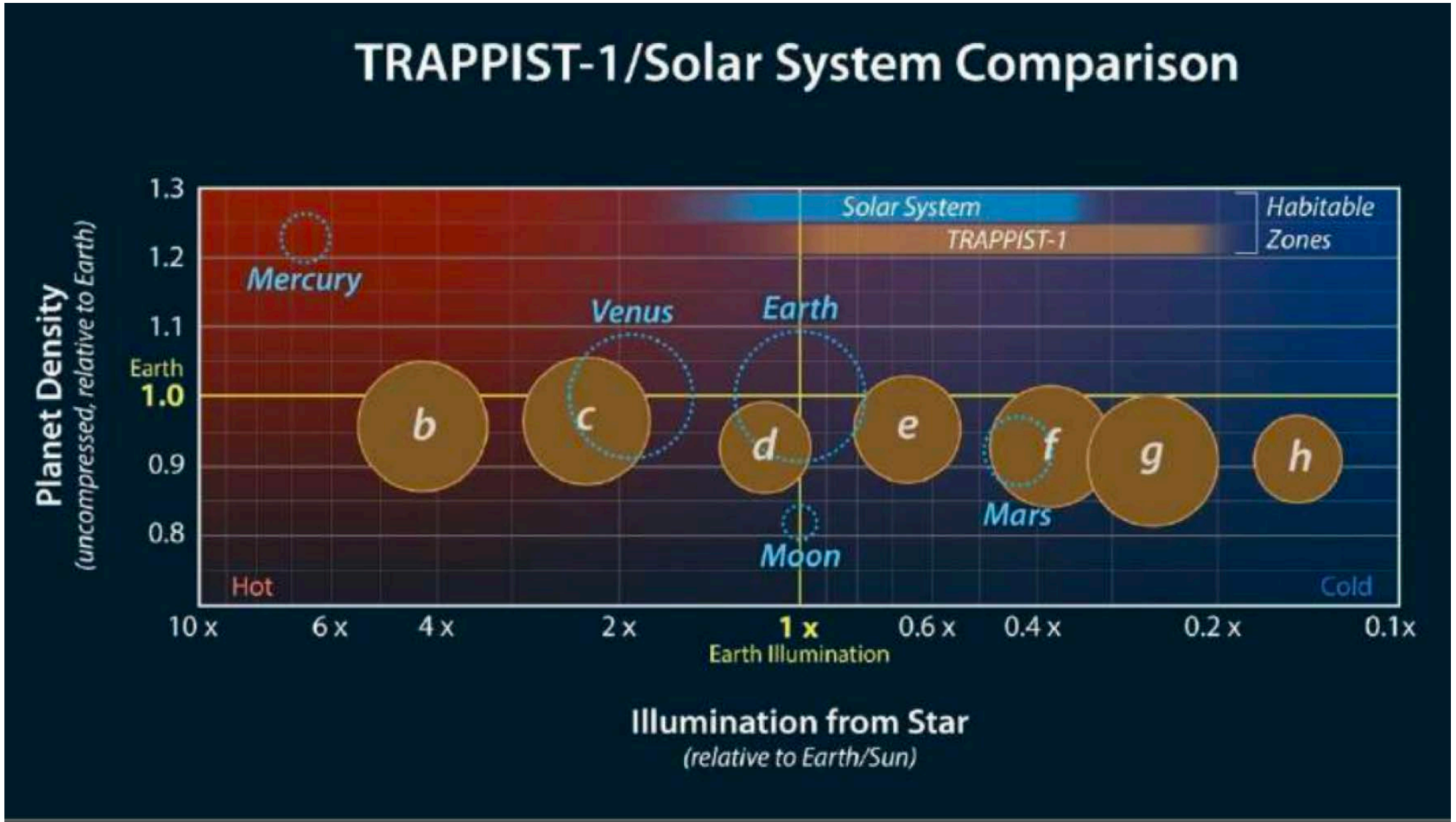

ROCKY EXOPLANET TRAPPIST-1 b

SECONDARY ECLIPSE LIGHT CURVE

MIRI | Time-Series Photometr

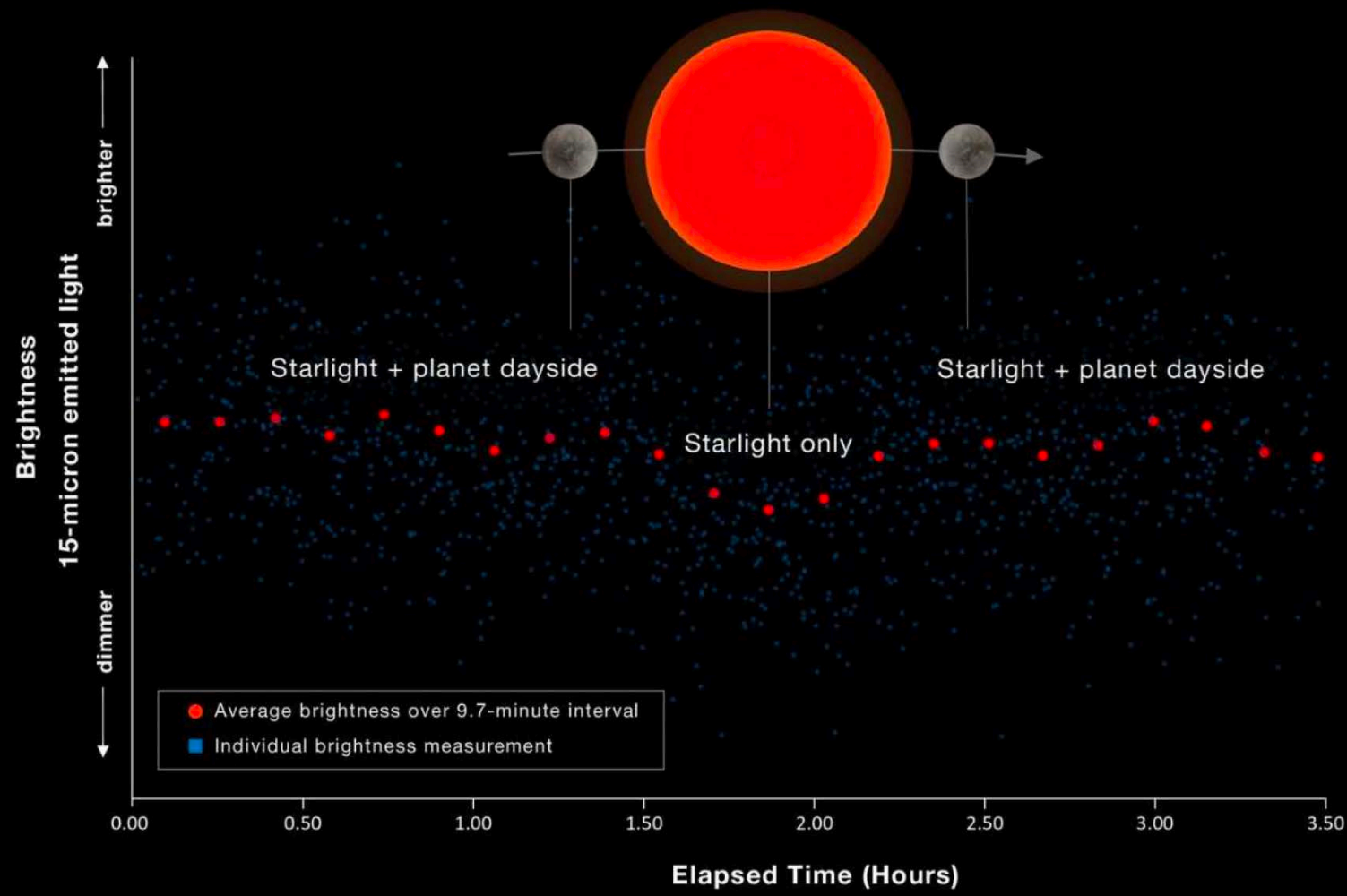

Emission detected !

publshed in Nature , T. Greene et al. 2023

Atmospheres on Trappist-1b ?

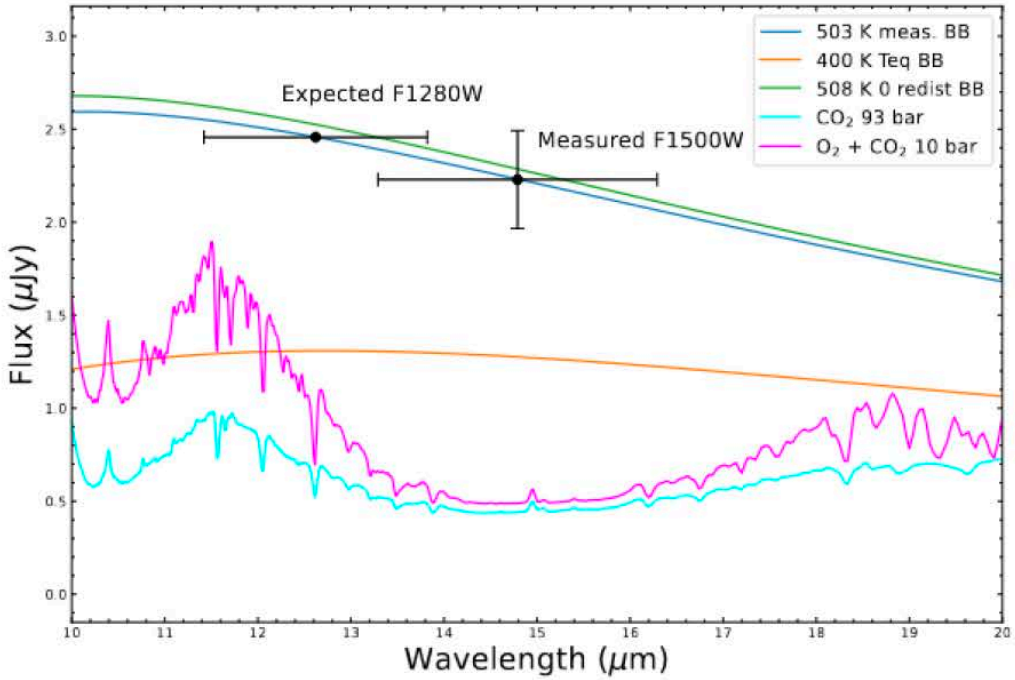

Figure – *Greene et al. 2023*, Thermal emission from TRAPPIST-1b (JWST Miri instrument, 5 eclipses)

Very bright dayside (@ 15μm)

- No atmosphere ? (=no heat redistribution towards nightside)
- Thin residual atmosphere ?
- Thick atmosphere, transparent at 15μm ?

Alice can tell you about it !

Trappist 1 c

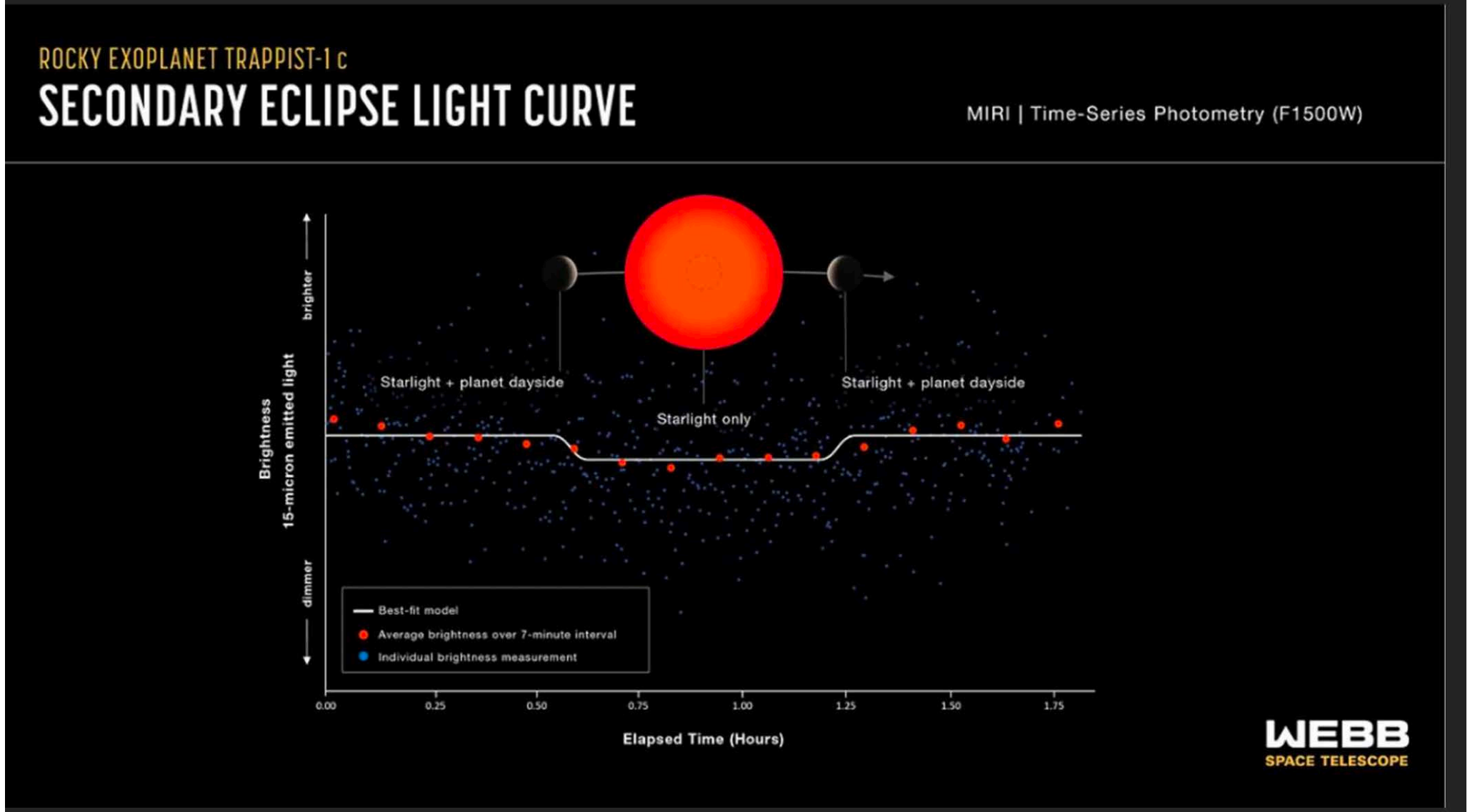

Emission detected ! T = 380 k +/- 31 k → No CO2 as for Venus

publshed in Nature , S. Sieba et al. 2023

Some JWST headlines

- https://www.jameswebbdiscovery.com/exoplanets/james-webb-telescope-exoplanet-discoveries

List of exoplanets :
https://www.stsci.edu/~nnikolov/TrExoLiSTS/JWST/trexolists.html

August 05, 2023 - Kepler-186f: The Earth-Like Exoplanet in the Habitable Zone Explained - Details here

- *March 27, 2023 - James Webb Telescope measures temperature of rocky exoplanet TRAPPIST-1b - Details here*
- *March 19, 2023 - Swirling, Gritty Clouds on exoplanet VHS 1256 b Spotted by Webb Telescope - Details here*
- *March 08, 2023 - Webb is observing six exoplanet systems this week including TOI-836, WASP-17 - Details here*
- *November 22, 2022 - Webb reveals molecular and chemical portrait of Wasp - 39b atmosphere - Details here*
- *October 20, 2022 - James Webb Telescope observes Jupiter-like extrasolar planet 51 Eridani b - Details here*
- *September 02, 2022 - James Webb Discovery - First Direct Image of Exoplanet - HIP 65426 b - Details here*
- *August 25, 2022 - James Webb Discovery - First Evidence of Carbon Dioxide on an Exoplanet - Details here*

JWST as of september 1, 2023

check *https://www.stsci.edu/~nnikolov/TrExoLiSTS/JWST/trexolists.html*

355 observations, including 236 transits, 89 eclipses, 24 phase curves

88 Targets

Instruments, NIRSPEC : 175, MIRI : 89, NIRISS:55, NIRCAM: 36

- NIRISS SOS : 55
- NIRSPEC BOTS+G395H : 103
- NIRSPEC BOTS+PRISM : 59
- NIRSPEC BOTS+G235H :3
- NIRCAM GRISMR+F444W: 21
- NIRCAM GRISMR+F322W2 : 15
- MIRI LRS : 47
- MIRI F1280W : 6
- MIRI F1500W : 33

Mass histogram of planets observed by JWST

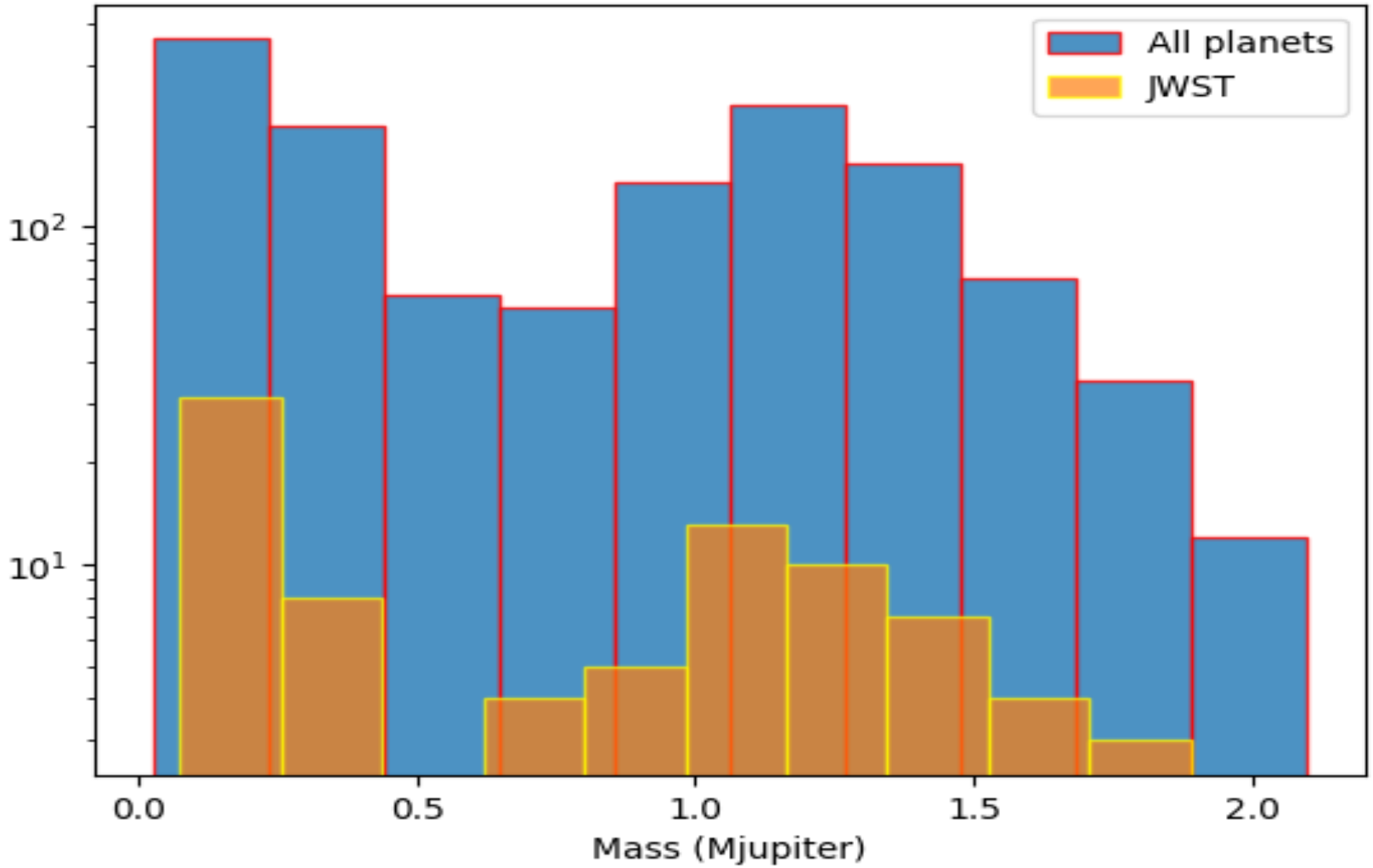

Radius histogram of planets observed by JWST

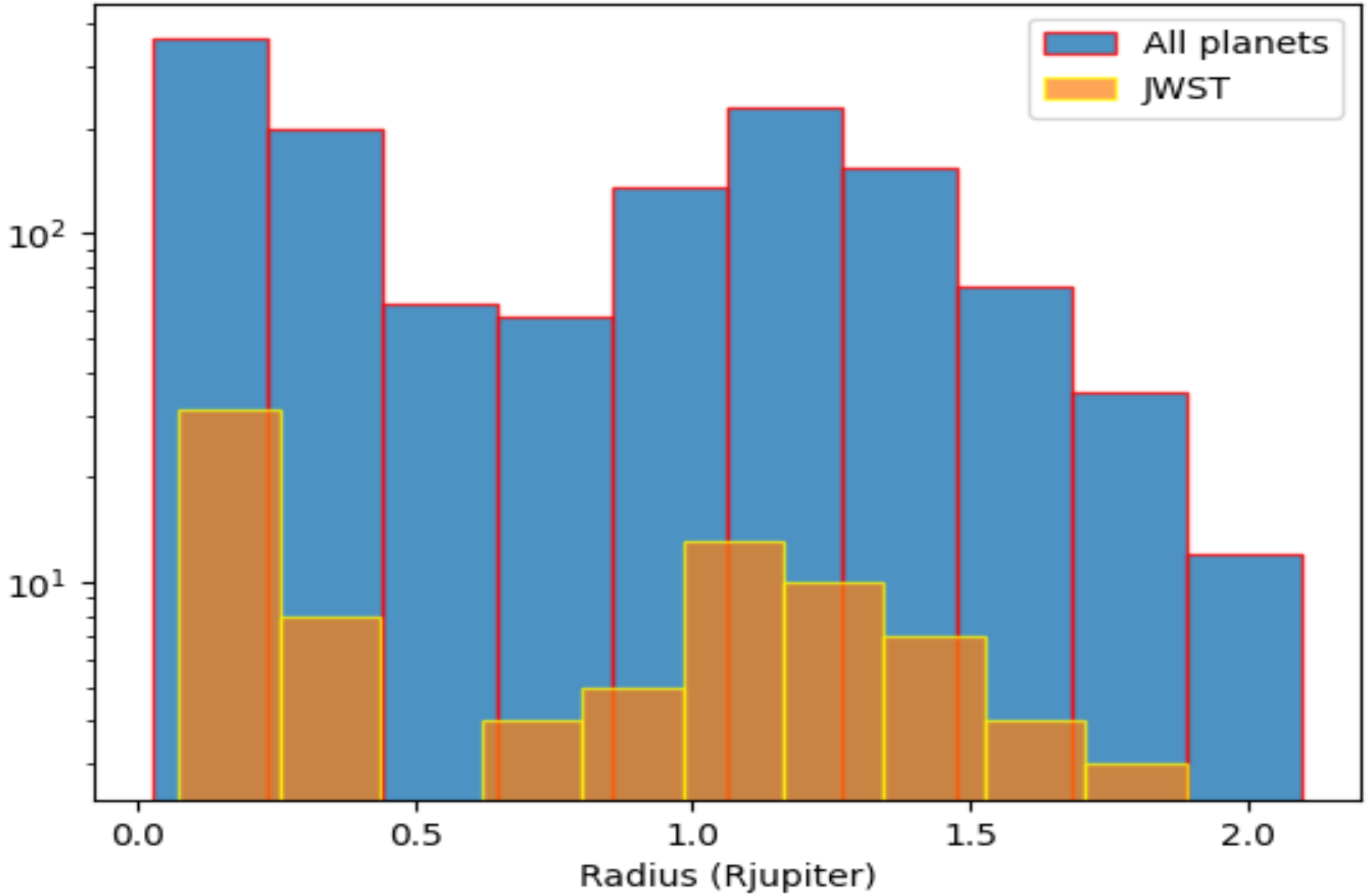

Radius histogram of planets observed by JWST

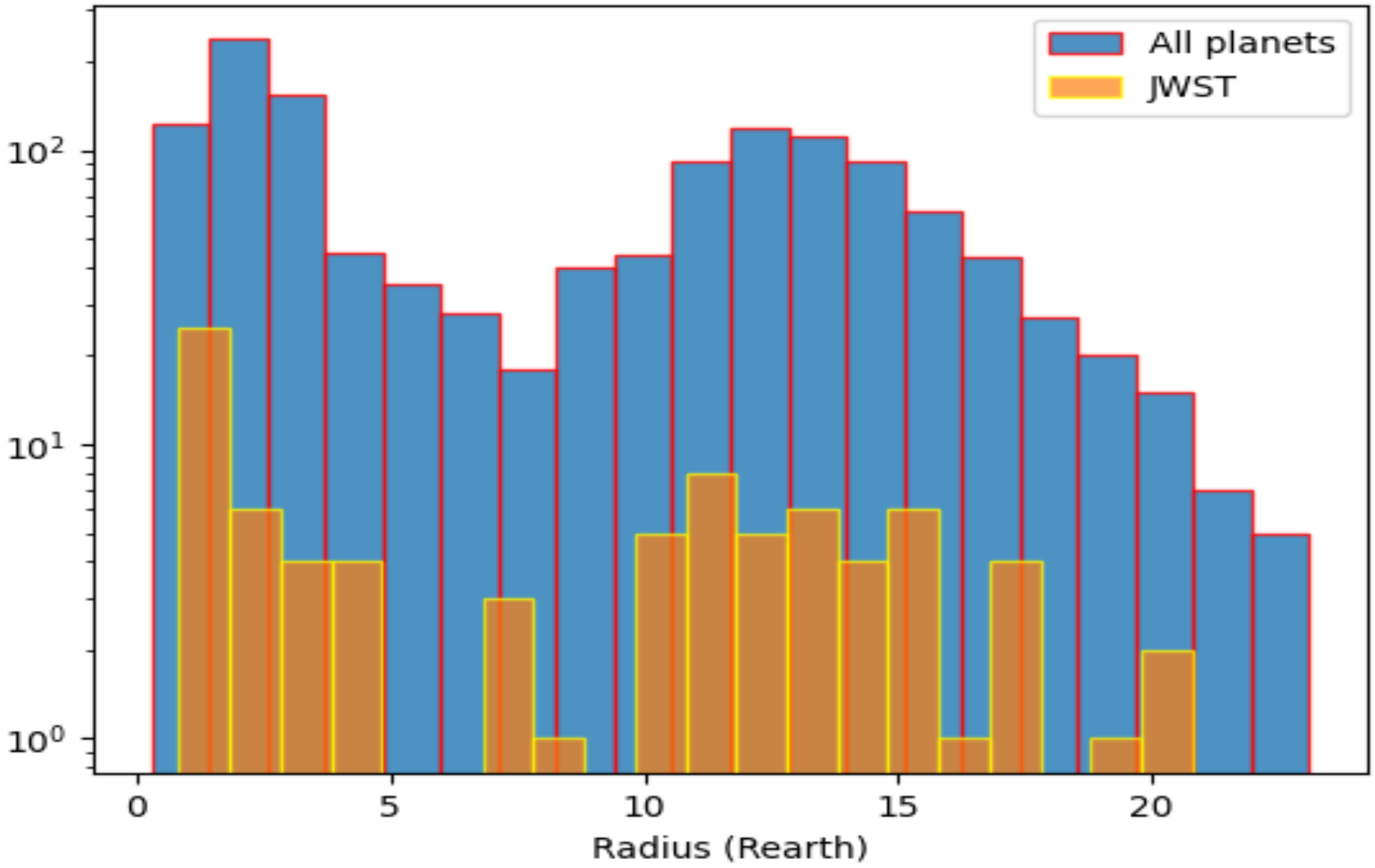

Mass radius of known planets, and JWST targets

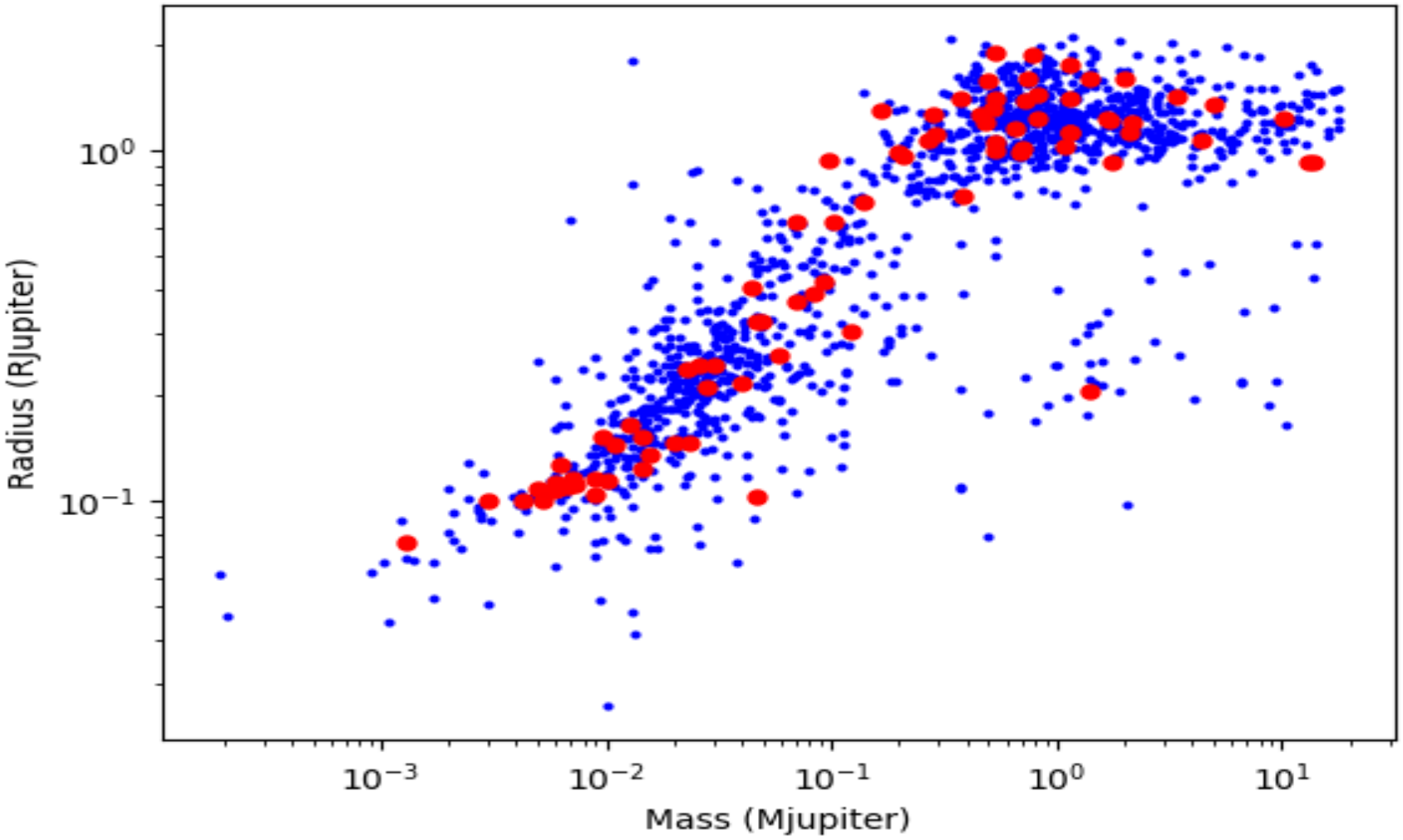

Temperature of known planets, and JWST targets

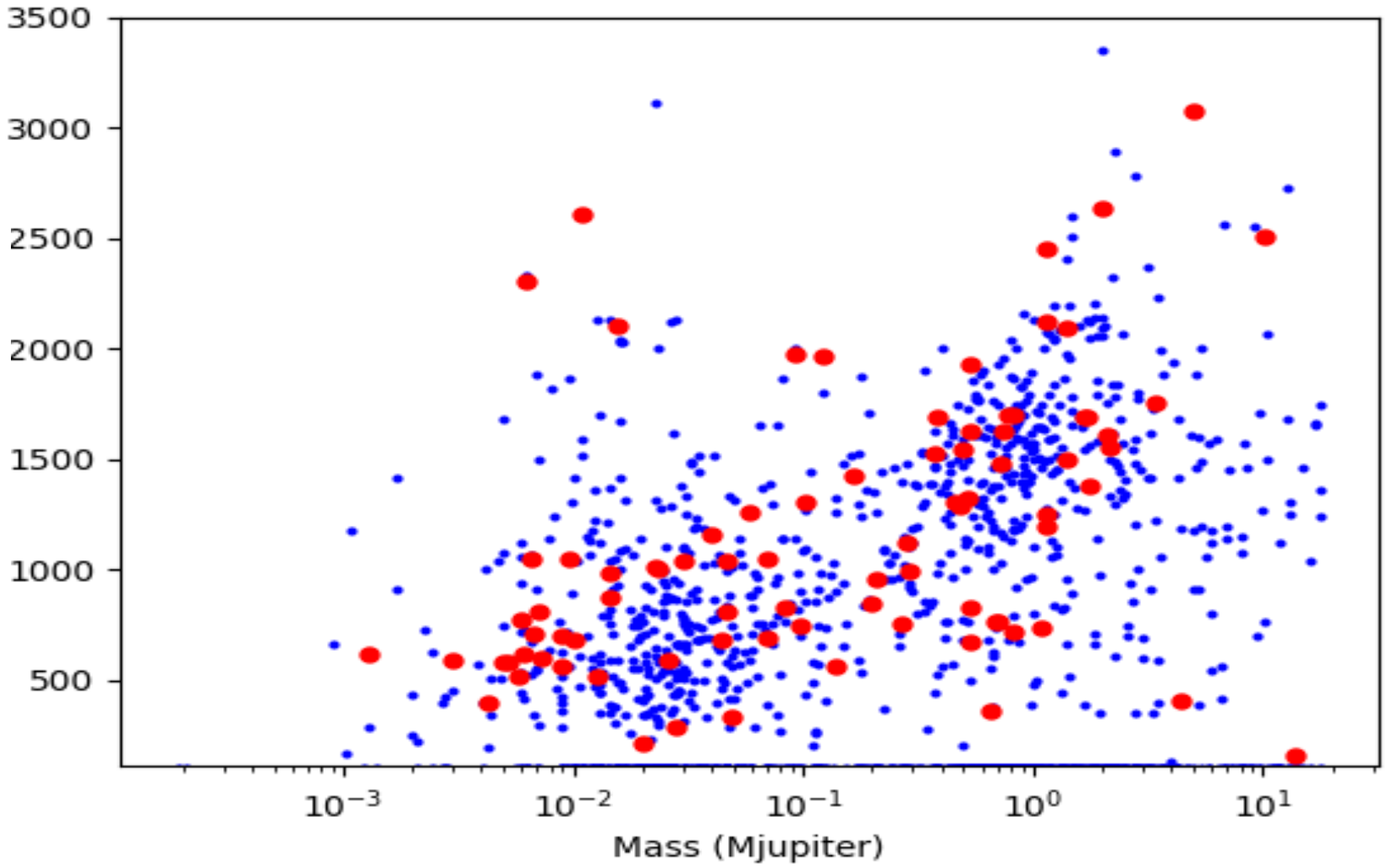

	Name		type	radius	mass	temp
1.	HAT-p-65 b		NIRSPEC BOTS+PRISM	1.89	0.527	1930
2.	WASP-17b		NIRSPEC BOTS+G395H NIRISS SOSS MIRI LRS	1.87	0.78	1700
3.	WASP-121b		NIRSPEC BOTS+G395H MIRI LRS NIRISS SOSS	1.75	1.157	2450
4.	HD 133112b		NIRISS SOSS	1.61	1.99	2636
5.	KELT-7b		NIRSPEC BOTS+G395H	1.60	1.39	2089
6.	NGTS-2b		NIRSPEC BOTS+G395H	1.595	0.74	1622
7.						
8.	WASP-94Ab		NIRSPEC BOTS+G395H	1.58	0.5	1540
9.	HAT-P-30 b		NIRSPEC BOTS+PRISM	1.44	0.83	1700
10.	HAT-P-14 b		NIRSPEC BOTS+G395H NIRCAM GRISMR+F322W2 NIRISS SOSS	1.43	3.44	1756
11.	WASP-19b		NIRSPEC BOTS+PRISM	1.415	1.154	2117
12.	WASP-63b CD-38 2551 b		NIRISS SOSS	1.41	0.37	1526
13.	WASP-15b		NIRSPEC BOTS+G395	1.41	0.54	1626
14.	HD 209458b		NIRCAM GRISMR+F322W2 NIRCAM GRISMR+F444W MIRI LRS	1.39	0.73	1476
15.	TOI-2109b		NIRSPEC BOTS+G395H	1.347	5.02	3072
16.	WASP-127b		NIRSPEC BOTS+G395H NIRISS SOSS	1.31	0.165	1420
17.	HAT-P-1 b		NIRISS SOSS MIRI LRS	1.32	0.525	1322
18.	WASP-52b		NIRSPEC BOTS+PRISM NIRISS SOSS NIRSPEC BOTS+G395H	1.27	0.46	1300
19.	WASP-39b		NIRSPEC BOTS+G395H NIRSPEC BOTS+PRISM NIRISS SOSS NIRCAM GRISMR+F322W2 MIRI LRS	1.27	0.28	1120
20.	WASP-18b		NIRCAM GRISMR+F322W2 NIRISS SOSS	1.24	10.2	2504
21.	55 Cnc b		NIRCAM GRISMR+F444W MIRI LRS	1.24	0.83	718
22.	WASP-77Ab		NIRSPEC BOTS+G395H	1.23	1.667	1690
23.	K2-34b		NIRISS SOSS	1.227	1.698	1685
24.	NGTS-10b		NIRSPEC BOTS+PRISM	1.205	2.162	1551
25.	WASP-96b		NIRSPEC BOTS+G395H NIRISS SOSS	1.2	0.48	1286
26.	TOI-1899b		NIRSPEC BOTS+PRISM	1.15	0.66	363
27.	HD189733b		NIRCAM GRISMR+F322W2 NIRCAM GRISMR+F444W MIRI MRS MIRI LRS	1.13	1.13	1193
28.	WASP-164b		NIRISS SOSS MIRI LRS	1.128	2.13	1608
29.	WASP-47b		NIRSPEC BOTS+G395H	1.128	1.144	1253
30.	WASP-69b		NIRCAM GRISMR+F322W2 NIRCAM GRISMR+F444W NIRSPEC BOTS+G395H MIRI LRS	1.11	0.29	988
31.	TOI-3757b		NIRSPEC BOTS+PRISM	1.07	0.2684	757
32.	TOI-5293b		NIRSPEC BOTS+PRISM	1.06	0.54	675
33.	HD 80606b		NIRSPEC BOTS+G395H MIRI F1500W MIRI LRS	1.07	4.38	404
34.	TOI-5205b		NIRSPEC BOTS+PRISM	1.03	1.08	732
35.	TOI-3714b		NIRSPEC BOTS+PRISM	1.01	0.7	767
36.	HAT-P-12 b		NIRSPEC BOTS+G395H MIRI LRS	0.959	0.21	957
37.	WASP-80 b		NIRCAM GRISMR+F322W2 NIRCAM GRISMR+F444W NIRISS SOSS NIRSPEC BOTS+G395H NIRSPEC BOTS+PRISM MIRI LRS	0.999	0.538	827
38.	HAT-P-18 b		NIRISS SOSS	0.995	0.197	848
39.	TOI-3714		NIRSPEC BOTS+PRISM	0.994	0.69	764
40.	WASP-107b		NIRCAM GRISMR+F322W2 NIRCAM GRISMR+F444W NIRISS SOSS NIRSPEC BOTS+G395H	0.94	0.096	744

			MIRI LRS			
41.	WASP-43b		NIRSPEC BOTS+G395H MIRI LRS	0.93	1.78	1380
42.	WD 1856		NIRSPEC BOTS+PRISM	0.93	13 .8	163
43.	LP 141-14b		NIRSPEC BOTS+G395M	0.928	13.8	159
44.	HD 149026b		NIRCAM GRISMR+F322W2 NIRCAM GRISMR+F444W NIRISS SOSS NIRSPEC BOTS+G395H NIRSPEC BOTS+PRISM MIRI MRS MIRI LRS	0.74	0.38	1693
45.	TOI-3984		NIRSPEC BOTS+PRISM	0.71	0.138	563
46.	HAT-P-26 b		NIRSPEC BOTS+G395H NIRISS SOSS MIRI LRS	0.63	0.07	1043
47.	WASP-166b		NIRSPEC BOTS+G395M NIRISS SOSS	0.63	0.101	1300
48.	LTT 9779b		NIRSPEC BOTS+G395H NIRISS SOSS	0.421	0.0923	1974
49.	GJ3470		NIRCAM GRISMR+F322W2 NIRCAM GRISMR+F444W NIRSPEC BOTS+G395H	0.408	0.0437	683
50.	HAT-P-11b		NIRSPEC BOTS+G395H MIRI LRS	0.389	0.084	829
51.	GJ436b		NIRCAM GRISMR+F322W2 NIRCAM GRISMR+F444W MIRI LRS	0.372	0.07	687
52.	TOI-1231b		NIRSPEC BOTS+G395H MIRI LRS	0.326	0.0485	330
53.	TOI-1130b		NIRSPEC BOTS+G395H NIRISS SOSS	0.326	0.047	812
54.	TOI-849b		NIRSPEC BOTS+PRISM	0.307	0.123	1966
55.	TOI-824b		NIRSPEC BOTS+G395H	0.261	0.0581	1257
56.	GJ 1214b		NIRSPEC BOTS+G395H MIRI LRS	0.245	0.0257	588
57.	TOI-125b		NIRSPEC BOTS+G395H	0.243	0.0299	1038
58.	TOI 421b		NIRISS SOSS NIRSPEC BOTS+G395M	0.239	0.0226	1012
59.	HD106315b		MIRI LRS	0.218	0.0396	1155
60.	K2-18b		NIRSPEC BOTS+G235H NIRSPEC BOTS+G395H NIRISS SOSS MIRI LRS	0.211	0.0281	282
61.	K2-22b		MIRI LRS	0.205	1.4	1500
62.	TOI-776b		NIRSPEC BOTS+G395H	0.165	0.0126	514
63.	TOI-1685b		NIRSPEC BOTS+G395H	0.152	0.0097	1045
64.	TOI-836b		NIRSPEC BOTS+G395H	0.152	0.0143	874
65.	LHS1140b		MIRI F1500W	0.146	0.02	213
66.	TOI 402b HD 15337b		NIRSPEC BOTS+G395H	0.146	0.0236	1003
67.	TOI-260B		NIRSPEC BOTS+G395H	0.1445	0.011	2610
68.	K2-141b		NIRSPEC BOTS+G395H MIRI LRS	0.135	0.0156	2100
69.	TOI-561b		NIRSPEC BOTS+G395H	0.127	0.0063	2305
70.	L168-8 TOI 134b		MIRI LRS	0.124	0.0145	980
71.				0		
72.	GJ1132b		NIRSPEC BOTS+G395H MIRI LRS	0.101	0.0052	584
73.	GJ-4102b LHS475b		NIRSPEC BOTS+G395H	0.1	0.003	586
74.	GJ341		NIRCAM GRISMR+F444W			
75.	LHS 3844		NIRSPEC BOTS+G395H MIRI LRS	0.116	0.0071	810
76.	WOLF 437 b, GJ486		NIRSPEC BOTS+G395H	0.116	0.0089	702
77.	TOI-1468b		NIRISS SOSS NIRSPEC BOTS+G395H MIRI LRS	0.114	0.0101	682
78.	GJ-3473		MIRI F1500W	0.113	0.0059	768
79.	MASS J02531581 +0003087 b TOI 2445b		NIRSPEC BOTS+PRISM	0.112	0.0066	1043
80.	LHS 1478b		MIRI F1500W	0.111	0.0073	600
81.	HD260655b		MIRI F1500W	0.11	0.0067	710
82.	LP 791 18b		NIRSPEC BOTS+PRISM	0.108	0.0061	612
83.	L231-32b TOI-270b		NIRSPEC BOTS+G395H	0.108	0.005	582

			NIRISS SOSS MIRI F1500W			
84.	GJ-357B TOI-562B		NIRISS SOSS NIRSPEC BOTS+G395H MIRI F1500W	0.107	0.0058	519
85.	TOI-455b LTT1445Ab		NIRSPEC BOTS+G395H	0.105	0.009	564
86.	TOI-178b		NIRSPEC BOTS+G395M	0.103	0.047	1039
87.	TRAPPIST-1b	34 obs sur 355	NIRISS SOSS NIRSPEC BOTS+PRISM MIRI F1280W MIRI F1500W	0.1	0.0043	400
88.	L98-59b TOI 175 b		NIRSPEC BOTS+G395H NIRSPEC BOTS+PRISM NIRISS SOSS MIRI F1500W MIRI MRS	0.076	0.0013	618

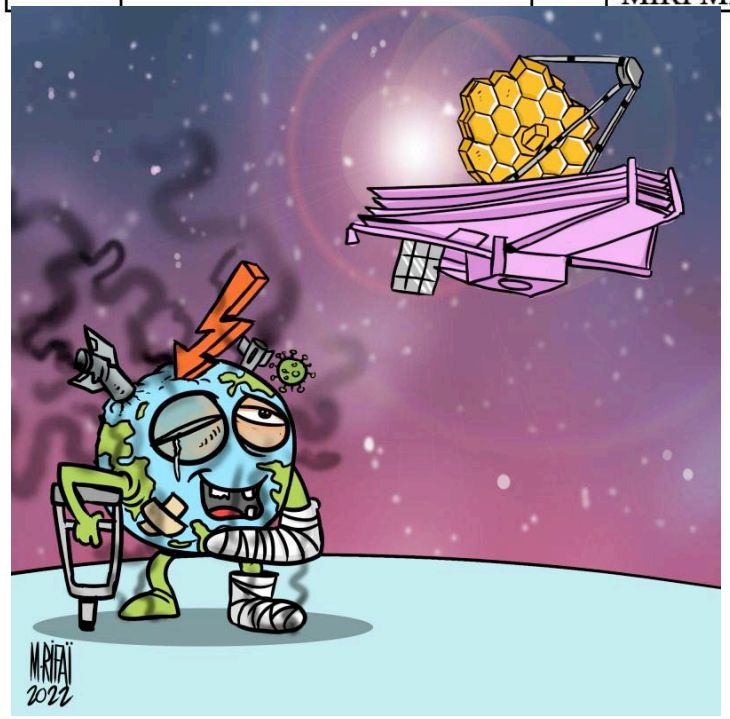

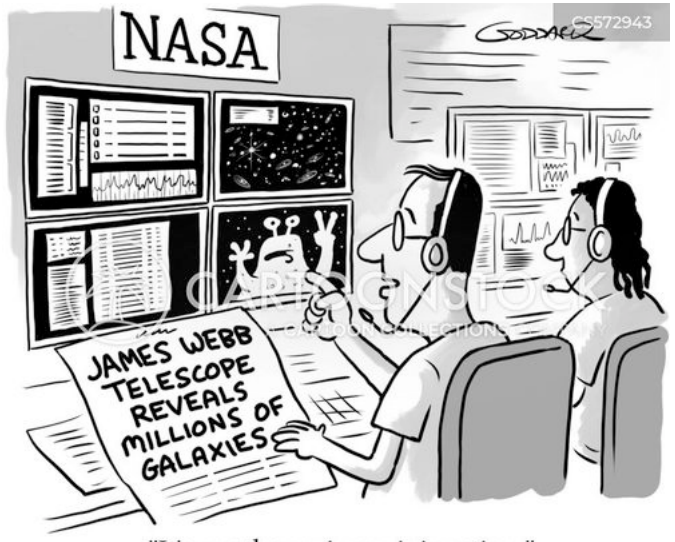

"It's another privacy injunction."